Scanning Probe Microscopy

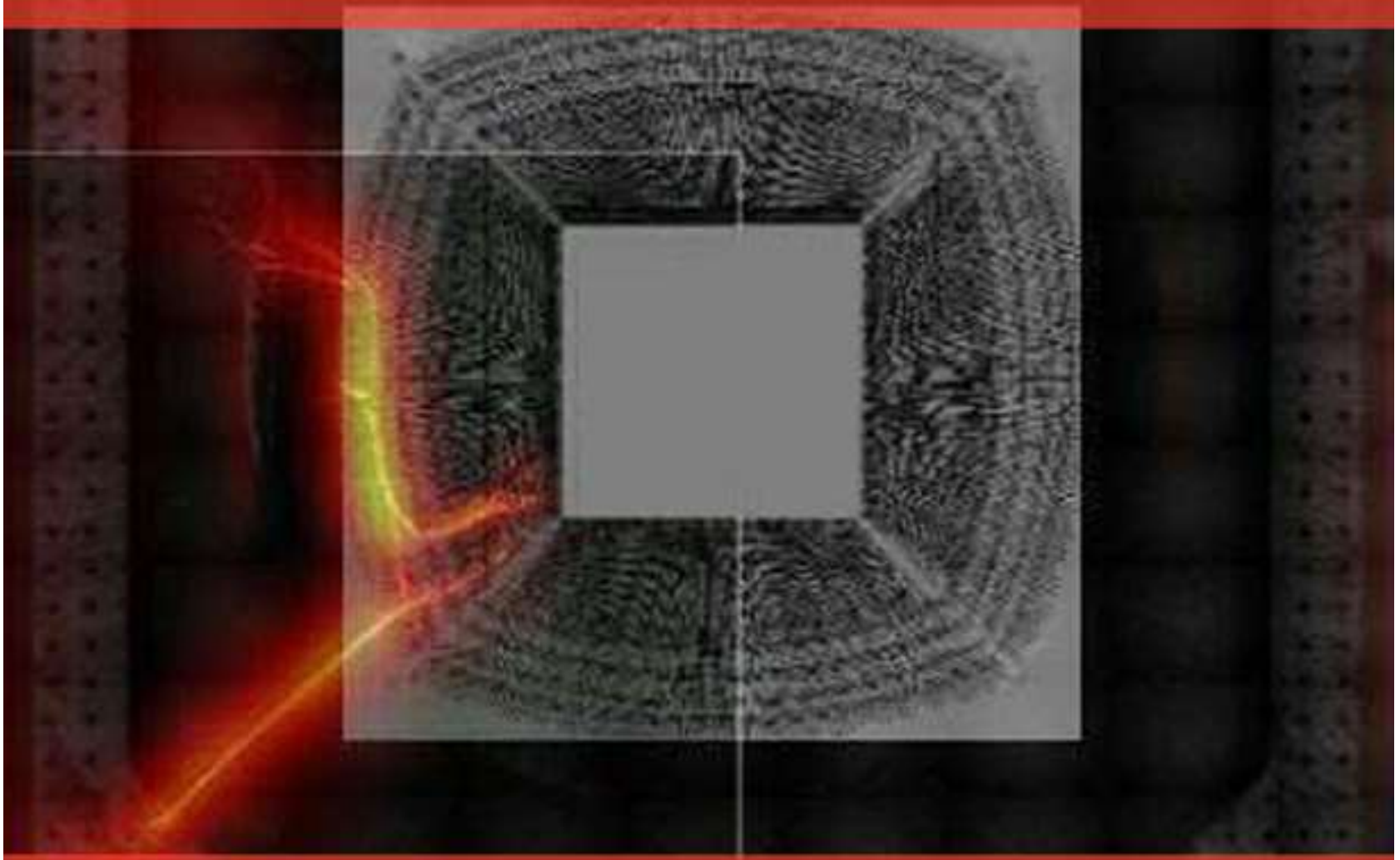

Jacinda Derosa

First Edition, 2011

ISBN 978-93-81157-92-3

Published by:
The English Press
4735/22 Prakashdeep Bldg,
Ansari Road, Darya Ganj,
Delhi - 110002
Email: info@wtbooks.com

Table of Contents

Chapter- 1

Scanning Probe Microscopy

Scanning Probe Microscopy (SPM) is a branch of microscopy that forms images of surfaces using a physical probe that scans the specimen. An image of the surface is obtained by mechanically moving the probe in a raster scan of the specimen, line by line, and recording the probe-surface interaction as a function of position. SPM was founded with the invention of the scanning tunneling microscope in 1981.

Many scanning probe microscopes can image several interactions simultaneously. The manner of using these interactions to obtain an image is generally called a mode.

The resolution varies somewhat from technique to technique, but some probe techniques reach a rather impressive atomic resolution. They owe this largely to the ability of piezoelectric actuators to execute motions with a precision and accuracy at the atomic level or better on electronic command. One could rightly call this family of techniques 'piezoelectric techniques'. The other common denominator is that the data are typically obtained as a two-dimensional grid of data points, visualized in false color as a computer image.

Probe tips

Probe tips are normally made of platinum/iridium, silicon nitride or gold. There are two main methods for obtaining a sharp probe tip, acid etching and cutting. The first involves dipping a wire end first into an acid bath and waiting until it has etched through the wire and the lower part drops away. The remainder is then removed and the resulting tip is often one atom in diameter. An alternative and much quicker method is to take a thin wire and cut it with a pair of scissors or a scalpel. Testing the tip produced via this method on a sample with a known profile will indicate whether the tip is good or not and a single sharp point is achieved roughly 50% of the time. It is not uncommon for this method to result in a tip with more than one peak; one can easily discern this upon scan due to a high level of ghost images.

Advantages of scanning probe microscopy

- The resolution of the microscopes is not limited by diffraction, but only by the size of the probe-sample interaction volume (i.e., point spread function), which can be as small as a few picometres. Hence the ability to measure small local differences in object height (like that of 135 picometre steps on <100> silicon) is unparalleled. Laterally the probe-sample interaction extends only across the tip atom or atoms involved in the interaction.
- The interaction can be used to modify the sample to create small structures (nanolithography).
- Unlike electron microscope methods, specimens do not require a partial vacuum but can be observed in air at standard temperature and pressure or while submerged in a liquid reaction vessel.

Disadvantages of scanning probe microscopy

- The detailed shape of the scanning tip is sometimes difficult to determine. Its effect on the resulting data is particularly noticeable if the specimen varies greatly in height over lateral distances of 10 nm or less.

- The scanning techniques are generally slower in acquiring images, due to the scanning process. As a result, efforts are being made to greatly improve the scanning rate. Like all scanning techniques, the embedding of spatial information into a time sequence opens the door to uncertainties in metrology, say of lateral spacings and angles, which arise due to time-domain effects like specimen drift, feedback loop oscillation, and mechanical vibration.

- The maximum image size is generally smaller.

- Scanning probe microscopy is often not useful for examining buried solid-solid or liquid-liquid interfaces.

Established types of scanning probe microscopy: -

Atomic force microscopy

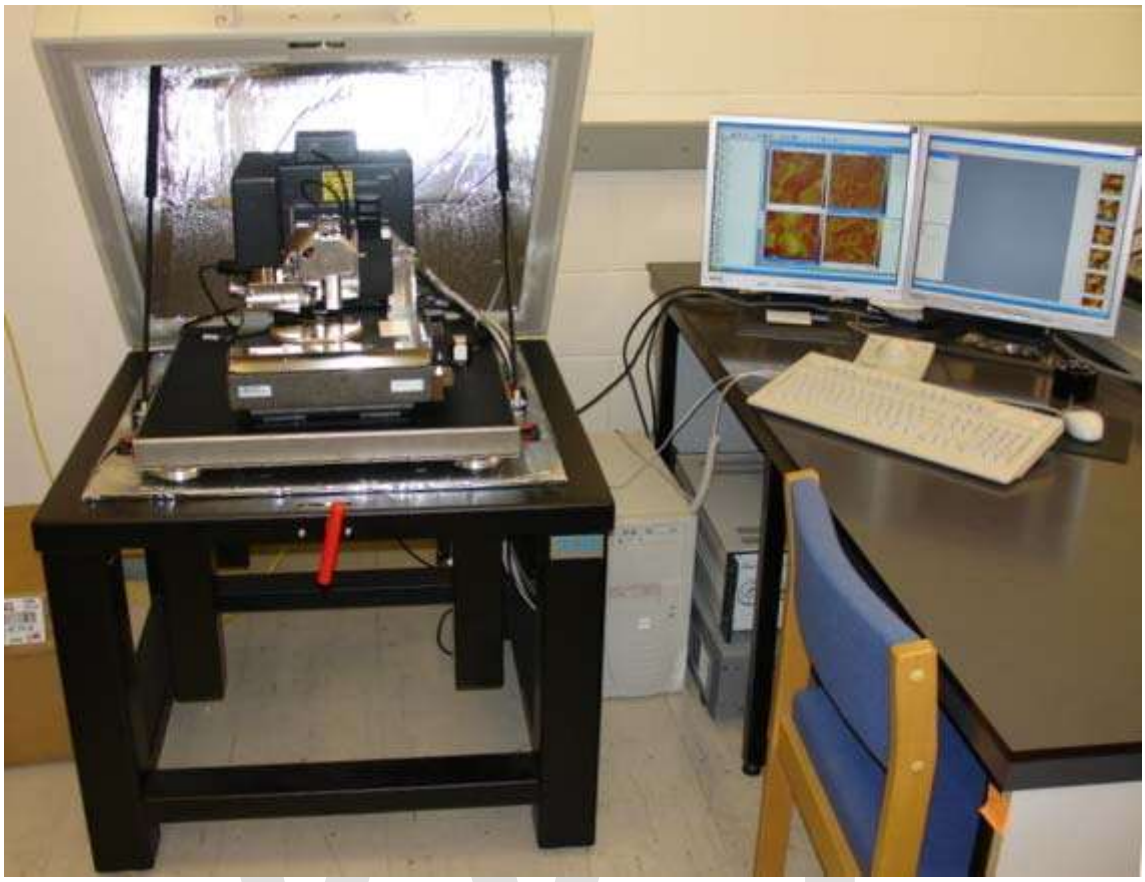

A commercial AFM setup

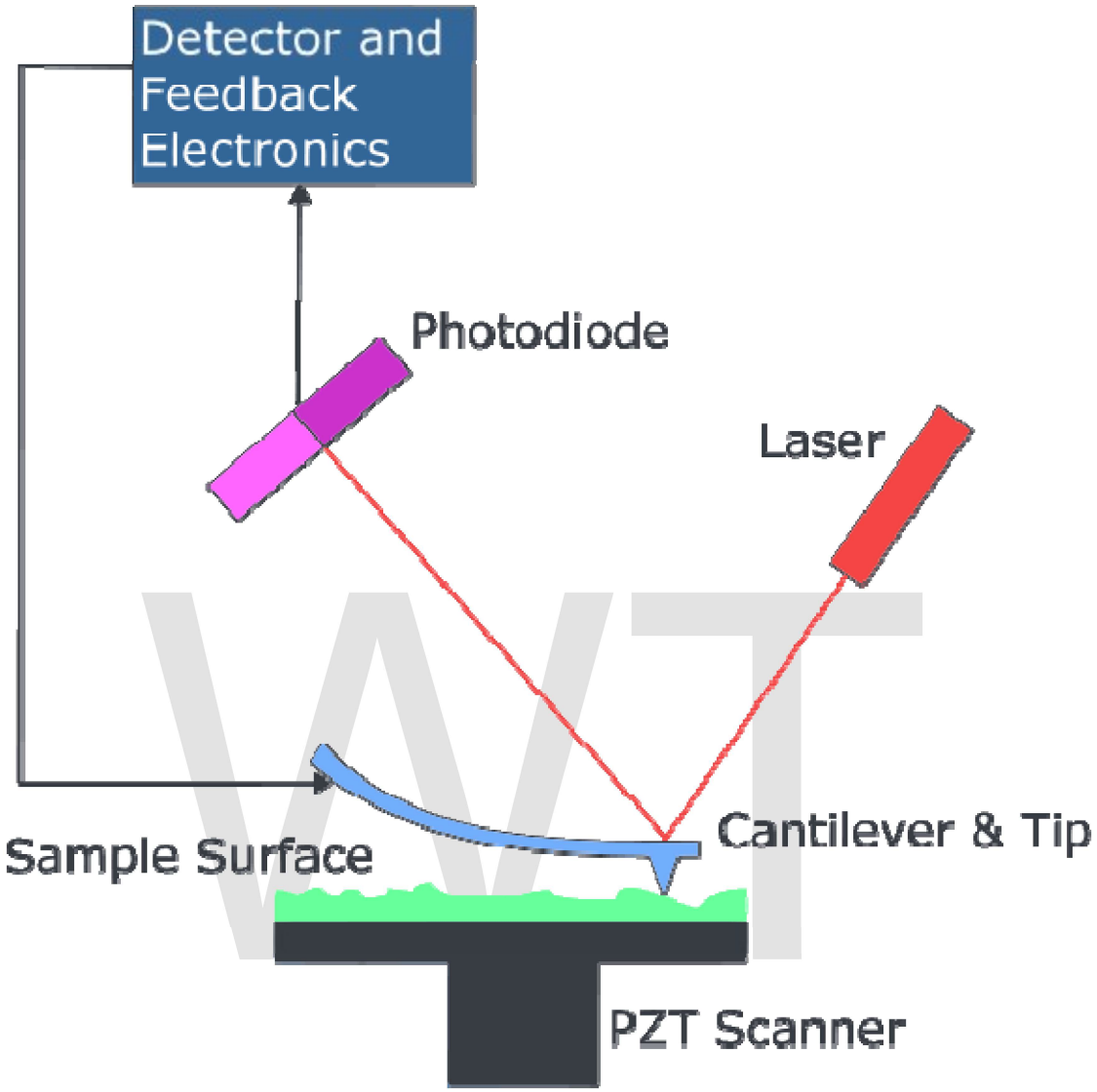

Block diagram of atomic force microscope

Atomic force microscopy (AFM) or scanning force microscopy (SFM) is a very high-resolution type of scanning probe microscopy, with demonstrated resolution on the order of fractions of a nanometer, more than 1000 times better than the optical diffraction limit. The precursor to the AFM, the scanning tunneling microscope, was developed by Gerd Binnig and Heinrich Rohrer in the early 1980s at IBM Research - Zurich, a development that earned them the Nobel Prize for Physics in 1986. Binnig, Quate and Gerber invented the first atomic force microscope (also abbreviated as AFM) in 1986. The first commercially available atomic force microscope was introduced in 1989. The AFM is one of the foremost tools for imaging, measuring, and manipulating matter at the nanoscale. The information is gathered by "feeling" the surface with a mechanical probe. Piezoelectric elements that facilitate tiny but accurate and precise movements on

(electronic) command enable the very precise scanning. In some variations, electric potentials can also be scanned using conducting cantilevers. In newer more advanced versions, currents can even be passed through the tip to probe the electrical conductivity or transport of the underlying surface, but this is much more challenging with very few groups reporting reliable data.

Basic principles

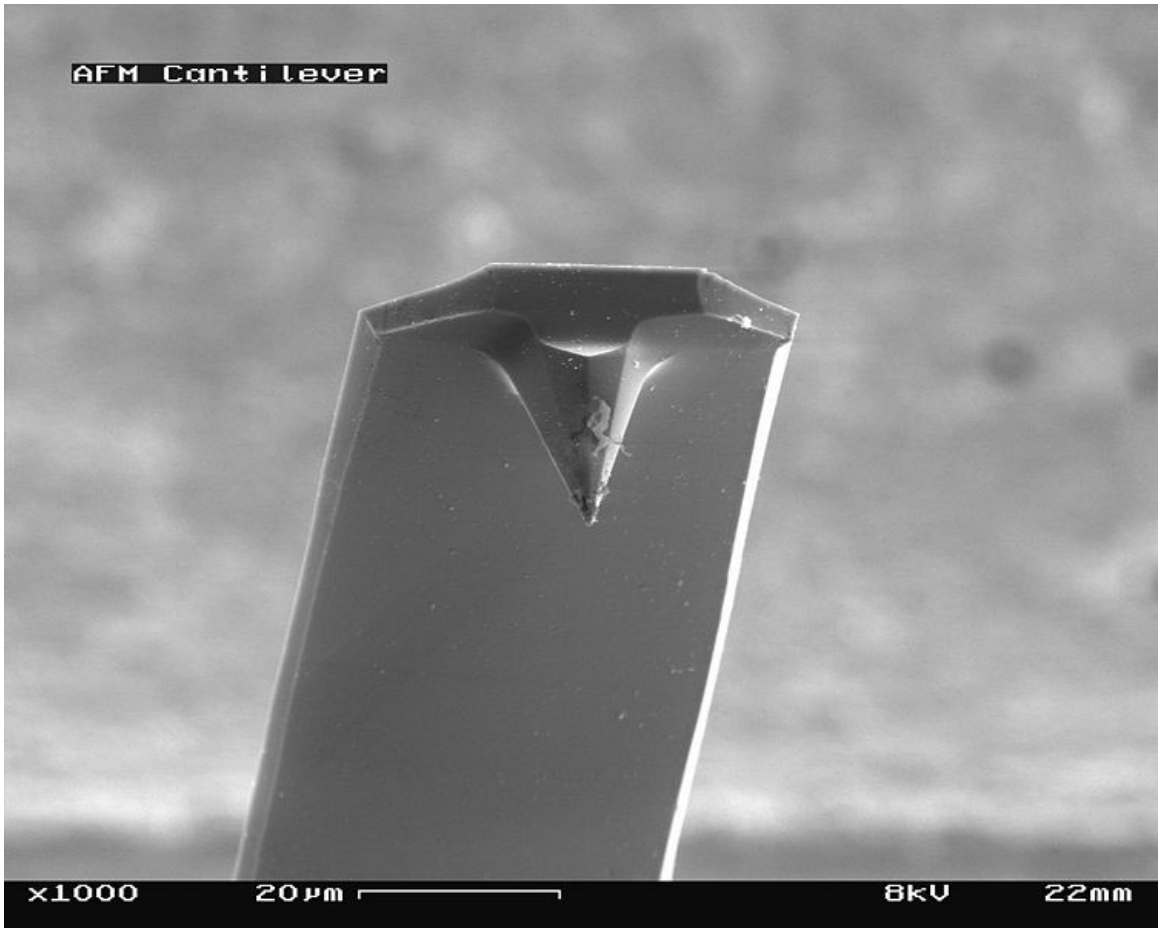

Electron micrograph of a used AFM cantilever image width ~100 micrometers...

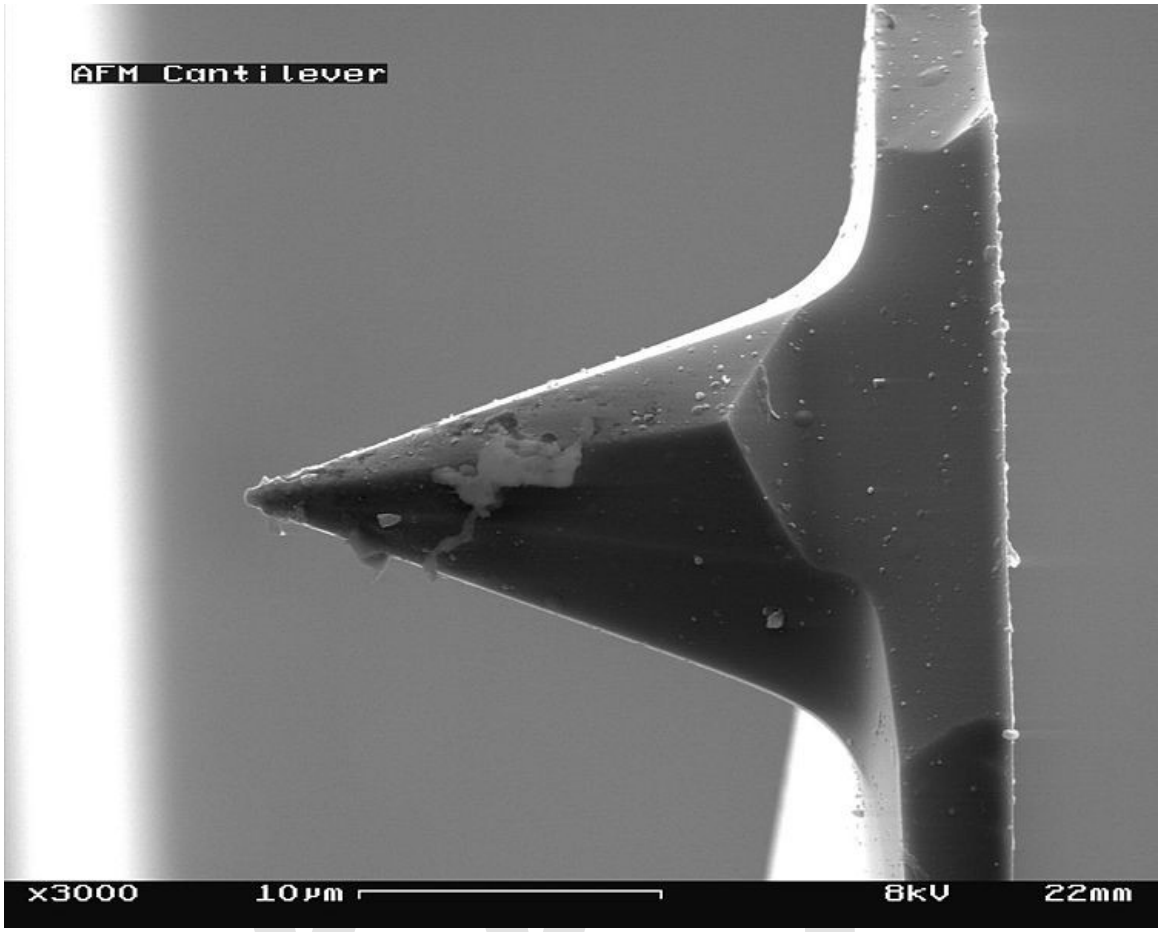

and ~30 micrometers

The AFM consists of a cantilever with a sharp tip (probe) at its end that is used to scan the specimen surface. The cantilever is typically silicon or silicon nitride with a tip radius of curvature on the order of nanometers. When the tip is brought into proximity of a sample surface, forces between the tip and the sample lead to a deflection of the cantilever according to Hooke's law. Depending on the situation, forces that are measured in AFM include mechanical contact force, van der Waals forces, capillary forces, chemical bonding, electrostatic forces, magnetic forces, Casimir forces, solvation forces, etc. Along with force, additional quantities may simultaneously be measured through the use of specialized types of probe. Typically, the deflection is measured using a laser spot reflected from the top surface of the cantilever into an array of photodiodes. Other methods that are used include optical interferometry, capacitive sensing or piezoresistive AFM cantilevers. These cantilevers are fabricated with piezoresistive elements that act as a strain gauge. Using a Wheatstone bridge, strain in the AFM cantilever due to deflection can be measured, but this method is not as sensitive as laser deflection or interferometry.

If the tip was scanned at a constant height, a risk would exist that the tip collides with the surface, causing damage. Hence, in most cases a feedback mechanism is employed to adjust the tip-to-sample distance to maintain a constant force between the tip and the sample. Traditionally, the sample is mounted on a piezoelectric tube, that can move the

sample in the *z* direction for maintaining a constant force, and the *x* and *y* directions for scanning the sample. Alternatively a 'tripod' configuration of three piezo crystals may be employed, with each responsible for scanning in the x,y and z directions. This eliminates some of the distortion effects seen with a tube scanner. In newer designs, the tip is mounted on a vertical piezo scanner while the sample is being scanned in X and Y using another piezo block. The resulting map of the area $s = f(x,y)$ represents the topography of the sample.

The AFM can be operated in a number of modes, depending on the application. In general, possible imaging modes are divided into static (also called *contact*) modes and a variety of dynamic (or non-contact) modes where the cantilever is vibrated.

Imaging modes

The primary modes of operation for an AFM are static mode and dynamic mode. In static mode, the cantilever is "dragged" across the surface of the sample and the contours of the surface are measured directly using the deflection of the cantilever. In the dynamic mode, the cantilever is externally oscillated at or close to its fundamental resonance frequency or a harmonic. The oscillation amplitude, phase and resonance frequency are modified by tip-sample interaction forces. These changes in oscillation with respect to the external reference oscillation provide information about the sample's characteristics.

Contact mode

In the static mode operation, the static tip deflection is used as a feedback signal. Because the measurement of a static signal is prone to noise and drift, low stiffness cantilevers are used to boost the deflection signal. However, close to the surface of the sample, attractive forces can be quite strong, causing the tip to "snap-in" to the surface. Thus static mode AFM is almost always done in contact where the overall force is repulsive. Consequently, this technique is typically called "contact mode". In contact mode, the force between the tip and the surface is kept constant during scanning by maintaining a constant deflection.

Non-contact mode

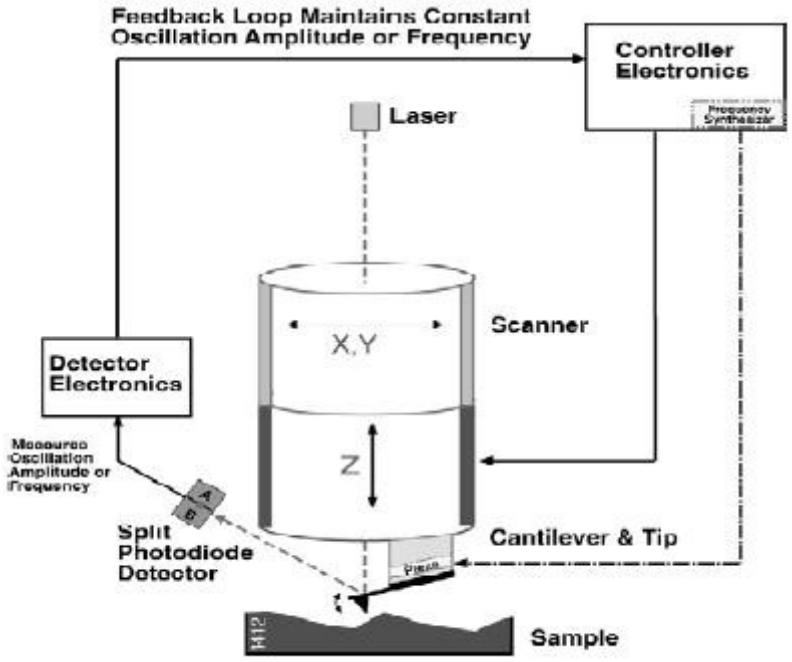

AFM - non-contact mode

In this mode, the tip of the cantilever does not contact the sample surface. The cantilever is instead oscillated at a frequency slightly above its resonance frequency where the amplitude of oscillation is typically a few nanometers (<10 nm). The van der Waals forces, which are strongest from 1 nm to 10 nm above the surface, or any other long range force which extends above the surface acts to decrease the resonance frequency of the cantilever. This decrease in resonance frequency combined with the feedback loop system maintains a constant oscillation amplitude or frequency by adjusting the average tip-to-sample distance. Measuring the tip-to-sample distance at each (x,y) data point allows the scanning software to construct a topographic image of the sample surface.

Non-contact mode AFM does not suffer from tip or sample degradation effects that are sometimes observed after taking numerous scans with contact AFM. This makes non-contact AFM preferable to contact AFM for measuring soft samples. In the case of rigid samples, contact and non-contact images may look the same. However, if a few monolayers of adsorbed fluid are lying on the surface of a rigid sample, the images may look quite different. An AFM operating in contact mode will penetrate the liquid layer to image the underlying surface, whereas in non-contact mode an AFM will oscillate above the adsorbed fluid layer to image both the liquid and surface.

Schemes for dynamic mode operation include frequency modulation and the more common amplitude modulation. In frequency modulation, changes in the oscillation frequency provide information about tip-sample interactions. Frequency can be measured with very high sensitivity and thus the frequency modulation mode allows for the use of

very stiff cantilevers. Stiff cantilevers provide stability very close to the surface and, as a result, this technique was the first AFM technique to provide true atomic resolution in ultra-high vacuum conditions.

In amplitude modulation, changes in the oscillation amplitude or phase provide the feedback signal for imaging. In amplitude modulation, changes in the phase of oscillation can be used to discriminate between different types of materials on the surface. Amplitude modulation can be operated either in the non-contact or in the intermittent contact regime. In dynamic contact mode, the cantilever is oscillated such that the separation distance between the cantilever tip and the sample surface is modulated.

Amplitude modulation has also been used in the non-contact regime to image with atomic resolution by using very stiff cantilevers and small amplitudes in an ultra-high vacuum environment.

Tapping mode

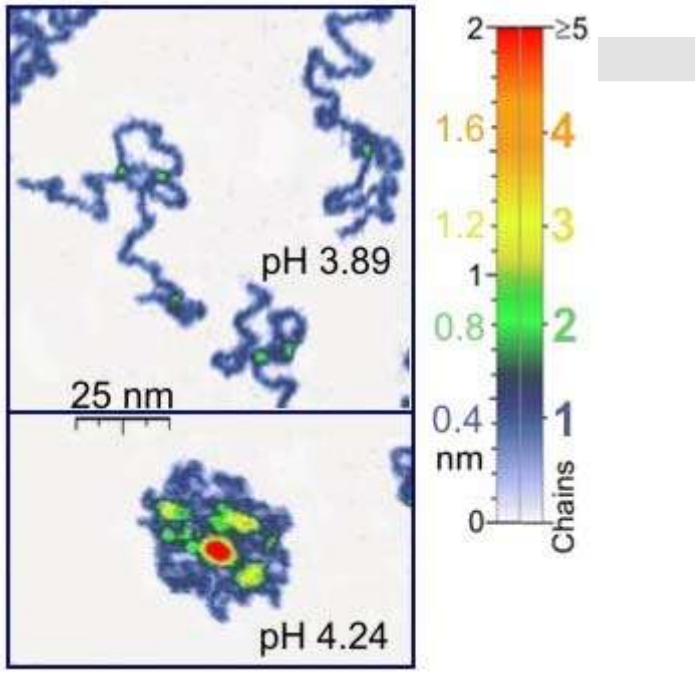

Single polymer chains (0.4 nm thick) recorded in a tapping mode under aqueous media with different pH.

In ambient conditions, most samples develop a liquid meniscus layer. Because of this, keeping the probe tip close enough to the sample for short-range forces to become detectable while preventing the tip from sticking to the surface presents a major problem for non-contact dynamic mode in ambient conditions. Dynamic contact mode (also called intermittent contact or tapping mode) was developed to bypass this problem.

In *tapping mode*, the cantilever is driven to oscillate up and down at near its resonance frequency by a small piezoelectric element mounted in the AFM tip holder similar to

non-contact mode. However, the amplitude of this oscillation is greater than 10 nm, typically 100 to 200 nm. Due to the interaction of forces acting on the cantilever when the tip comes close to the surface, Van der Waals force, dipole-dipole interaction, electrostatic forces, etc. cause the amplitude of this oscillation to decrease as the tip gets closer to the sample. An electronic servo uses the piezoelectric actuator to control the height of the cantilever above the sample. The servo adjusts the height to maintain a set cantilever oscillation amplitude as the cantilever is scanned over the sample. A *tapping AFM* image is therefore produced by imaging the force of the intermittent contacts of the tip with the sample surface.

This method of "tapping" lessens the damage done to the surface and the tip compared to the amount done in contact mode. Tapping mode is gentle enough even for the visualization of supported lipid bilayers or adsorbed single polymer molecules (for instance, 0.4 nm thick chains of synthetic polyelectrolytes) under liquid medium. With proper scanning parameters, the conformation of single molecules can remain unchanged for hours.

AFM cantilever deflection measurement

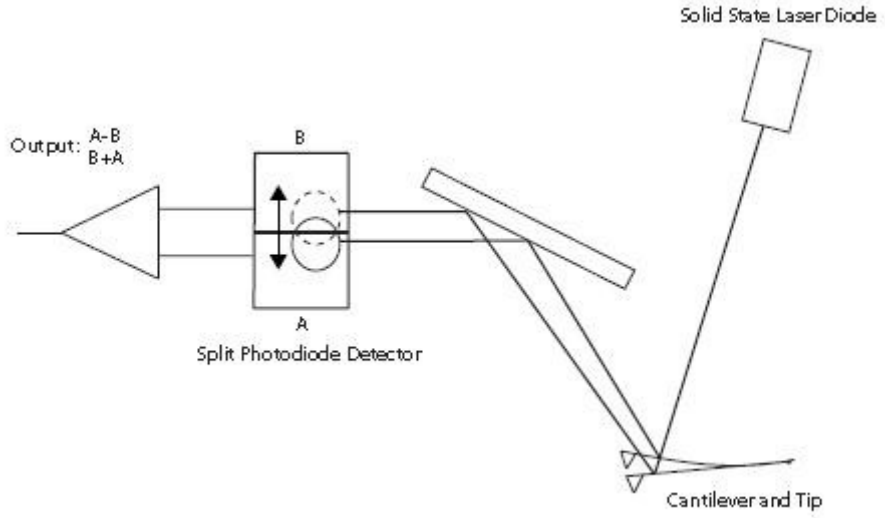

AFM beam deflection detection

Laser light from a solid state diode is reflected off the back of the cantilever and collected by a position sensitive detector (PSD) consisting of two closely spaced photodiodes whose output signal is collected by a differential amplifier. Angular displacement of cantilever results in one photodiode collecting more light than the other photodiode, producing an output signal (the difference between the photodiode signals normalized by their sum) which is proportional to the deflection of the cantilever. It detects cantilever deflections <10 nm (thermal noise limited). A long beam path (several centimeters) amplifies changes in beam angle.

Force spectroscopy

Another major application of AFM (besides imaging) is force spectroscopy, the direct measurement of tip-sample interaction forces as a function of the gap between the tip and sample (the result of this measurement is called a force-distance curve). For this method, the AFM tip is extended towards and retracted from the surface as the deflection of the cantilever is monitored as a function of piezoelectric displacement. These measurements have been used to measure nanoscale contacts, atomic bonding, Van der Waals forces, and Casimir forces, dissolution forces in liquids and single molecule stretching and rupture forces. Furthermore, AFM was used to measure in aqueous environment dispersion force due to polymer adsorbed on the substrate. Forces of the order of a few piconewtons can now be routinely measured with a vertical distance resolution of better than 0.1 nanometers. Force spectroscopy can be performed with either static or dynamic modes. In dynamic modes, information about the cantilever vibration is monitored in addition to the static deflection.

Problems with the technique include no direct measurement of the tip-sample separation and the common need for low stiffness cantilevers which tend to 'snap' to the surface. The snap-in can be reduced by measuring in liquids or by using stiffer cantilevers, but in the latter case a more sensitive deflection sensor is needed. By applying a small dither to the tip, the stiffness (force gradient) of the bond can be measured as well.

Identification of individual surface atoms

The AFM can be used to image and manipulate atoms and structures on a variety of surfaces. The atom at the apex of the tip "senses" individual atoms on the underlying surface when it forms incipient chemical bonds with each atom. Because these chemical interactions subtly alter the tip's vibration frequency, they can be detected and mapped. This principle was used to distinguish between atoms of silicon, tin and lead on an alloy surface, by comparing these 'atomic fingerprints' to values obtained from large-scale density functional theory (DFT) simulations.

The trick is to first measure these forces precisely for each type of atom expected in the sample, and then to compare with forces given by DFT simulations. The team found that the tip interacted most strongly with silicon atoms, and interacted 23% and 41% less strongly with tin and lead atoms, respectively. Thus, each different type of atom can be identified in the matrix as the tip is moved across the surface.

Such a technique has been used now in biology and extended recently to cell biology. Forces corresponding to (i) the unbinding of receptor ligand couples (ii) unfolding of proteins (iii) cell adhesion at single cell scale have been gathered.

Advantages and disadvantages

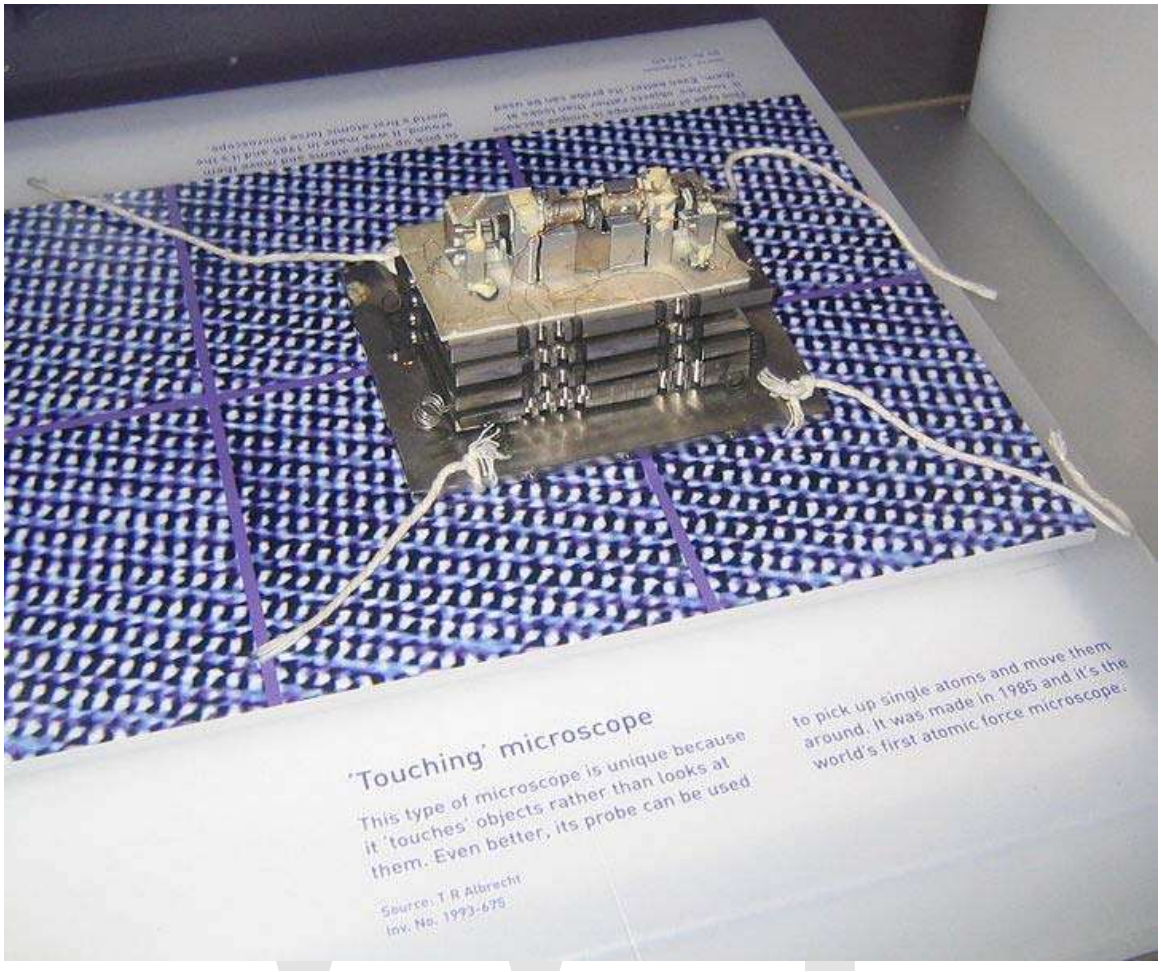

The first atomic force microscope

Just like any other tool, an AFM's usefulness has limitations. When determining whether or not analyzing a sample with an AFM is appropriate, there are various advantages and disadvantages that must be considered.

Advantages

AFM has several advantages over the scanning electron microscope (SEM). Unlike the electron microscope which provides a two-dimensional projection or a two-dimensional image of a sample, the AFM provides a three-dimensional surface profile. Additionally, samples viewed by AFM do not require any special treatments (such as metal/carbon coatings) that would irreversibly change or damage the sample. While an electron microscope needs an expensive vacuum environment for proper operation, most AFM modes can work perfectly well in ambient air or even a liquid environment. This makes it possible to study biological macromolecules and even living organisms. In principle, AFM can provide higher resolution than SEM. It has been shown to give true atomic resolution in ultra-high vacuum (UHV) and, more recently, in liquid environments. High

resolution AFM is comparable in resolution to scanning tunneling microscopy and transmission electron microscopy.

Disadvantages

A disadvantage of AFM compared with the scanning electron microscope (SEM) is the single scan image size. In one pass, the SEM can image an area on the order of square millimeters with a depth of field on the order of millimeters. Whereas the AFM can only image a maximum height on the order of 10-20 micrometers and a maximum scanning area of about 150×150 micrometers. One method of improving the scanned area size for AFM is by using parallel probes in a fashion similar to that of millipede data storage.

The scanning speed of an AFM is also a limitation. Traditionally, an AFM cannot scan images as fast as a SEM, requiring several minutes for a typical scan, while a SEM is capable of scanning at near real-time, although at relatively low quality. The relatively slow rate of scanning during AFM imaging often leads to thermal drift in the image making the AFM microscope less suited for measuring accurate distances between topographical features on the image. However, several fast-acting designs were suggested to increase microscope scanning productivity including what is being termed videoAFM (reasonable quality images are being obtained with videoAFM at video rate: faster than the average SEM). To eliminate image distortions induced by thermal drift, several methods have been introduced.

AFM images can also be affected by hysteresis of the piezoelectric material and cross-talk between the *x*, *y*, *z* axes that may require software enhancement and filtering. Such filtering could "flatten" out real topographical features. However, newer AFMs utilize closed-loop scanners which practically eliminate these problems. Some AFMs also use separated orthogonal scanners (as opposed to a single tube) which also serve to eliminate part of the cross-talk problems.

As with any other imaging technique, there is the possibility of image artifacts, which could be induced by an unsuitable tip, a poor operating environment, or even by the sample itself. These image artifacts are unavoidable however, their occurrence and effect on results can be reduced through various methods.

Due to the nature of AFM probes, they cannot normally measure steep walls or overhangs. Specially made cantilevers and AFMs can be used to modulate the probe sideways as well as up and down (as with dynamic contact and non-contact modes) to measure sidewalls, at the cost of more expensive cantilevers, lower lateral resolution and additional artifacts.

Piezoelectric scanners

AFM scanners are made from piezoelectric material, which expands and contracts proportionally to an applied voltage. Whether they elongate or contract depends upon the polarity of the voltage applied. The scanner is constructed by combining independently

operated piezo electrodes for X, Y, and Z into a single tube, forming a scanner which can manipulate samples and probes with extreme precision in 3 dimensions.

Scanners are characterized by their sensitivity which is the ratio of piezo movement to piezo voltage, i.e., by how much the piezo material extends or contracts per applied volt. Because of differences in material or size, the sensitivity varies from scanner to scanner. Sensitivity varies non-linearly with respect to scan size. Piezo scanners exhibit more sensitivity at the end than at the beginning of a scan. This causes the forward and reverse scans to behave differently and display hysteresis between the two scan directions. This can be corrected by applying a non-linear voltage to the piezo electrodes to cause linear scanner movement and calibrating the scanner accordingly.

The sensitivity of piezoelectric materials decreases exponentially with time. This causes most of the change in sensitivity to occur in the initial stages of the scanner's life. Piezoelectric scanners are run for approximately 48 hours before they are shipped from the factory so that they are past the point where they may have large changes in sensitivity. As the scanner ages, the sensitivity will change less with time and the scanner would seldom require recalibration.

Chapter- 2

Scanning Tunneling Microscope

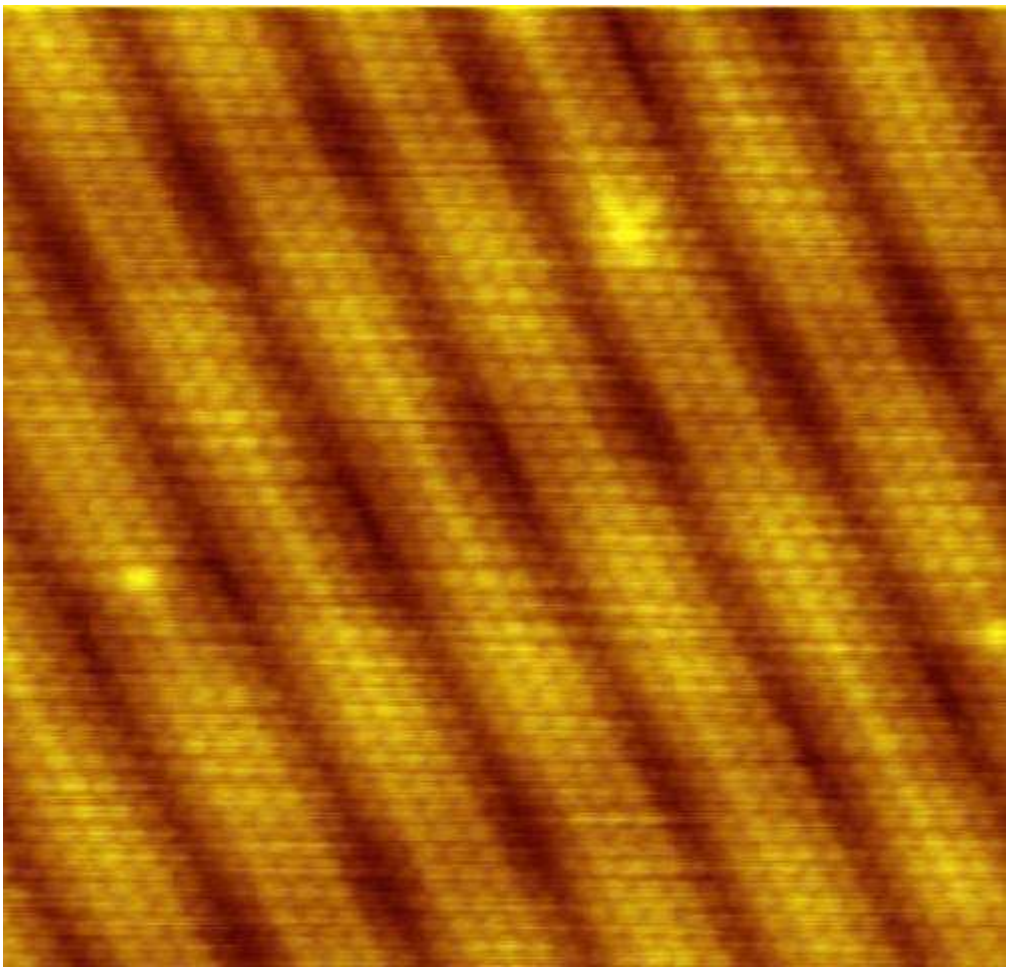

Image of reconstruction on a clean Gold(100) surface

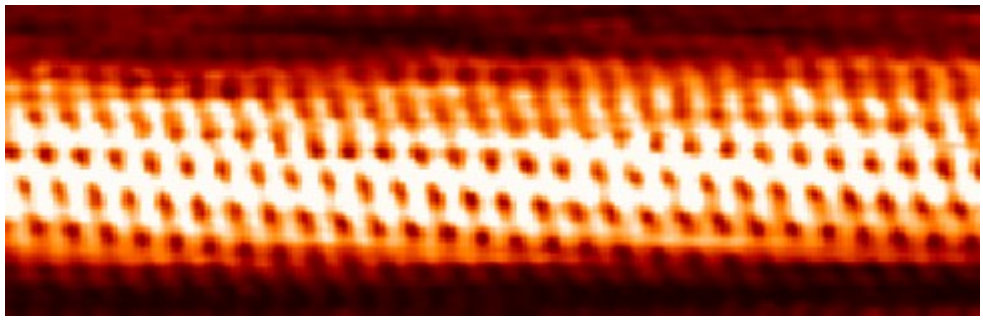

An STM image of single-walled carbon nanotube

A **scanning tunneling microscope** (STM) is an instrument for imaging surfaces at the atomic level. Its development in 1981 earned its inventors, Gerd Binnig and Heinrich Rohrer (at IBM Zürich), the Nobel Prize in Physics in 1986. For an STM, good resolution is considered to be 0.1 nm lateral resolution and 0.01 nm depth resolution. With this resolution, individual atoms within materials are routinely imaged and manipulated. The STM can be used not only in ultra high vacuum but also in air, water, and various other liquid or gas ambients, and at temperatures ranging from near zero kelvin to a few hundred degrees Celsius.

The STM is based on the concept of quantum tunneling. When a conducting tip is brought very near to the surface to be examined, a bias (voltage difference) applied between the two can allow electrons to tunnel through the vacuum between them. The resulting *tunneling current* is a function of tip position, applied voltage, and the local density of states (LDOS) of the sample. Information is acquired by monitoring the current as the tip's position scans across the surface, and is usually displayed in image form. STM can be a challenging technique, as it requires extremely clean and stable surfaces, sharp tips, excellent vibration control, and sophisticated electronics.

Procedure

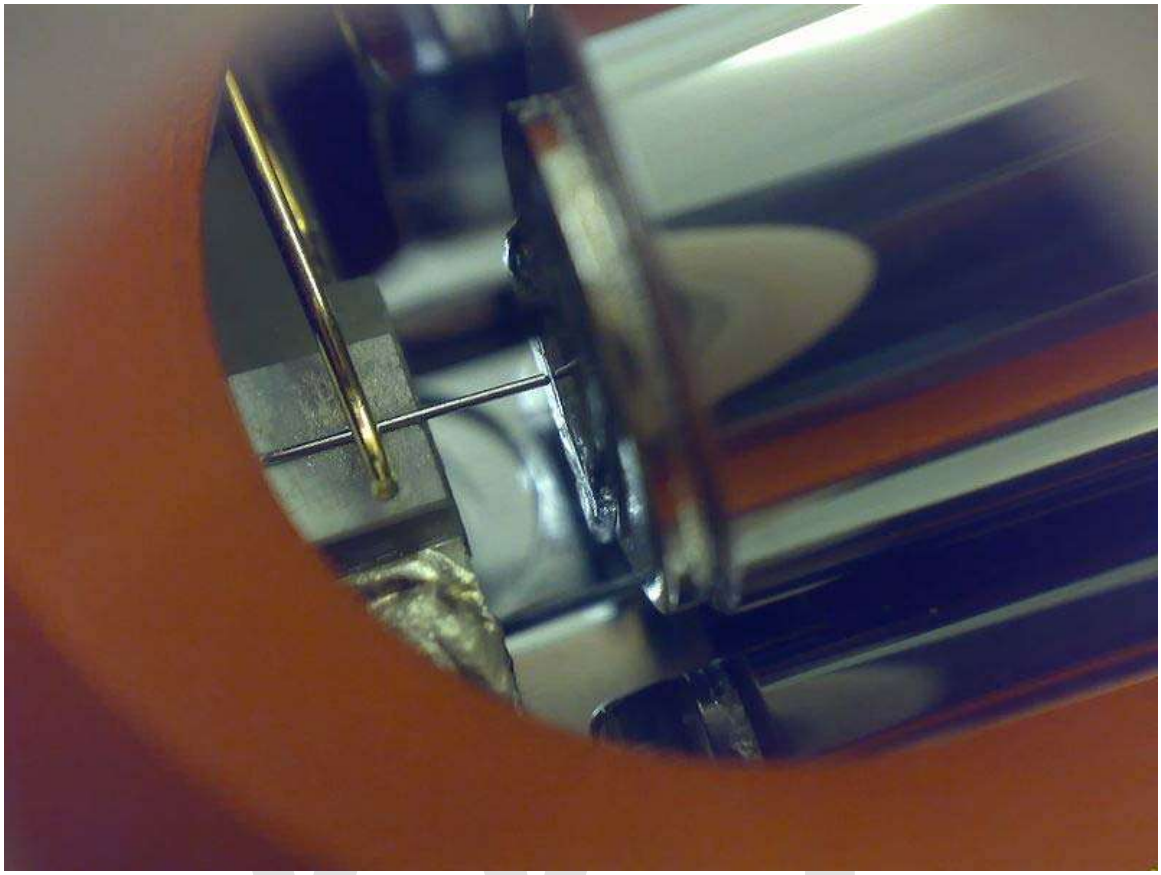

A close-up of a simple scanning tunneling microscope head using a platinum-iridium stylus.

First, a voltage bias is applied and the tip is brought close to the sample by some coarse sample-to-tip control, which is turned off when the tip and sample are sufficiently close. At close range, fine control of the tip in all three dimensions when near the sample is typically piezoelectric, maintaining tip-sample separation W typically in the 4-7 Å range, which is the equilibrium position between attractive (3<W<10Å) and repulsive (W<3Å) interactions. In this situation, the voltage bias will cause electrons to tunnel between the tip and sample, creating a current that can be measured. Once tunneling is established, the tip's bias and position with respect to the sample can be varied (with the details of this variation depending on the experiment) and data is obtained from the resulting changes in current.

If the tip is moved across the sample in the x-y plane, the changes in surface height and density of states cause changes in current. These changes are mapped in images. This change in current with respect to position can be measured itself, or the height, z, of the tip corresponding to a constant current can be measured. These two modes are called constant height mode and constant current mode, respectively. In constant current mode, feedback electronics adjust the height by a voltage to the piezoelectric height control mechanism. This leads to a height variation and thus the image comes from the tip

topography across the sample and gives a constant charge density surface; this means contrast on the image is due to variations in charge density. In constant height mode, the voltage and height are both held constant while the current changes to keep the voltage from changing; this leads to an image made of current changes over the surface, which can be related to charge density. The benefit to using a constant height mode is that it is faster, as the piezoelectric movements require more time to register the change in constant current mode than the voltage response in constant height mode. All images produced by STM are grayscale, with color optionally added in post-processing in order to visually emphasize important features.

In addition to scanning across the sample, information on the electronic structure at a given location in the sample can be obtained by sweeping voltage and measuring current at a specific location. This type of measurement is called scanning tunneling spectroscopy (STS) and typically results in a plot of the local density of states as a function of energy within the sample. The advantage of STM over other measurements of the density of states lies in its ability to make extremely local measurements: for example, the density of states at an impurity site can be compared to the density of states far from impurities.

Framerates of at least 1 Hz enable so called Video-STM (up to 50 Hz is possible). This can be used to scan surface diffusion.

Instrumentation

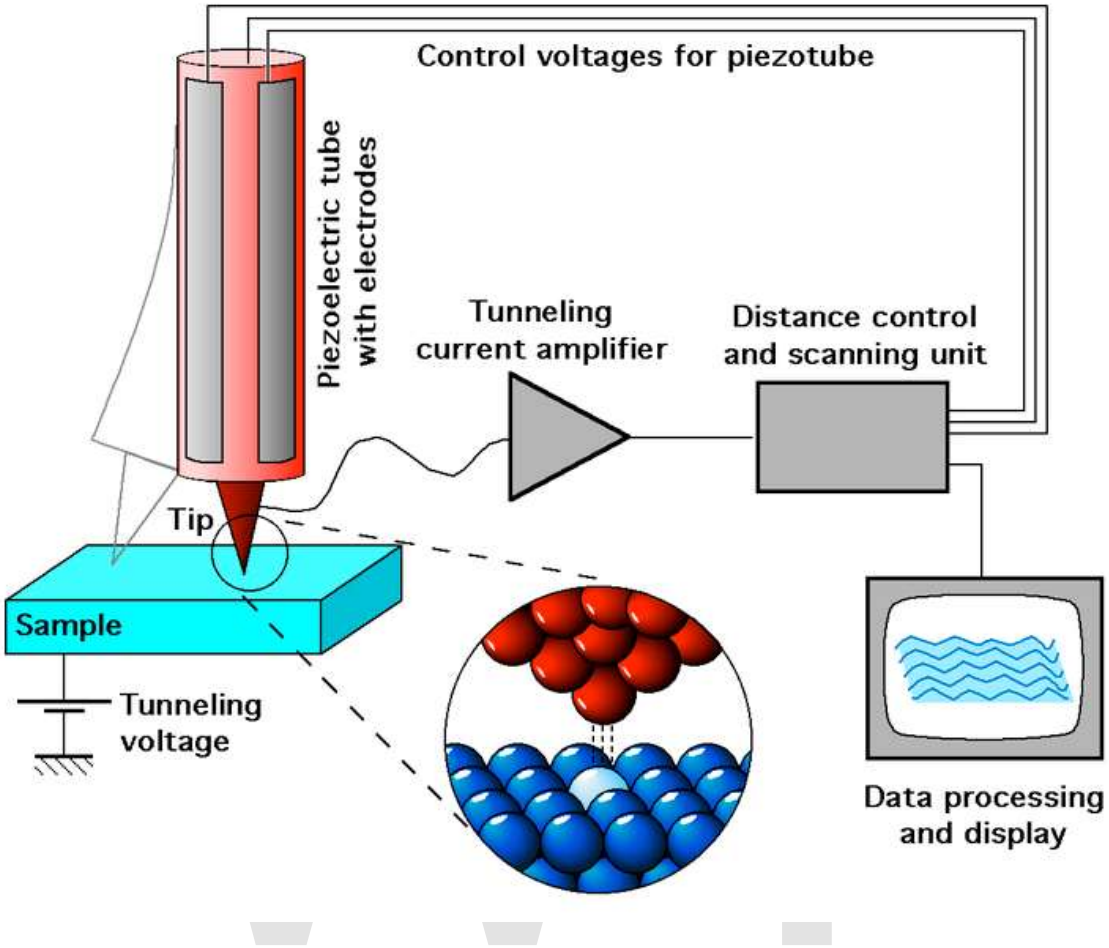

Schematic view of an STM

The components of an STM include scanning tip, piezoelectric controlled height and x,y scanner, coarse sample-to-tip control, vibration isolation system, and computer.

The resolution of an image is limited by the radius of curvature of the scanning tip of the STM. Additionally, image artifacts can occur if the tip has two tips at the end rather than a single atom; this leads to “double-tip imaging,” a situation in which both tips contribute to the tunneling. Therefore it has been essential to develop processes for consistently obtaining sharp, usable tips. Recently, carbon nanotubes have been used in this instance.

The tip is often made of tungsten or platinum-iridium, though gold is also used. Tungsten tips are usually made by electrochemical etching, and platinum-iridium tips by mechanical shearing.

Due to the extreme sensitivity of tunnel current to height, proper vibration isolation or an extremely rigid STM body is imperative for obtaining usable results. In the first STM by Binnig and Rohrer, magnetic levitation was used to keep the STM free from vibrations;

now mechanical spring or gas spring systems are often used. Additionally, mechanisms for reducing eddy currents are sometimes implemented.

Maintaining the tip position with respect to the sample, scanning the sample and acquiring the data is computer controlled. The computer may also be used for enhancing the image with the help of image processing as well as performing quantitative measurements.

Other STM related studies

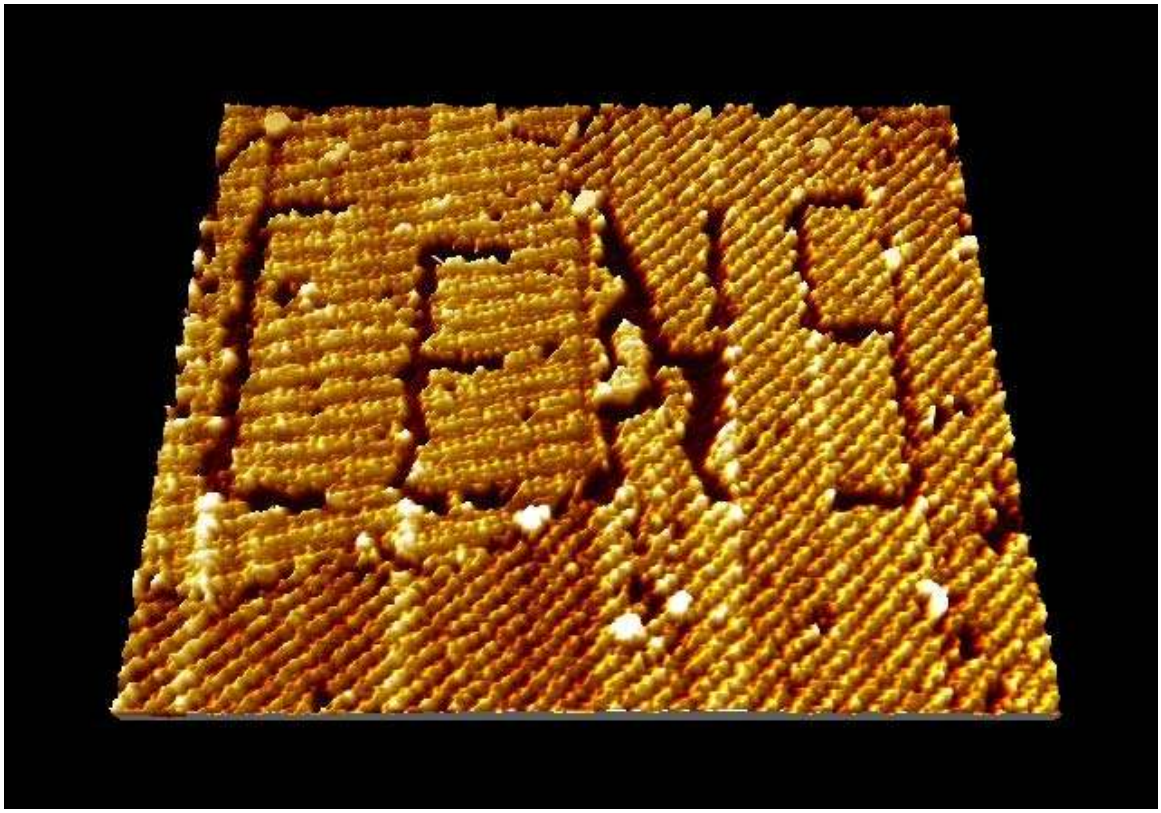

Nanomanipulation via STM of a self-assembled organic semiconductor monolayer (here: PTCDA molecules) on graphite, in which the logo of the Center for NanoScience (CeNS), LMU has been written.

Many other microscopy techniques have been developed based upon STM. These include photon scanning microscopy (PSTM), which uses an optical tip to tunnel photons; scanning tunneling potentiometry (STP), which measures electric potential across a surface; spin polarized scanning tunneling microscopy (SPSTM), which uses a ferromagnetic tip to tunnel spin-polarized electrons into a magnetic sample, and atomic force microscopy (AFM), in which the force caused by interaction between the tip and sample is measured.

Other STM methods involve manipulating the tip in order to change the topography of the sample. This is attractive for several reasons. Firstly the STM has an atomically

precise positioning system which allows very accurate atomic scale manipulation. Furthermore, after the surface is modified by the tip, it is a simple matter to then image with the same tip, without changing the instrument. IBM researchers developed a way to manipulate Xenon atoms absorbed on a nickel surface This technique has been used to create electron "corrals" with a small number of adsorbed atoms, which allows the STM to be used to observe electron Friedel oscillations on the surface of the material. Aside from modifying the actual sample surface, one can also use the STM to tunnel electrons into a layer of E-Beam photoresist on a sample, in order to do lithography. This has the advantage of offering more control of the exposure than traditional Electron beam lithography. Another practical application of STM is atomic deposition of metals (Au, Ag, W, etc.) with any desired (pre-programmed) pattern, which can be used as contacts to nanodevices or as nanodevices themselves.

Recently groups have found they can use the STM tip to rotate individual bonds within single molecules. The electrical resistance of the molecule depends on the orientation of the bond, so the molecule effectively becomes a molecular switch.

Principle of operation

Tunneling is a functioning concept that arises from quantum mechanics. Classically, an object hitting an impenetrable barrier will not pass through. In contrast, objects with a very small mass, such as the electron, have wavelike characteristics which permit such an event, referred to as tunneling.

Electrons behave as beams of energy, and in the presence of a potential $U(z)$, assuming 1-dimensional case, the energy levels $\psi_n(z)$ of the electrons are given by solutions to Schrödinger's equation,

$$-\frac{\hbar^2}{2m}\frac{\partial^2\psi_n(z)}{\partial z^2} + U(z)\psi_n(z) = E\psi_n(z),$$

where $\hbar$ is the reduced Planck's constant, z is the position, and m is the mass of an electron. If an electron of energy E is incident upon an energy barrier of height $U(z)$, the electron wave function is a traveling wave solution,

$$\psi_n(z) = \psi_n(0)e^{\pm ikz},$$

where

$$k = \frac{\sqrt{2m(E - U(z))}}{\hbar}$$

if $E > U(z)$, which is true for a wave function inside the tip or inside the sample. Inside a barrier, $E < U(z)$ so the wave functions which satisfy this are decaying waves,

$$\psi_n(z) = \psi_n(0)e^{\pm\kappa z},$$

where

$$\kappa = \frac{\sqrt{2m(U-E)}}{\hbar}$$

quantifies the decay of the wave inside the barrier, with the barrier in the +*z* direction for $-\kappa$.

Knowing the wave function allows one to calculate the probability density for that electron to be found at some location. In the case of tunneling, the tip and sample wave functions overlap such that when under a bias, there is some finite probability to find the electron in the barrier region and even on the other side of the barrier. Let us assume the bias is *V* and the barrier width is *W*. This probability, *P*, that an electron at *z*=0 (left edge of barrier) can be found at *z*=*W* (right edge of barrier) is proportional to the wave function squared,

$$P \propto |\psi_n(0)|^2 e^{-2\kappa W}.$$

If the bias is small, we can let $U - E \approx \varphi M$ in the expression for κ, where φM, the work function, gives the minimum energy needed to bring an electron from an occupied level, the highest of which is at the Fermi level (for metals at *T*=0 kelvins), to vacuum level. When a small bias *V* is applied to the system, only electronic states very near the Fermi level, within *eV* (a product of electron charge and voltage, not to be confused here with electronvolt unit), are excited. These excited electrons can tunnel across the barrier. In other words, tunneling occurs mainly with electrons of energies near the Fermi level.

However, tunneling does require that there is an empty level of the same energy as the electron for the electron to tunnel into on the other side of the barrier. It is because of this restriction that the tunneling current can be related to the density of available or filled states in the sample. The current due to an applied voltage *V* (assume tunneling occurs sample to tip) depends on two factors: 1) the number of electrons between E_f and *eV* in the sample, and 2) the number among them which have corresponding free states to tunnel into on the other side of the barrier at the tip. The higher density of available states the greater the tunneling current. When *V* is positive, electrons in the tip tunnel into empty states in the sample; for a negative bias, electrons tunnel out of occupied states in the sample into the tip.

Mathematically, this tunneling current is given by

$$I \propto \sum_{E_f - eV}^{E_f} |\psi_n(0)|^2 e^{-2\kappa W}.$$

One can sum the probability over energies between $E_f - eV$ and eV to get the number of states available in this energy range per unit volume, thereby finding the local density of states (LDOS) near the Fermi level. The LDOS near some energy E in an interval ε is given by

$$\rho_s(z, E) = \frac{1}{\epsilon} \sum_{E-\epsilon}^{E} |\psi_n(z)|^2,$$

and the tunnel current at a small bias V is proportional to the LDOS near the Fermi level, which gives important information about the sample. It is desirable to use LDOS to express the current because this value does not change as the volume changes, while probability density does. Thus the tunneling current is given by

$$I \propto V \rho_s(0, E_f) e^{-2\kappa W}$$

where $\rho_s(0,E_f)$ is the LDOS near the Fermi level of the sample at the sample surface. This current can also be expressed in terms of the LDOS near the Fermi level of the sample at the tip surface,

$$I \propto V \rho_s(W, E_f) V$$

The exponential term in the above equations means that small variations in W greatly influence the tunnel current. If the separation is decreased by 1 Å, the current increases by an order of magnitude, and vice versa.

This approach fails to account for the *rate* at which electrons can pass the barrier. This rate should affect the tunnel current, so it can be treated using the Fermi's golden rule with the appropriate tunneling matrix element. John Bardeen solved this problem in his study of the metal-insulator-metal junction. He found that if he solved Schrödinger's equation for each side of the junction separately to obtain the wave functions ψ and χ for each electrode, he could obtain the tunnel matrix, M, from the overlap of these two wave functions. This can be applied to STM by making the electrodes the tip and sample, assigning ψ and χ as sample and tip wave functions, respectively, and evaluating M at some surface S between the metal electrodes, where z=0 at the sample surface and z=W at the tip surface.

Now, Fermi's Golden Rule gives the rate for electron transfer across the barrier, and is written

$$w = \frac{2\pi}{\hbar} |M|^2 \delta(E_\psi - E_\chi),$$

where $\delta(E_\psi - E_\chi)$ restricts tunneling to occur only between electron levels with the same energy. The tunnel matrix element, given by

$$M = \frac{\hbar}{2\pi} \int_{z=z_0} (\chi * \frac{\partial \psi}{\partial z} - \psi \frac{\partial \chi *}{\partial z}) dS$$,

is a description of the lower energy associated with the interaction of wave functions at the overlap, also called the resonance energy.

Summing over all the states gives the tunneling current as

$$I = \frac{4\pi e}{\hbar} \int_{-\infty}^{+\infty} [f(E_f - eV + \epsilon) - f(E_f + \epsilon)] \rho_s (E_f - eV + \epsilon) \rho_T (E_f + \epsilon) |M|^2 d\epsilon$$

where *f* is the Fermi function, ρ_s and ρ_T are the density of states in the sample and tip, respectively. The Fermi distribution function describes the filling of electron levels at a given temperature T.

Early invention

An earlier, similar invention, the *Topografiner* of R. Young, J. Ward, and F. Scire from the NIST , relied on field emission. However, Young is credited by the Nobel Committee as the person who realized that it should be possible to achieve better resolution by using the tunnel effect.

Chapter- 3

Magnetic Force Microscope

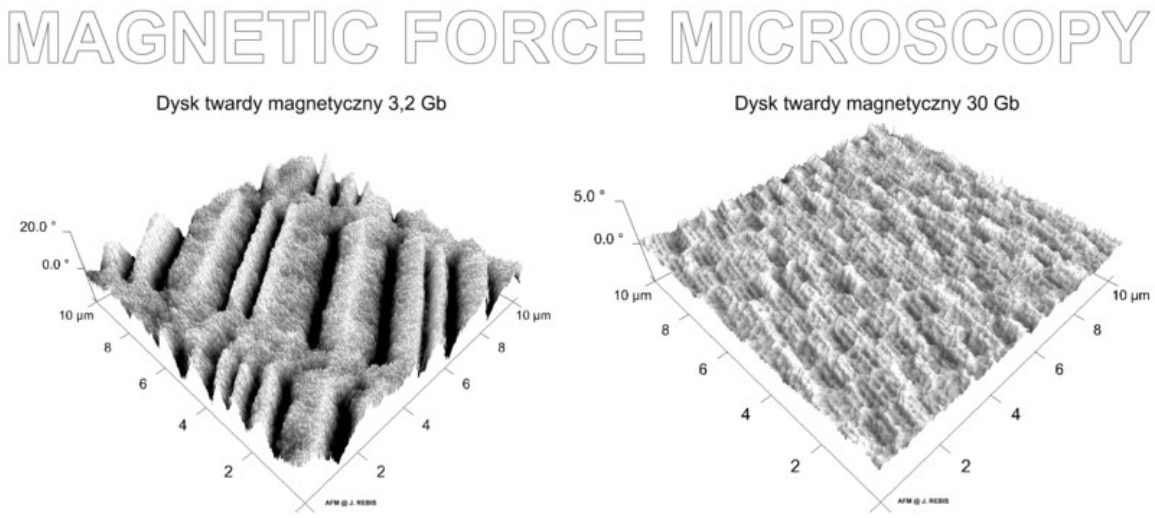

MFM images of 3.2 GB and 30 GB computer hard-drive surfaces.

Magnetic force microscope (MFM) is a variety of atomic force microscope, where a sharp magnetized tip is scanning the magnetic sample; the tip-sample magnetic interactions are detected and used to reconstruct the magnetic structure of the sample surface. Many kinds of magnetic interactions are measured by MFM, including magnetic dipole–dipole interaction. MFM scanning often uses non-contact AFM (NC-AFM) mode.

Overview

In MFM measurements, the magnetic force between the sample and the tip can be expressed as

$$\vec{F} = \mu_o(\vec{m} \cdot \nabla)\vec{H}$$

where $\vec{m}$ is the magnetic moment of the tip (approximated as a point dipole), $\vec{H}$ is the magnetic stray field from the sample surface, and μ_0 is the magnetic permeability of free space.

Because the stray magnetic field from the sample can affect the magnetic state of the tip, and vice versa, interpretation of the MFM measurement is not straightforward. For instance, the geometry of the tip magnetization must be known for quantitative analysis.

Typical resolution of 30 nm can be achieved, although resolutions as low as 10 to 20 nm are attainable.

Important dates

A boost in the interest to MFM resulted from the following inventions :

1982 - Scanning Tunneling Microscopy (STM)

- Tunneling current between the tip and sample is used as the signal.
- Both the tip and sample must be electrically conductive.

1986 - Atomic force microscopy (AFM)

- Forces (atomic/electrostatic) between the tip and sample are sensed from the deflections of a flexible lever (cantilever).
- The cantilever tip flies above the sample with a typical distance of tens of nanometers.

1987 - Magnetic Force Microscopy (MFM)

- Derives from AFM. The magnetic forces between the tip and sample are sensed.

- Image of the magnetic stray field is obtained by scanning the magnetized tip over the sample surface in a raster scan.

MFM components

The main components of an MFM system are: Piezoelectric scanning

- Moves the sample in an *x*, *y* and *z* directions.
- Voltage is applied to separate electrodes for different directions. Typically, a 1 volt potential results in 1 to 10 nm displacement.
- Image is put together by slowly scanning sample surface in a raster fashion.
- Scan areas range from a few to 200 micrometers.
- Imaging times range from a few minutes to 30 minutes.

- Restoring force constants on the cantilever range from 0.01 to 100 N/m depending on the material of the cantilever.

Magnetized tip at one end of a flexible lever (cantilever); generally an AFM probe with a magnetic coating.

- In the past, tips were made of etched magnetic metals such as nickel.
- Nowadays, tips are batch fabricated (tip-cantilever) using a combination of micromachining and photolithography. As a result, smaller tips are possible, and better mechanical control of the tip-cantilever is obtained.
- Cantilever can be made of single-crystalline silicon, silicon dioxide (SiO_2), or silicon nitride (Si_3N_4). The Si_3N_4 cantilever-tip modules are usually more durable and have smaller restoring force constants (k).
- Tips are coated with a thin (< 50 nm) magnetic film (such as Ni or Co), usually of high coercivity, so that the tip magnetic state (or magnetization M) does not change during the imaging.
- The tip-cantilever module is driven close to the resonance frequency by a piezoelectric crystal with typical frequencies ranging from 10 kHz to 1 MHz.

Scanning procedure

The scanning method when using an MFM is called the "lift height" method. When the tip scans the surface of a sample at close distances (< 100 nm), not only magnetic forces are sensed, but also atomic and electrostatic forces. The lift height method helps to enhance the magnetic contrast through the following:

- First, the topographic profile of each scan line is measured. That is, the tip is brought into a close proximity of the sample to take AFM measurements.
- The magnetized tip is then lifted further away from the sample.
- On the second pass, the magnetic signal is extracted.

Modes of operation

Static (DC) mode

- The stray field from the sample exerts a force on the magnetic tip. The force is detected by measuring the displacement of the cantilever by reflecting a laser beam from it.
- The cantilever end is either deflected away or towards the sample surface by a distance $\Delta z = F_z/k$ (perpendicular to the surface).
- *Static mode* corresponds to measurements of the cantilever deflection.
- Forces in the range of tens of piconewtons are normally measured.

Dynamic (AC) mode

- For small deflections, the tip-cantilever can be modeled as a damped harmonic oscillator with a proof mass (m) in [kg], an ideal spring constant (k) in [N/m], and a damper (D) in [N·s/m].
- If an external oscillating force F_z is applied to the cantilever, then the tip will be displaced by an amount z. Moreover, the displacement will also harmonically oscillate, but with a phase shift between applied force and displacement given by:

$$F_z = F_o \cos(\omega t),\ z = z_o \cos(\omega t + \theta)$$

where the amplitude and phase shifts are given by:

$$z_o = \frac{\frac{F_o}{m}}{\sqrt{(\omega_n^2 - \omega^2) + (\frac{\omega_n \omega}{Q})^2}},\ \theta = \arctan\left[\frac{\omega_n \omega}{Q(\omega_n^2 - \omega^2)}\right]$$

Here the quality factor of resonance, resonance angular frequency, and damping factor are:

$$Q = 2\pi \frac{\frac{1}{2}kz_o^2}{\pi D z_o^2 \omega_n} = \frac{1}{2\delta},\ \omega_n = \sqrt{\frac{k}{m}},\ \delta = \frac{D}{2\sqrt{mk}}$$

- Dynamic mode of operation refers to measurements of the shifts in the resonance frequency.
- The cantilever is driven to its resonance frequency and frequency shifts are detected.
- Assuming small vibration amplitudes (which is generally true in MFM measurements), to a first-order approximation, the resonance frequency can be related to the natural frequency and the force gradient. That is, the shift in the resonance frequency is a result of changes in the spring constant due to the (repelling and attraction) forces acting on the tip.

$$\omega_r = \omega_n \sqrt{1 - \frac{1}{k}\frac{\partial F_z}{\partial z}} \approx \omega_n \left(1 - \frac{1}{k}\frac{\partial F_z}{\partial z}\right)$$

The change in the natural resonance frequency is given by

$$\Delta f = f_r - f_n \approx -\frac{f_n}{2k}\frac{\partial F_z}{\partial z}, \text{ where } f = \frac{\omega}{2\pi}$$

For instance, the coordinate system is such that positive z is away from or perpendicular to the sample surface, so that an attractive force would be in the negative direction (F<0), and thus the gradient is positive. Consequently, for attractive forces, the resonance

frequency of the cantilever decreases (as described by the equation). The image is encoded in such a way that attractive forces are generally depicted in black color, while repelling forces are coded white.

Image formation

Calculating forces acting on magnetic tips

Analytically, the magnetostatic energy (*U*) of the tip-sample system can be calculated in one of two ways:

- One can either compute the magnetization (*M*) of the tip in the presence of the magnetic stray field (**H**) of the sample or
- Compute the magnetization of the sample in the presence of the magnetic stray field of the tip (whichever is easier)

Then, integrate the (dot) product of the magnetization and stray field over the interaction volume as

$$U = -\mu_o \int_V \vec{M} \cdot \vec{H}\, dV$$

and compute the gradient of the energy over distance to obtain the force *F*. Assuming that the cantilever deflects along the *z*-axis, and the tip is magnetized along a certain direction (e.g. the *z*-axis), then the equations can be simplified to

$$F_i = \mu_o \int_V \vec{M} \cdot \frac{\partial \vec{H}}{\partial x_i}\, dV$$

Since the tip is magnetized along a specific direction, it will be sensitive to the component of the magnetic stray field of the sample which is aligned to the same direction.

Imaging samples

The MFM can be used to image various magnetic structures including domain walls (Bloch and Neel), closure domains, recorded magnetic bits, etc. Furthermore, motion of domain wall can also be studied in an external magnetic field. MFM images of various materials can be seen in the following books and journal publications: thin films, nanoparticles, nanowires, permalloy disks and recording media.

Advantages

The popularity of MFM originates from several reasons, which include::

- The sample does not need to be electrically conductive.
- Measurement can be performed at ambient temperature, in ultra high vacuum (UHV), in liquid environment, and at different temperatures.
- Measurement is nondestructive to the crystal lattice or structure.
- Long-range magnetic interactions are not sensitive to surface contamination.
- No special surface preparation or coating is required.
- Deposition of thin non-magnetic layers on the sample does not alter the results.
- Detectable magnetic field intensity, **H**, is in the range of 10 A/m
- Detectable magnetic field, **B**, is in the range of 0.1 gauss (10 microteslas).
- Typical measured forces are as low as 10^{-14} N, with the spatial resolutions as low as 20 nm.
- MFM can be combined with other scanning methods like STM.

Limitations

There are some shortcomings or difficulties when working with an MFM, such as:

- The recorded image depends on the type of the tip and magnetic coating, due to tip-sample interactions.
- Magnetic field of the tip and sample can change each other's magnetization, *M*, which can result in nonlinear interactions. This hinders image interpretation.
- Relatively short lateral scanning range (order of hundreds micrometers).
- Scanning (lift) height affects the image.
- Housing of the MFM system is important to shield electromagnetic noise (Faraday cage), acoustic noise (anti-vibration tables), air flow (air isolation), and static charge on the sample.

Chapter- 4

Piezoresponse Force Microscopy

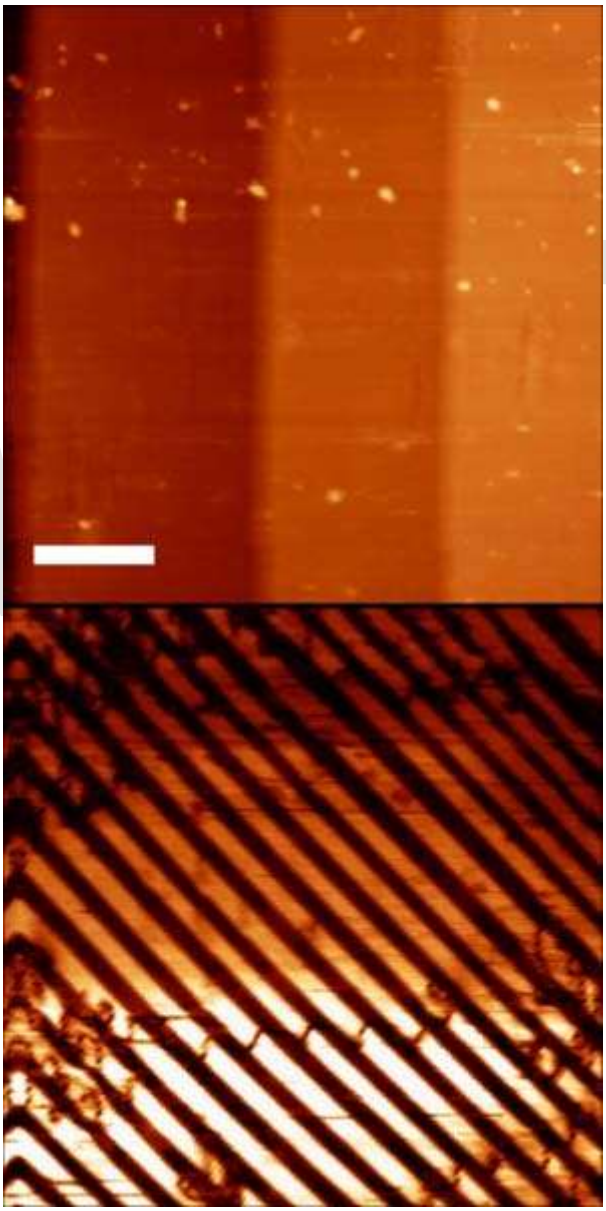

Piezoresponse Force Microscopy of single crystal $BaTiO_3$ showing simultaneously acquired topography (top) and domain structure (bottom). The scale bar is 10 μm

Piezoresponse Force Microscopy (PFM) is a variant of Atomic Force Microscopy (AFM) that allows imaging and manipulation of ferroelectric domains. This is achieved by bringing a sharp conductive probe into contact with a ferroelectric surface (or piezoelectric material) and applying an alternating current (AC) bias to the probe tip in order to excite deformation of the sample through the converse piezoelectric effect (CPE). The resulting deflection of the probe cantilever is detected through standard split photodiode detector methods and then demodulated by use of a Lock-in amplifier (LiA). In this way topography and ferroelectric domains can be imaged simultaneously with high resolution.

Basic Principles

General Overview

Piezoresponse Force Microscopy is a technique which since its inception and first implementation has steadily attracted more and more interest. This is due in large part to the many benefits and few drawbacks that PFM offers researchers in varying fields from ferroelectrics, semiconductors and even biology. In its most common format PFM allows for identification of domains from relatively large scale e.g. 100 x 100 μm^2 scans right down to the nanoscale with the added advantage of simultaneous imaging of sample surface topography. Also possible is the ability to switch regions of ferroelectric domains with the application of a sufficiently high bias to the probe which opens up the opportunity of investigating domain formation on nanometre length scales with nanosecond time resolution. Many recent advances have expanded the list of applications for PFM and further increased this powerful technique. Indeed what started as a user modified AFM has now attracted the attention of the major SPM manufacturers so much so that in fact many now supply ‘ready-made’ systems specifically for PFM each with novel features for research. This is testament to the growth of the field and reflects the numbers of users throughout the scientific world who are at the forefront of scientific research.

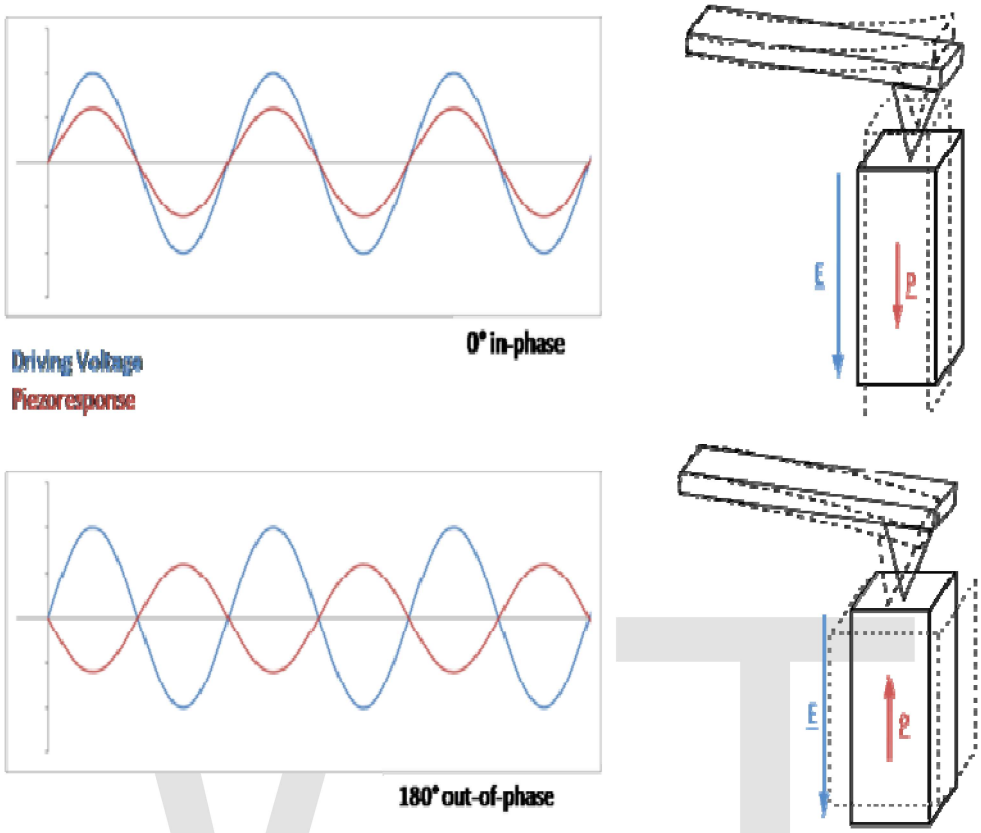

Top line shows an in-phase piezoresponse to the driving voltage and the bottom line shows a 180° out-of-phase piezoresponse to driving voltage. Alignment of electric field and polarisation orientation (top right) results in an expansion of the domain, giving a positive deflection as measured by the photodiode. When the bias is negative the domain contracts giving a negative deflection as measured by the photodiode meaning that the piezoresponse will always be in-phase with the driving voltage. For anti-alignment of electric field and polarisation orientation (bottom right) a positive bias results in a contraction of the domain and so gives a negative deflection as measured by the photodiode therefore the piezoresponse is 180° out-of-phase with the driving voltage. In this way the orientation of polarisation within a domain can be observed.

Consider that a static or DC voltage applied to a piezoelectric surface will produce a displacement but as applied fields are quite low and the piezoelectric tensor coefficients are relatively small then the physical displacement will also be small such that it is below the level of possible detection of the system. Take as an example, the d_{33} piezoelectric tensor coefficient of $BaTiO_3$, it has a value of 85.6 pmV^{-1} meaning that applying 1 V across the material results in a displacement of 85.6 pm or 0.0856 nm, a minute cantilever displacement even for the high precision of AFM deflection detection. In order to separate this low level signal from random noise a lock-in technique is used wherein a modulated voltage reference signal,

$$V(\omega) = V_{ac}\cos(\omega t)$$

of frequency ω and amplitude V_{ac} is applied to the tip giving rise to an oscillatory deformation of the sample surface,

$$d = d_0 + D\cos(\omega t + \varphi)$$

from the equilibrium position d_0 with amplitude D, and an associated phase difference φ. The resulting movement of the cantilever is detected by the photodiode and so an oscillating surface displacement is converted into an oscillating voltage. A lock-in-amplifier (LiA) is then able to retrieve the amplitude and phase of the CPE induced surface deformation by the process outlined below.

Converse Piezoelectric Effect

The converse piezoelectric effect (CPE) describes how an applied electric field will create a resultant strain which in turn leads to a physical deformation of the material. This effect can be described through the constitutive equations. The CPE can be written as

$$X_i = d_{ki}E_k$$

where X_i is the strain tensor, d_{ki} is the piezoelectric tensor, and E_k is the electric field. If the piezoelectric tensor is considered to be that of the tetragonal crystal system (that of $BaTiO_3$) then it is

$$\begin{bmatrix} X_1 \\ X_2 \\ X_3 \\ X_4 \\ X_5 \\ X_6 \end{bmatrix} = \begin{bmatrix} 0 & 0 & d_{31} \\ 0 & 0 & d_{31} \\ 0 & 0 & d_{33} \\ 0 & d_{15} & 0 \\ d_{15} & 0 & 0 \\ 0 & 0 & 0 \end{bmatrix} \begin{bmatrix} E_1 \\ E_2 \\ E_3 \end{bmatrix}$$

such that the equation will lead to the strain components for an applied field. If the field is applied exclusively in one direction i.e. E_3 for example, then the resulting strain components are: $d_{31}E_3$, $d_{31}E_3$, $d_{33}E_3$

Thus for an electric field applied along the c-axis of $BaTiO_3$ i.e. E_3, then the resulting deformation of the crystal will be an elongation along the c-axis and an axially symmetric contraction along the other orthogonal directions. PFM uses the effect of this deformation to detect domains and also to determine their orientation.

Conductive Probe

The most important property of the probe for use in PFM is that it should be conducting. This is generally required in order to provide a means of applying a bias to the sample, and can be achieved through manufacturing standard silicon probes and coating them in a conductive material. Common coatings are platinum, gold, tungsten and even conductive diamond.

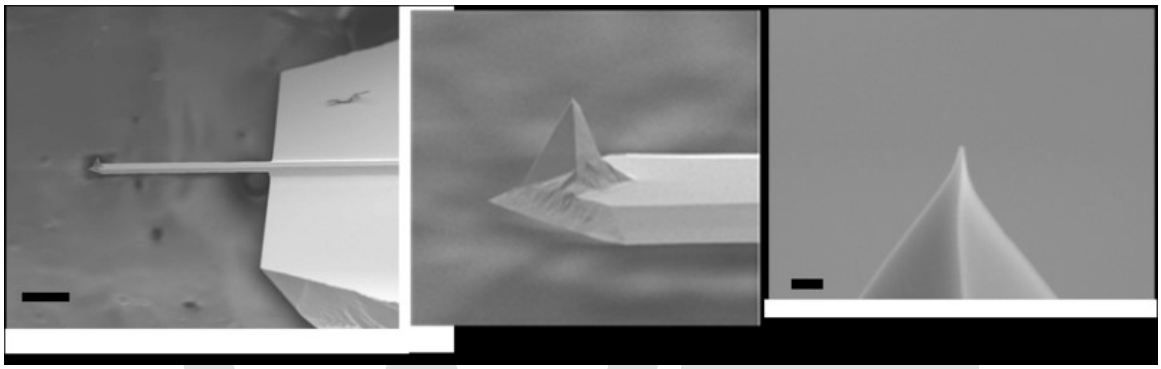

Scanning Electron Microscopy images of a $PtIr_5$ coated scanning probe. From left to right shows images of increasing magnification where the scale bar in the first image is 50 μm and in the third is 200 nm. The first image shows the substrate, cantilever and the tip whereas the second image shows the tip geometry whilst the last image shows the tip apex and demonstrates the fine point that is achieved e.g. radius of curvature of less than 40 nm.

Lock-in Amplifier

In the general case a LiA 'compares' an *input signal* against that of a *reference signal* (either generated internally or supplied by an external function generator) in order to separate the information contained in the input signal at the frequency of the reference signal. This is called *demodulation* and is done in a number of easy steps. The reference signal $V_{ref} = B\cos(\omega t)$, and input signal, $V_{in} = A\cos(\omega t + \varphi)$, are multiplied together to give the *demodulator output*,

$$V_{out} = \frac{1}{2}AB\cos(\varphi) + \frac{1}{2}AB\cos(2\omega t + \varphi)$$

where A is the input signal Amplitude and B is the reference signal Amplitude, ω is the frequency of both the reference and input signals, and φ is any phase shift between the two signals.

The above equation has an AC component at twice the frequency of the original signals (second term) and a DC component (first term) whose value is related to both the amplitude and phase of the input signal. The demodulator output is sent through a low-pass filter to remove the 2ω component and leave the DC component then the signal is

integrated over a period of time defined as the *Time Constant*, τ_{LiA} which is a user-definable parameter. Several different outputs are commonly available from a LiA: *X* output is the demodulator output and *Y* is the second demodulator output which is shifted by 90° in reference to the first output, together they hold both the phase, θ, and magnitude, *R*, information and are given by

$$X = \frac{1}{2}AB\cos(\theta)$$ and

$$Y = \frac{1}{2}AB\cos(\theta + \frac{\pi}{2}) = \frac{1}{2}AB\sin(\theta)$$

However, phase and amplitude of the input signal can also be calculated and outputted from the LiA if desired, so that the full amount of information is available. The Phase output can be determined from the following equation:

$$\theta = \tan^{-1}\frac{Y}{X}$$

The Magnitude is then given by:

$$R = \sqrt{X^2 + Y^2}$$

This allows *R* to be calculated even if the input signal differs in phase from the reference signal.

Differentiating Vertical and Lateral PFM signals

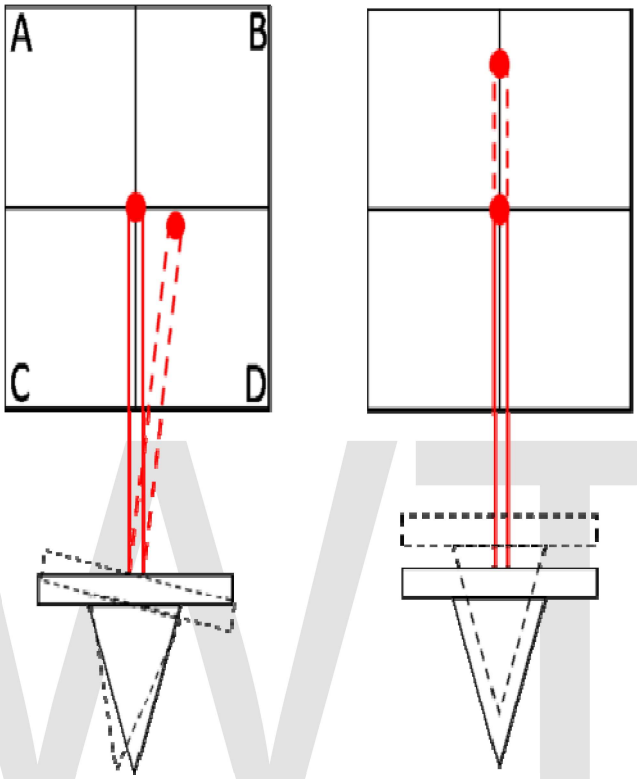

Diagrams showing the effect of cantilever movement with the photodetector represented by the square with quadrants labelled A, B, C & D. Torsional bending of the cantilever (left) leads to a change in lateral deflection and (right) vertical displacement of the cantilever leads to a change in vertical deflection

A basic interpretation of PFM (which is generally accepted) identifies that two modes of imaging are possible, one that is sensitive to out-of-plane & one to in-plane piezoresponse, termed, vertical & lateral PFM (VPFM & LPFM) respectively. The separation of these components is possible through the use of a split photodiode detector, standard to all optical detection AFM systems. In this setup the detector is split into quadrants, nominally A, B, C & D. The centre of the entire detector outputs 0 V but as the laser spot moves a radial distance from this centre point the magnitude of the outputted voltage will increase linearly. A vertical deflection can be defined as {(A+B)-(C+D)}/(ABCD) so that now positive and negative voltages are ascribed to positive and negative cantilever vertical displacements. Similarly a lateral deflection is defined as {(B+D)-(A+C)}/(ABCD) to describe positive and negative torsional movements of the cantilever. So VPFM will utilise the vertical deflection signal from the photodiode

detector so will only be sensitive to out-of-plane polar components and LPFM will utilise the lateral deflection signal from the photodiode and will only be sensitive to in-plane polar components.

For polar components orientated such that they are parallel to the electric field the resulting oscillating movement will be entirely in-phase with the modulated electric field but for an anti-parallel alignment the motion will be 180° out-of-phase. In this way it is possible to determine the orientation of the vertical components of polarisation from analysis of the phase information, φ, contained in the input signal, readily available after demodulation in the LiA, when using the VPFM mode. In a similar sense the orientations of in-plane polar components can also be determined from the phase difference when using the LPFM mode. The amplitude of the piezoresponse of either VPFM or LPFM is also given by the LiA, in the form of the magnitude, R.

Examples of PFM imaging

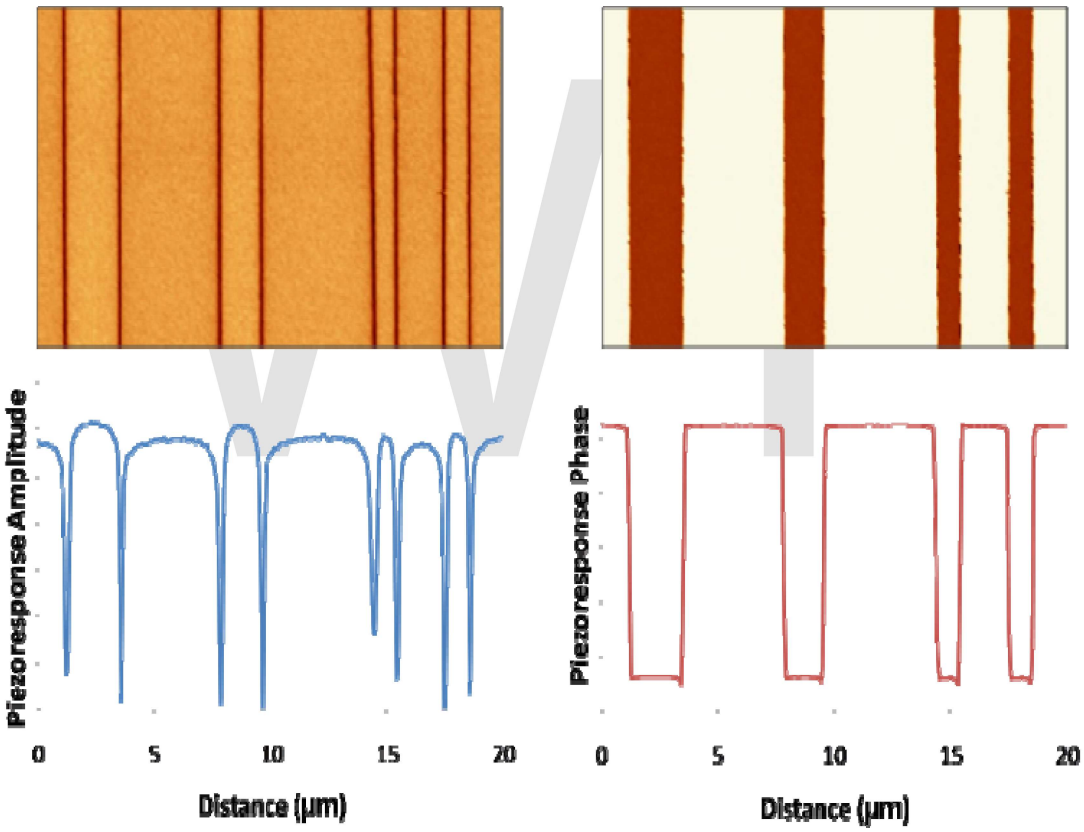

180° ferroelectric domains in KTP as imaged by PFM. Below are the associated line profiles across the domains

The image shows periodically poled 180° domains in KTP as imaged by VPFM. In the image piezoresponse amplitude can be seen where dark areas represent the zero amplitude that is expected at domain boundaries where the unit cell is cubic i.e.

centrosymmetric and so therefore not ferroelectric. On the left hand side piezoresponse phase can be seen where the measured phase changes to show the out-of-plane components that are pointing out of the screen, white areas, and into the screen, dark areas. The scan area is 20 x 10 μm^2. Below each scan is the relevant cross-section that shows in arbitrary units the PR amplitude and phase.

Advanced Modes of PFM

Several additions have been made to PFM that substantially increase the flexibility of the technique to probe nanoscale features.

Stroboscopic PFM

Stroboscopic PFM allows for time resolved imaging of switching in pseudo real-time. A voltage pulse of amplitude much higher than the coercive voltage of the sample but shorter in duration than the characteristic switching time is applied to the sample and subsequently imaged. Further pulses with the same amplitude but longer in time are then applied with regular PFM imaging at the intervals. In this way a series of images showing the switching of the sample can be obtained. Typical pulses are of tens of nanoseconds in duration and are therefore capable of resolving the first nucleation sites of domain reversal and then observing how these sites evolve.

Contact Resonance PFM

Remembering that in PFM an AC bias of a certain frequency causes a deformation of the sample material at that same frequency the system can be considered as a driven harmonic oscillator. As such there exists a resonance as a function of driving frequency. This effect has been exploited in PFM to provide an enhancement in the PR signal, thus allowing for a higher signal-to-noise or similar signal-to-noise at lower driving bias amplitude. Typically this contact resonance is in the kilo- to mega-hertz range which is several times higher in frequency than the first free harmonic in air of the cantilever used. However a drawback is that the contact resonance is dependent not only on the dynamic response of the cantilever but also on the Elastic Modulus of the sample material immediately in contact with the probe tip and so therefore can change during scanning over different areas. This leads to a change in the measured PR amplitude and so is undesirable. One method of bypassing the inherent disadvantages of Contact Resonance PFM is to change the driving frequency in order to shadow or track the changes in the frequency of the contact resonance. This feature as developed by Asylum Research called Dual Frequency Resonance Tracking (DFRT) uses two limit frequencies on either side of the contact resonance peak and so can sense changes in the peak position. It is then possible to adapt the AC bias driving frequency correspondingly in order to maintain the signal boost that results from the contact resonance.

Switching Spectroscopy (SS) PFM

In this technique the area underneath the PFM tip is switched with simultaneous acquisition of a hysteresis loop that can be analysed to obtain information about the sample properties. A series of hysteresis loops are acquired across the sample surface in order to map the switching characteristics as a function of position. In this way an image representing switching properties such as coercive voltage, remnant polarisation, imprint and work of switching amongst others can be displayed in which each pixel displays the desired data from the hysteresis loop acquired at that point. This allows spatial analysis of switching properties to be compared with sample topography etc.

Advantages and Disadvantages

Pros

- High resolution on the nanometre scale
- Simultaneous acquisition of topography and piezoresponse
- Allows manipulation of ferroelectric domains
- Non-destructive
- Little sample preparation required

Cons

- Scans can be slow e.g. tens of minutes
- Tip wear changes surface interaction and can affect contrast
- Limited to lateral range of AFM i.e. approx. 100 x 100 μm^2

Chapter- 5

Scanning Thermal Microscopy

Scanning thermal microscopy (SThM) is a type of scanning probe microscopy that maps the local temperature and thermal conductivity of an interface. The probe in a scanning thermal microscope is sensitive to local temperatures - providing a nanoscale thermometer. Thermal measurements at the nanometer scale are of both scientific and industrial interest.

Applications

SThM allows thermal measurements at the nanoscale. These measurements can include: temperature, thermal properties of materials, thermal conductivity, heat capacity, glass transition temperature, latent heat, enthalpy, etc. The applications include:

Joule heating

Joule heating, also known as **ohmic heating** and **resistive heating**, is the process by which the passage of an electric current through a conductor releases heat. It was first studied by James Prescott Joule in 1841. Joule immersed a length of wire in a fixed mass of water and measured the temperature rise due to a known current flowing through the wire for a 30 minute period. By varying the current and the length of the wire he deduced that the heat produced was proportional to the square of the current multiplied by the electrical resistance of the wire.

$$Q \propto I^2 \cdot R$$

This relationship is known as Joule's First Law. The SI unit of energy was subsequently named the joule and given the symbol *J*. The commonly known unit of power, the watt, is equivalent to one joule per second.

It is now known that Joule heating is caused by interactions between the moving particles that form the current (usually, but not always, electrons) and the atomic ions that make up the body of the conductor. Charged particles in an electric circuit are accelerated by an

electric field but give up some of their kinetic energy each time they collide with an ion. The increase in the kinetic or vibrational energy of the ions manifests itself as heat and a rise in the temperature of the conductor. Hence energy is transferred from the electrical power supply to the conductor and any materials with which it is in thermal contact.

Joule heating is referred to as *ohmic heating* or *resistive heating* because of its relationship to Ohm's Law. It forms the basis for the myriad of practical applications involving electric heating. However, in applications where heating is an unwanted by-product of current use (e.g., load losses in electrical transformers) the diversion of energy is often referred to as *resistive losses*. The use of high voltages in electric power transmission systems is specifically designed to reduce such losses in cabling by operating with commensurately lower currents. The ring circuits, or ring mains, used in homes are another example, where power is delivered to outlets at lower currents, thus reducing Joule heating in the wires. Joule heating can be defeated using superconducting materials.

Photothermal microspectroscopy

Photothermal microspectroscopy (PTMS), alternatively known as photothermal temperature fluctuation (PTTF), is derived from two parent instrumental techniques: infrared spectroscopy and atomic force microscopy (AFM). In one particular type of AFM, known as scanning thermal microscopy (SThM), the imaging probe is a sub-miniature temperature sensor, which may be a thermocouple or a resistance thermometer. This same type of detector is employed in a PTMS instrument, enabling it to provide AFM/SThM images: However, the chief additional use of PTMS is to yield infrared spectra from sample regions below a micrometer, as outlined below.

Technique

The AFM is interfaced with an infrared spectrometer. For work using Fourier transform infrared spectroscopy (FTIR), the spectrometer is equipped with a conventional black body infrared source. A particular region of the sample may first be chosen on the basis of the image obtained using the AFM imaging mode of operation. Then, when material at this location absorbs the electromagnetic radiation, heat is generated, which diffuses, giving rise to a decaying temperature profile. The thermal probe then detects the photothermal response of this region of the sample. The resultant measured temperature fluctuations provide an interferogram that replaces the interferogram obtained by a conventional FTIR setup, e.g., by direct detection of the radiation transmitted by a sample. The temperature profile can be made sharp by modulating the excitation beam. This results in the generation of thermal waves whose diffusion length is inversely proportional to the root of the modulation frequency. An important advantage of the thermal approach is that it permits to obtain depth-sensitive subsurface information from

surface measurement, thanks to the dependence of thermal diffusion length on modulation frequency.

Applications

The two particular features of PTMS that have determined its applications so far are:

- spectroscopic mapping may be performed at a spatial resolution well below the diffraction limit of IR radiation, ultimately at a scale of 20-30 nm. In principle, this opens the way to sub-wavelength IR microscopy where the image contrast is to be determined by the thermal response of individual sample regions to particular spectral wavelengths.

- In general, no special preparation technique is required when solid samples are to be studied. For most standard FTIR methods, this is not the case.

Related technique

This spectroscopic technique complements another recently-developed method of chemical characterisation or fingerprinting, namely micro-thermal analysis (micro-TA). This also uses an "active" SThM probe, which acts as a heater as well as a thermometer, so as to inject evanescent temperature waves into a sample and to allow sub-surface imaging of polymers and other materials. The sub-surface detail detected corresponds to variations in heat capacity or thermal conductivity. Ramping the temperature of the probe, and thus the temperature of the small sample region in contact with it, allows localized thermal analysis and/or thermomechanometry to be performed.

Calorimetry

The world's first **ice-calorimeter**, used in the winter of 1782-83, by Antoine Lavoisier and Pierre-Simon Laplace, to determine the heat evolved in various chemical changes; calculations which were based on Joseph Black's prior discovery of latent heat. These experiments mark the foundation of thermochemistry.

Calorimetry is the science of measuring the heat of chemical reactions or physical changes. Calorimetry is performed with a calorimeter. The word calorimetry is derived from the Latin word *calor*, meaning heat. Scottish physician and scientist Joseph Black, who was the first to recognize the distinction between heat and temperature, is said to be the founder of calorimetry.

Indirect calorimetry calculates heat that living organisms produce from their production of carbon dioxide and nitrogen waste (frequently ammonia in aquatic organisms, or urea

in terrestrial ones), OR from their consumption of oxygen. Lavoisier noted in 1780 that heat production can be predicted from oxygen consumption this way, using multiple regression. The Dynamic Energy Budget theory explains why this procedure is correct. Of course, heat generated by living organisms may also be measured by **direct calorimetry**, in which the entire organism is placed inside the calorimeter for the measurement.

Calculation of heat

The specific heat formula is as follows:

$$q = ms\Delta T$$

where

q is energy, or heat,
m is mass,
s is specific heat,
ΔT is change in temperature.

Constant-volume calorimetry (Bomb Calorimetry)

Constant-volume calorimetry is calorimetry performed at a constant volume. This involves the use of a constant-volume calorimeter.

No work is performed in constant-volume calorimetry, so the heat measured equals the change in internal energy of the system. The equation for constant-volume calorimetry is (the heat capacity at constant volume is assumed to be constant):

$$q = C_V\Delta T = \Delta U$$

where

ΔU is change in internal energy,
ΔT is change in temperature and
C_V is the heat capacity at constant volume.

Since in *constant-volume calorimetry* the pressure is not kept constant, the heat measured does not represent the *enthalpy change.*

Differential scanning calorimetry

A widely used modern instrument is the Differential scanning calorimeter, a device which allows thermal data to be obtained on small amounts of material. It involves heating the sample at a controlled rate and recording the heat flow either into or from the specimen.

History

Scanning thermal microscopy (SThM) was invented by Williams and Wickramasinghe in 1986.

Technique

SThM requires the use of specialized probes. There are two types of thermal probes. Thermocouple probes where the probe temperature is monitored by a thermocouple junction at the probe tip and resistive or bolometer probes where the probe temperature is monitored by a thin film resistor at probe tip. These probes are generally made from thin dielectric films on a silicon substrate and use a metal or semiconductor film bolometer to sense the tip temperature. Other approaches, using more involved micromachining methods, have also been reported . In a bolometer probe the resistor is used as a local heater and the fractional change in probe resistance is used to detect the temperature and/or the thermal conductance of the sample . When the tip is placed in contact with the sample, heat flows from the tip to sample. As the probe is scanned, the amount of heat flow changes. By monitoring the heat flow, we can create a thermal map of the sample .

Tip-sample heat transfer can include

- Solid-solid conduction. Probe tip to sample. This is the transfer mechanism which yields the thermal scan.
- Liquid-liquid conduction. When scanning in non-zero humidity, a liquid meniscus forms between the tip and sample. Conduction can occur through this liquid drop.
- Gas conduction. Heat can be transferred through the edges of the probe tip to the sample.

Chapter- 6

Scanning SQUID Microscope

A **Scanning SQUID Microscope** is a sensitive near-field imaging system for the measurement of weak magnetic fields by moving a Superconducting Quantum Interference Device (SQUID) across an area. The microscope can map out buried current-carrying wires by measuring the magnetic fields produced by the currents, or can be used to image fields produced by magnetic materials. By mapping out the current in an integrated circuit or a package, short circuits can be localized and chip designs can be verified to see that current is flowing where expected.

High temperature scanning SQUID microscope

Scanning SQUID microscope

A high temperature Scanning SQUID Microscope using a YBCO SQUID is capable of measuring magnetic fields as small as 20 pT (about 2 million times weaker than the earth's magnetic field). The SQUID sensor is sensitive enough that it can detect a wire even if it is carrying only 10 nA of current at a distance of 100 μm from the SQUID sensor with 1 second averaging. The microscope uses a patented design to allow the sample under investigation to be at room temperature and in air while the SQUID sensor is under vacuum and cooled to less than 80 K using a cryo cooler. No Liquid Nitrogen is used. During non-contact, non-destructive imaging of room temperature samples in air, the system achieves a raw, unprocessed spatial resolution equal to the distance separating the sensor from the current or the effective size of the sensor, whichever is larger. To best locate a wire short in a buried layer, however, a Fast Fourier Transform (FFT) back-evolution technique can be used to transform the magnetic field image into an equivalent map of the current in an integrated circuit or printed wiring board. The resulting current map can then be compared to a circuit diagram to determine the fault location. With this post-processing of a magnetic image and the low noise present in SQUID images, it is

possible to enhance the spatial resolution by factors of 5 or more over the near-field limited magnetic image. The system's output is displayed as a false-color image of magnetic field strength or current magnitude (after processing) versus position on the sample. After processing to obtain current magnitude, this microscope has been successful at locating shorts in conductors to within ±3 μm at a sensor-current distance of 150 μm.

SQUID operation

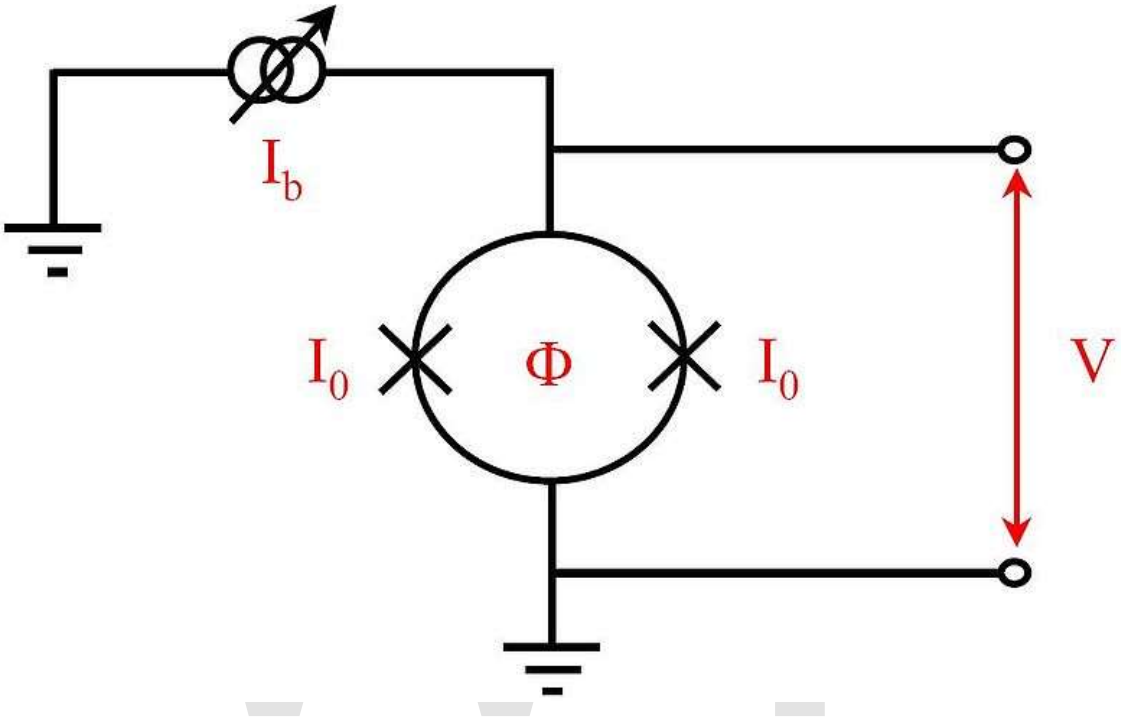

Figure 1: Electrical schematic of a SQUID where I_b is the bias current, I_0 is the critical current of the SQUID, Φ is the flux threading the SQUID and V is the voltage response to that flux.

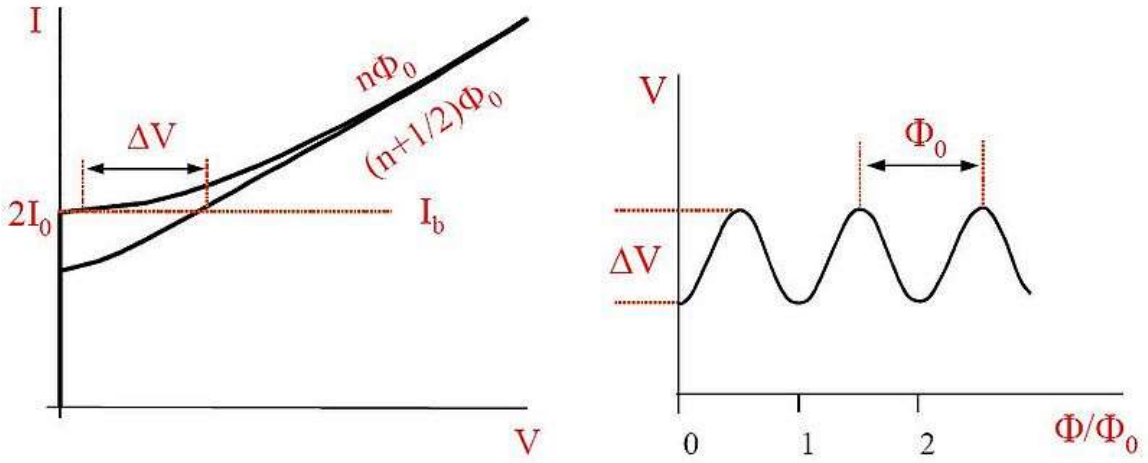

Figure 2 a) Plot of current vs. voltage for a SQUID. Upper and lower curves correspond to $n\Phi_0$ and $(n+1/2)\Phi_0$ respectively. Figure 2 b) Periodic voltage response due to flux through a SQUID. The periodicity is equal to one flux quantum, Φ_0

As the name implies, SQUIDs are made from superconducting material. As a result, they need to be cooled to cryogenic temperatures of less than 90 K (liquid nitrogen temperatures) for high temperature SQUIDs and less than 9 K (liquid helium temperatures) for low temperature SQUIDs. For magnetic current imaging systems, a small (about 30 μm wide) high temperature SQUID is used. This system has been designed to keep a high temperature SQUID, made from $YBa_2Cu_3O_7$, cooled below 80K and in vacuum while the device under test is at room temperature and in air. A SQUID consists of two Josephson tunnel junctions that are connected together in a superconducting loop (see Figure 1). A Josephson junction is formed by two superconducting regions that are separated by a thin insulating barrier. Current exists in the junction without any voltage drop, up to a maximum value, called the critical current, I_o. When the SQUID is biased with a constant current that exceeds the critical current of the junction, then changes in the magnetic flux, Φ, threading the SQUID loop produce changes in the voltage drop across the SQUID (see Figure 1). Figure 2(a) shows the I-V characteristic of a SQUID where ΔV is the modulation depth of the SQUID due to external magnetic fields. The voltage across a SQUID is a nonlinear periodic function of the applied magnetic field, with a periodicity of one flux quantum, $\Phi_0=2.07\times10^{-15}$ Tm^2 (see Figure 2(b)). In order to convert this nonlinear response to a linear response, a negative feedback circuit is used to apply a feedback flux to the SQUID so as to keep the total flux through the SQUID constant. In such a flux locked loop, the magnitude of this feedback flux is proportional to the external magnetic field applied to the SQUID. Further description of the physics of SQUIDs and SQUID microscopy can be found elsewhere.

Magnetic field detection using SQUID

$$d\vec{B} = \frac{\mu_0}{4\pi}\frac{Id\vec{\ell}\times\vec{r}}{r^2}$$

Figure 3: Biot-Savart Law (B is the magnetic induction, Idℓ is an element of the current, the constant μ_0 is the permeability of free space, and r is the distance between the current and the sensor)

Magnetic current imaging uses the magnetic fields produced by currents in electronic devices to obtain images of those currents. This is accomplished though the fundamental physics relationship between magnetic fields and current, the Biot-Savart Law (Figure 3). As a result, the current can be directly calculated from the magnetic field knowing only the separation between the current and the magnetic field sensor. The details of this mathematical calculation can be found elsewhere, but what is important to know here is that this is a direct calculation that is not influenced by other materials or effects, and that through the use of Fast Fourier Transforms these calculations can be performed very

quickly. A magnetic field image can be converted to a current density image in about 1 or 2 seconds.

Applications using a Scanning SQUID Microscope

Scanning SQUID Microscope can detect all types of shorts and conductive paths including Resistive Opens (RO) defects such as cracked or voided bumps, Delaminated Vias, Cracked traces/mouse bites and Cracked Plated Through Holes (PTH). It can map power distributions in packages as well as in 3D Integrated Circuits (IC) with Through-Silicon Via (TSV), System in Package (SiP), Multi-Chip Module (MCM) and stacked die. SQUID scanning can also isolate defective components in assembled devices or Printed Circuit Board (PCB).

Short Localization in Advanced Wirebond Semiconductor Package

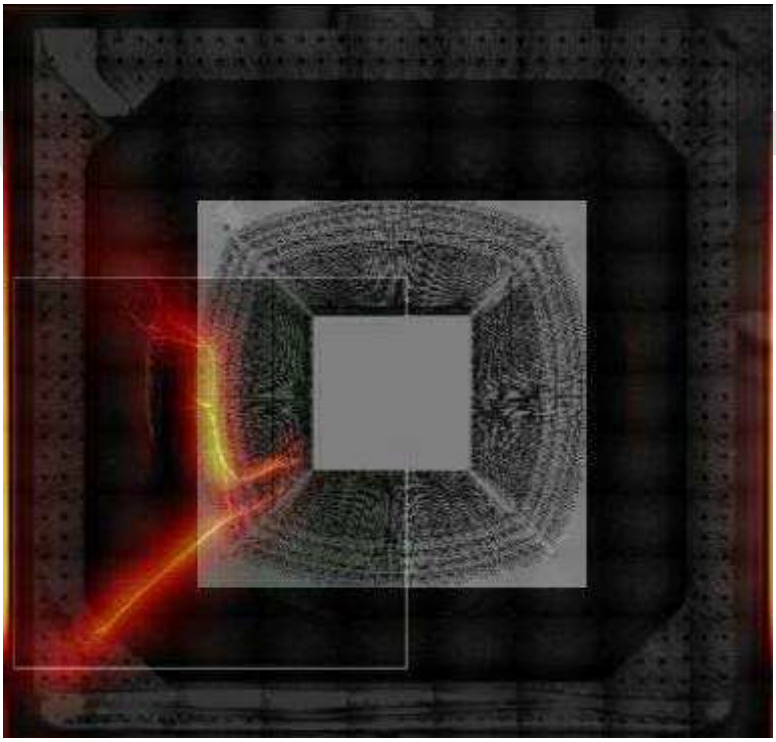

Current Image overlaid the optical image of the part and the layout of the part

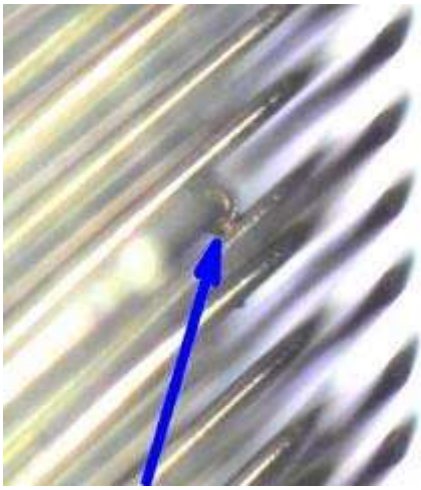

Optical image of the decapped wire bonds that are lifted from the die and touching another wire bond

Advanced wire-bond packages, unlike traditional Ball Grid Array (BGA) packages, have multiple pad rows on the die and multiple tiers on the substrate. This package technology has brought new challenges to failure analysis. To date, Scanning Acoustic Microscopy (SAM), Time Domain Reflectometry (TDR) analysis, and Real-Time X-ray (RTX) inspection were the non-destructive tools used to detect short faults. Unfortunately, these techniques do not work very well in advanced wire-bond packages. Because of the high density wire bonding in advanced wire-bond packages, it is extremely hard to localize the short with conventional RTX inspection. Without detailed information as to where the short might occur, attempting destructive decapsualtion to expose both die surface and bond wires is full of risk. Wet chemical etching to remove mold compound in a large area often results in over-etching. Furthermore, even if the package is successfully decapped, visual inspection of the multi-tiered bond wires is a blind search.

The Scanning SQUID Microscopy (SSM) data are current density images and current peak images. The current density images give the magnitude of the current, while the current peak images reveal the current path with a ± 3 μm resolution. Obtaining the SSM data from scanning advanced wire-bond packages is only half the task; fault localization is still necessary. The critical step is to overlay the SSM current images or current path images with CAD files such as bonding diagrams or RTX images to pinpoint the fault location. To make alignment of overlaying possible, an optical two-point reference alignment is made. The package edge and package fiducial are the most convenient package markings to align to. Based on the data analysis, fault localization by SSM should isolate the short in the die, bond wires or package substrate. After all non-destructive approaches are exhausted, the final step is destructive deprocessing to verify SSM data. Depending on fault isolation, the deprocessing techniques include decapsulation, parallel lapping or cross-section.

Short in multi-stacked packages

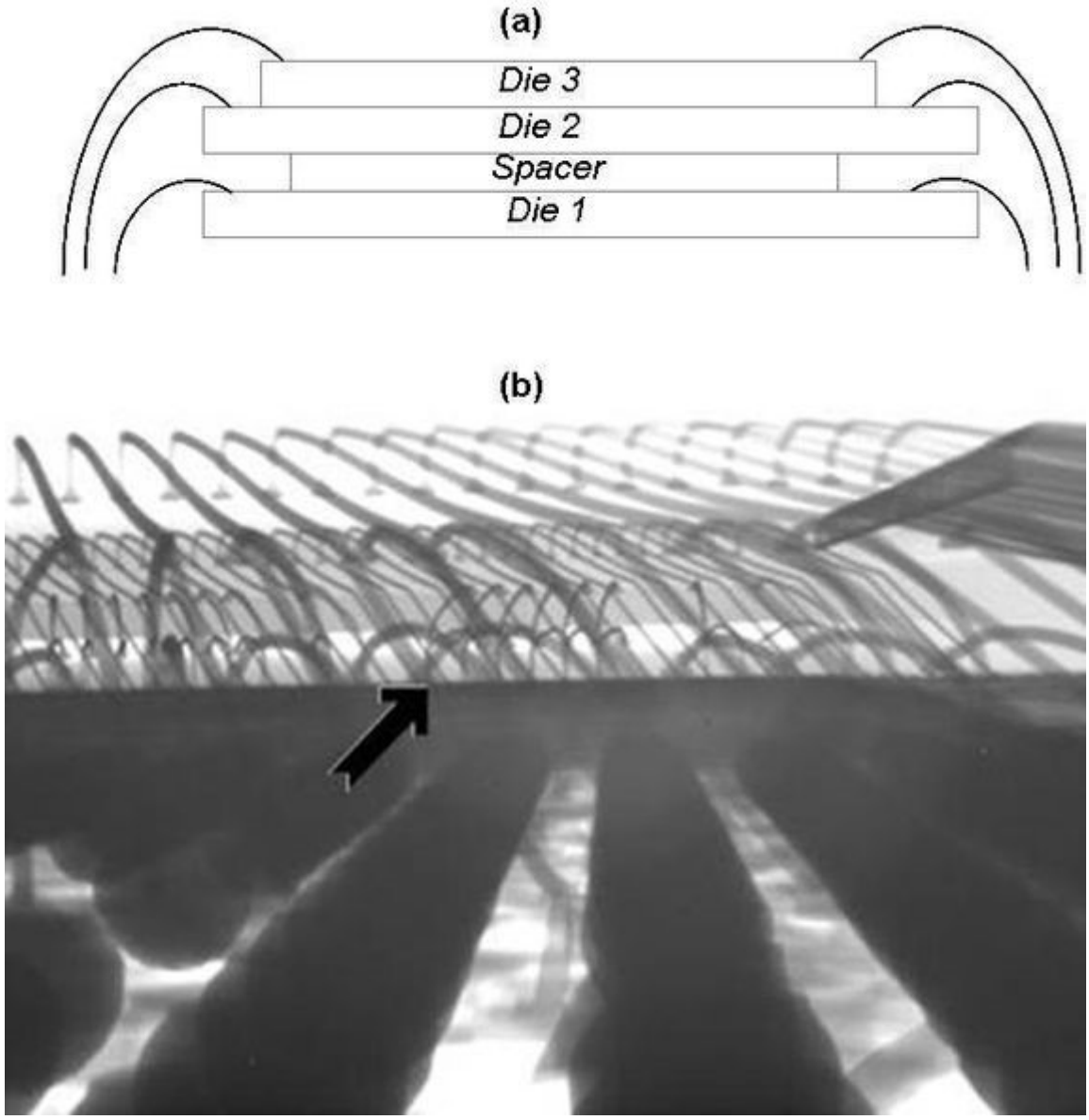

Figure 1(a) Schematic showing typical bond wires in a triple-stacked die package, Figure 1(b) x-ray lateral view of actual triple-stacked die package.

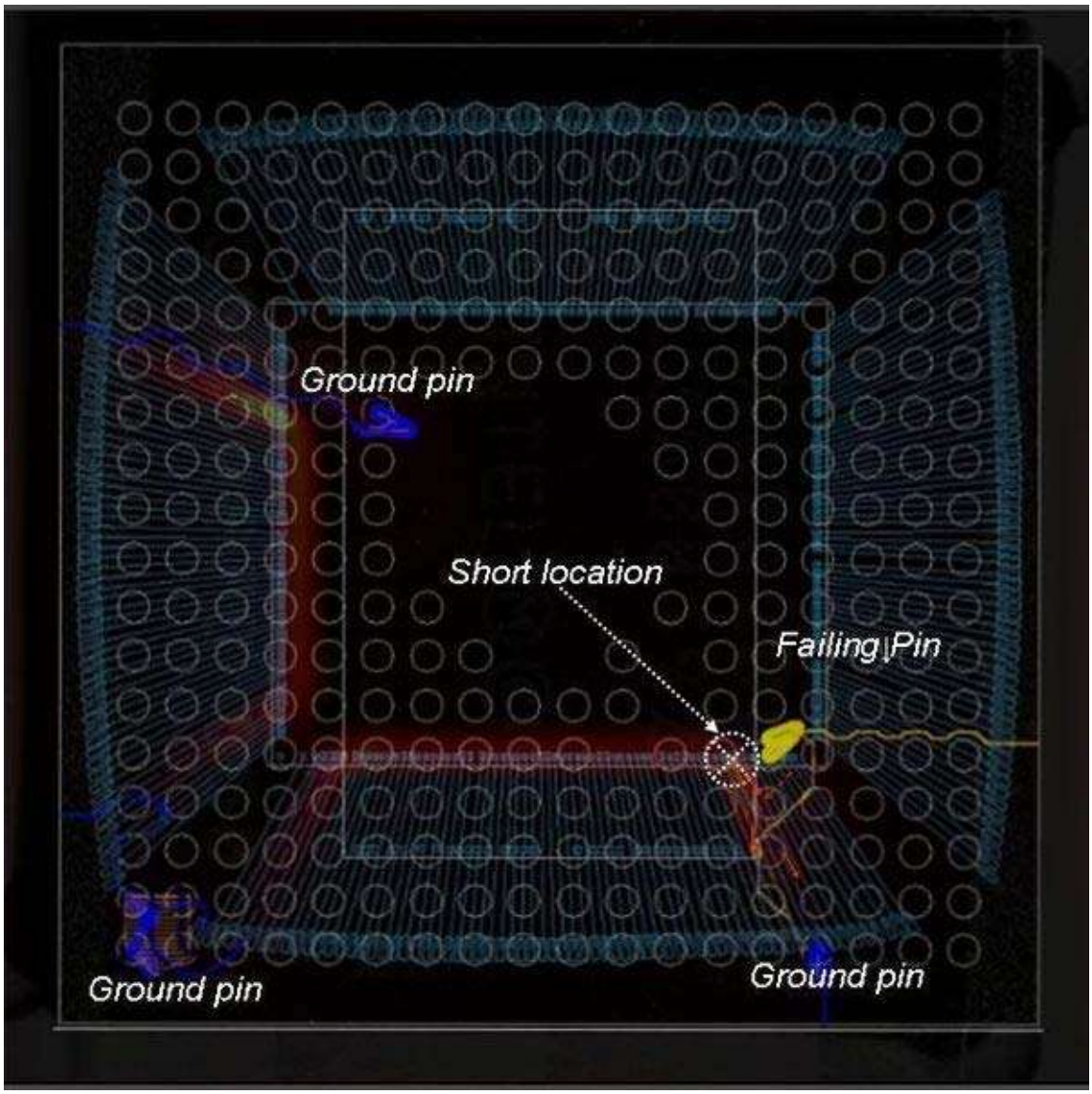

Figure 2: Overlay of current density, optical, and CAD images in triple-stacked die package with electric short failure mode.

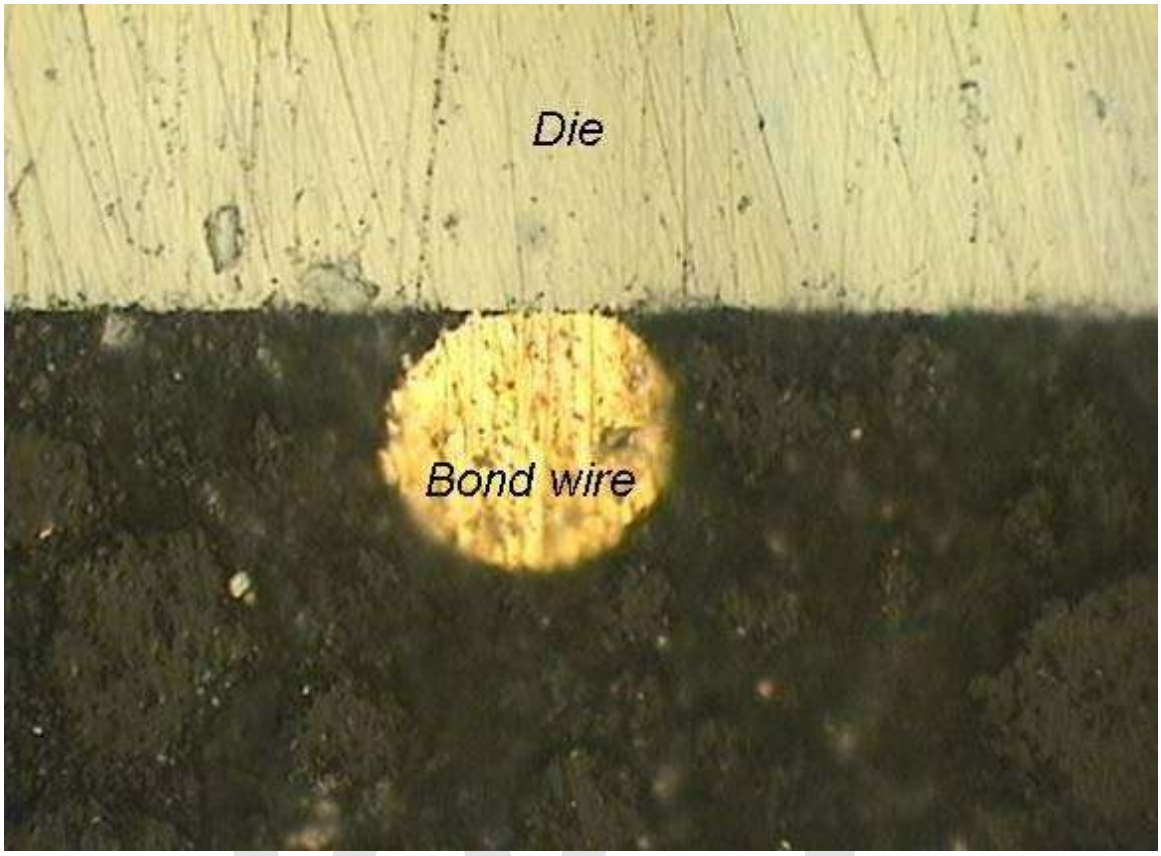

Figure 3: Cross sectional image showing a bond wire touching the die causing signal to ground leakage.

Electric shorts in multi-stacked die packages can be very difficult to isolate non-destructively; especially when a large number of bond wires are somehow shorted. For instance, when an electric short is produced by two bond wires touching each other, x-ray analysis may help to identify potential defect locations; however, defects like metal migration produced at wirebond pads, or bond wires somehow touching any other conductive structures, may be very difficult to catch with non-destructive techniques that are not electrical in nature. Here, the availability of analytical tools that can map out the flow of electrical current inside the package provide valuable information to guide the failure analyst to potential defect locations.

Figure 1a shows the schematic of our first case study consisting of a triple-stacked die package. The x-ray image of figure 1b is intended to illustrate the challenge of finding the potential short locations represented for failure analysts. In particular, this is one of a set of units that were inconsistently failing and recovering under reliability tests. Time domain reflectometry and X-ray analysis were performed on these units with no success in isolating the defects. Also there was no clear indication of defects that could potentially produce the observed electrical short failure mode. Two of those units were analyzed with SSM.

Electrically connecting the failing pin to a ground pin produced the electrical current path shown in figure 2. This electrical path strongly suggests that the current is somehow flowing through all the ground nets though a conductive path located very close to the wirebond pads from the top down view of the package. Based on electrical and layout analysis of the package, it can be inferred that current is either flowing through the wirebond pads or that the wirebonds are somehow touching a conductive structure at the specified location. After obtaining similar SSM results on the two units under test, further destructive analysis focused around the small potential short region, and it showed that the failing pin wirebond is touching the bottom of one of the stacked dice at the specific XY position highlighted by SSM analysis. The cross section view of one of those units is shown in figure 3.

A similar defect was found in the second unit.

Short between pins in molding compound package

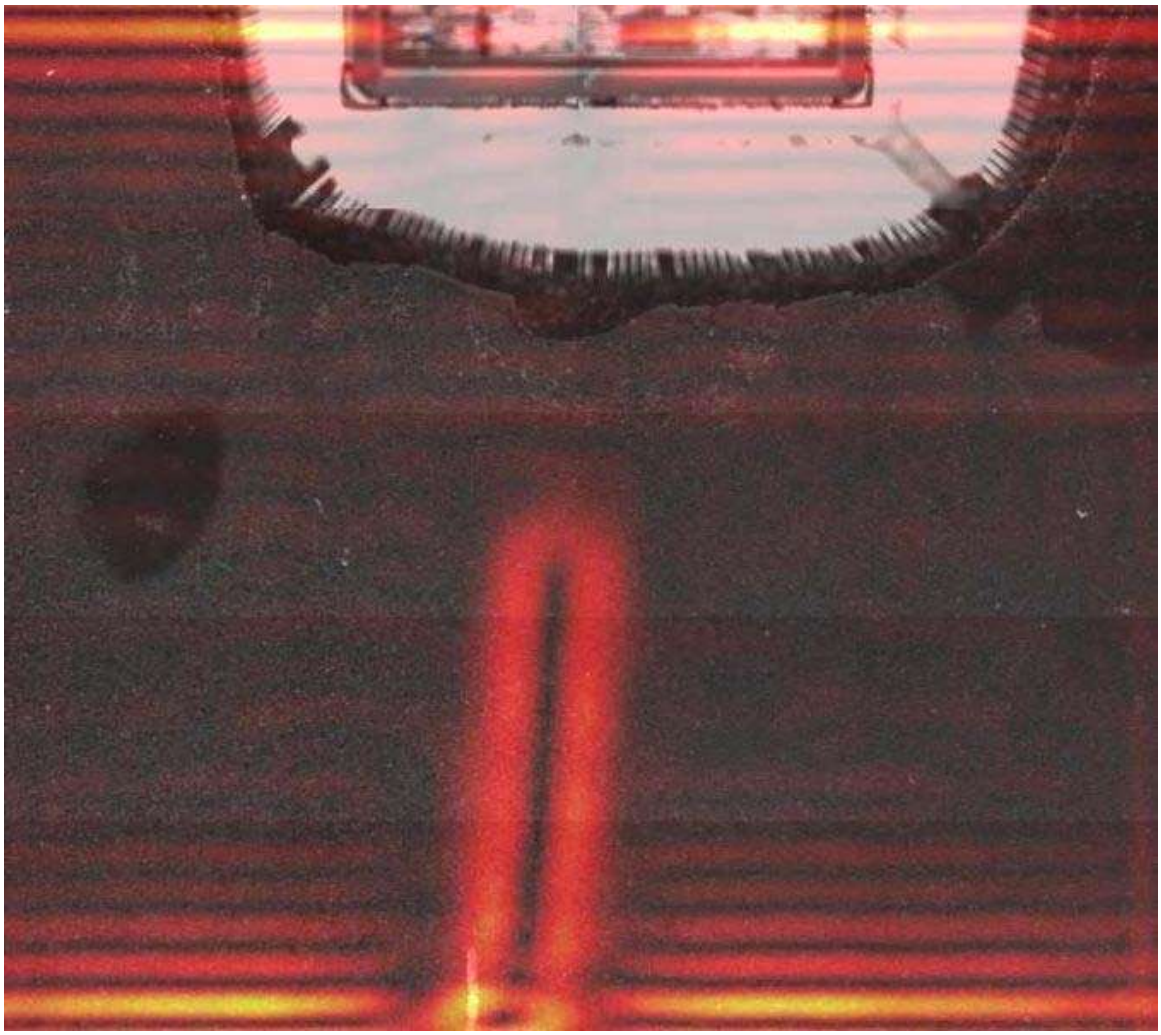

Figure 1 SQUID image of package indicating location of short.

Figure 2: High-resolution radiographic image of filament, measured at 2.9 micrometres wide. Image shows filament running under both shorted leads.

The failure in this example was characterized as an eight-ohm short between two adjacent pins. The bond wires to the pins of interest were cut with no effect on the short as measured at the external pins, indicating that the short was present in the package. Initial attempts to identify the failure with conventional radiographic analysis were unsuccessful. Arguably the most difficult part of the procedure is identifying the physical location of the short with a high enough degree of confidence to permit destructive techniques to be used to reveal the shorting material. Fortunately, two analytical techniques are now available that can significantly increase the effectiveness of the fault localization process.

Superconducting Quantum Interference Device (SQUID) Detection

One characteristic that all shorts have in common is the movement of electrons from a high potential to a lower one. This physical movement of the electrical charge creates a small magnetic field around the electron. With enough electrons moving, the aggregate magnetic field can be detected by superconducting sensors. Instruments equipped with

such sensors can follow the path of a short circuit along its course through a part. The SQUID detector has been used in failure analysis for many years, and is now commercially available for use at the package level. The ability of SQUID to track the flow of current provides a virtual roadmap of the short, including the location in plan view of the shorting material in a package. We used the SQUID facilities at Neocera to investigate the failure in the package of interest, with pins carrying 1.47 milliamps at 2 volts. SQUID analysis of the part revealed a clear current path between the two pins of interest, including the location of the conductive material that bridged the two pins. The SQUID scan of the part is shown in Figure 1.

Low-power radiography

The second fault location technique will be taken somewhat out of turn, as it was used to characterize this failure after the SQUID analysis, as an evaluation sample for an equipment vendor. The ability to focus and resolve low-power x-rays and detect their presence or absence has improved to the point that radiography can now be used to identify features heretofore impossible to detect. The equipment at Xradia was used to inspect the failure of interest in this analysis. An example of their findings is shown in Figure 2. The feature shown (which is also the material responsible for the failure) is a copper filament approximately three micrometres wide in cross-section, which was impossible to resolve in our in-house radiography equipment.

The principal drawback of this technique is that the depth of field is extremely short, requiring many ‘cuts’ on a given specimen to detect very small particles or filaments. At the high magnification required to resolve micrometre-sized features, the technique can become prohibitively expensive in both time and money to perform. In effect, to get the most out of it, the analyst really needs to know already where the failure is located. This makes low-power radiography a useful supplement to SQUID, but not a generally effective replacement for it. It would likely best be used immediately after SQUID to characterize morphology and depth of the shorting material once SQUID had pinpointed its location.

Short in a 3D Package

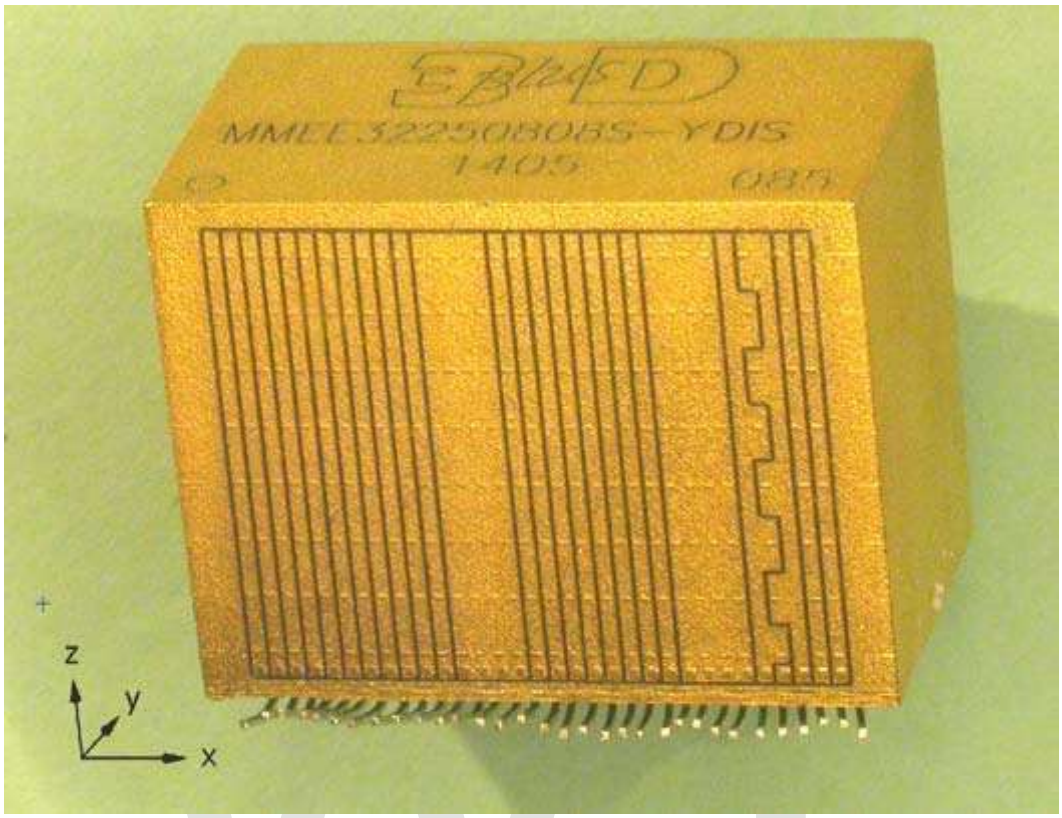

Figure 1: An external view of the EEPROM module shows the coordinate axis used while performing orthogonal magnetic current imaging. These axes are used to define the scanning planes in the body of the paper.

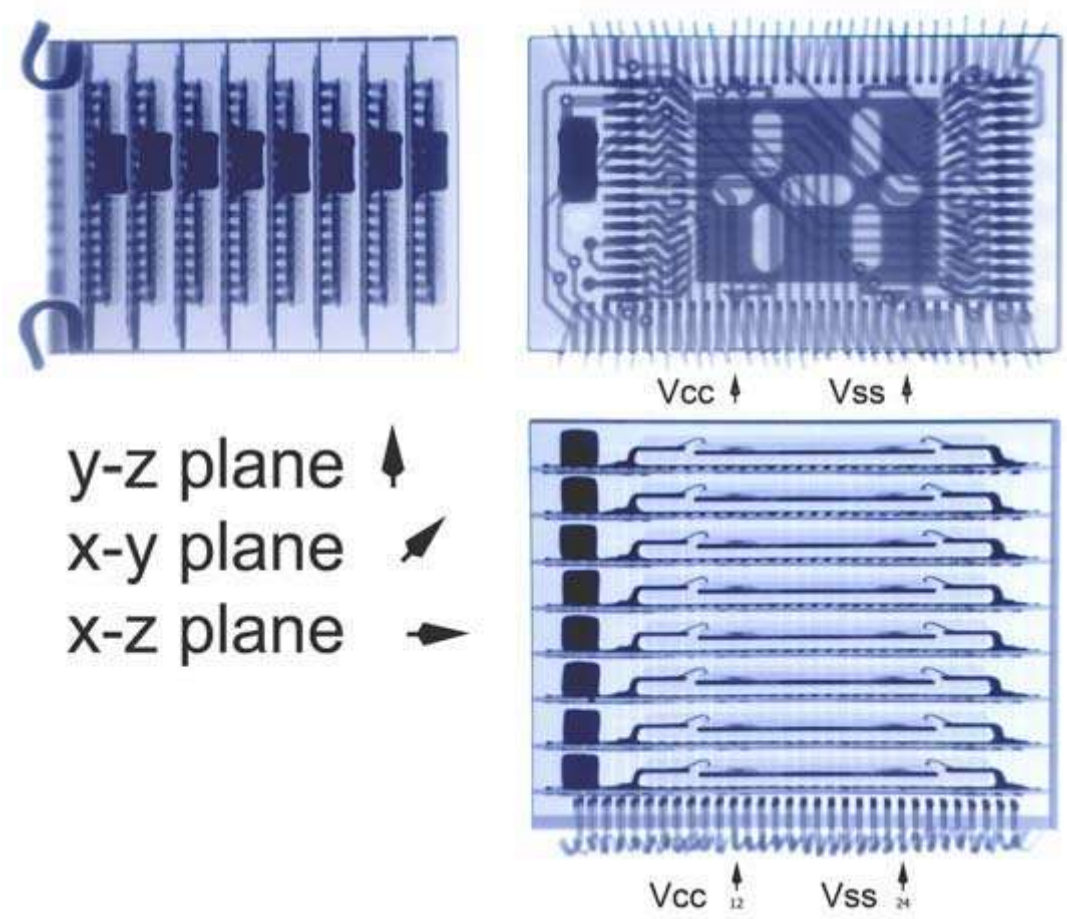

Figure 2: Radiography, showing three orthogonal views of the part, reveals internal construction of the module.

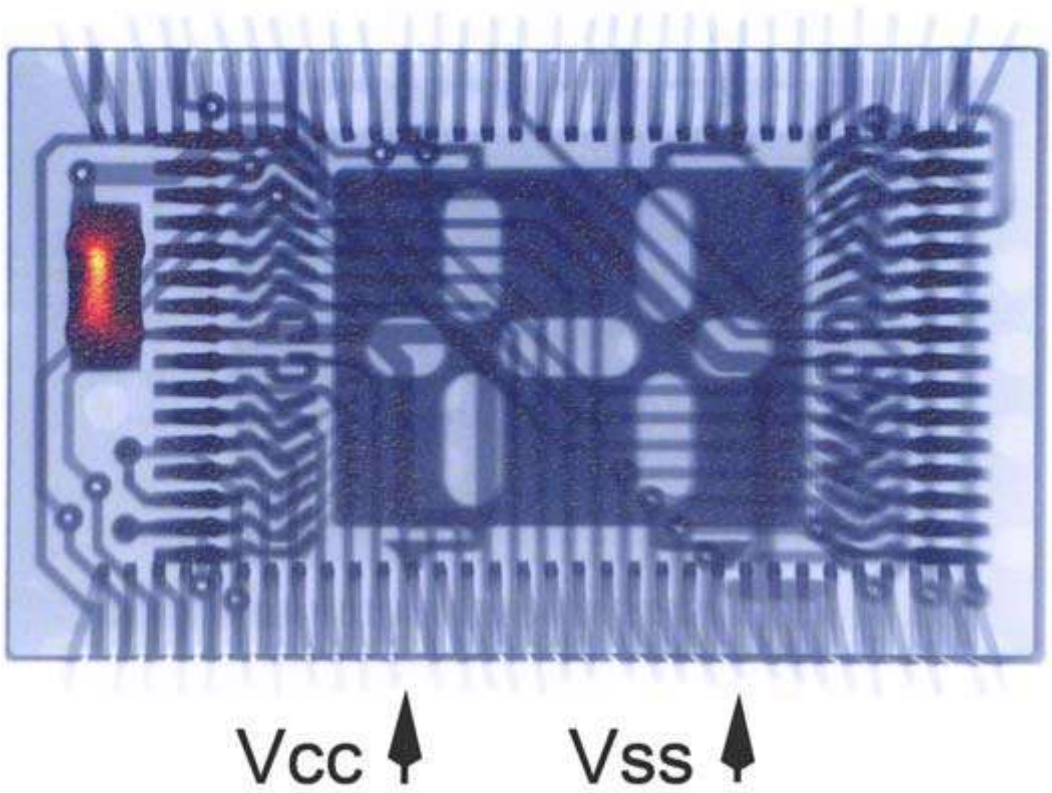

Figure 3: A magnetic current image overlay on an x-ray image of the EEPROM module. Thresholding was used to show only the strongest current at the capacitor of the TSOP08 mini-board. Arrows indicate Vcc and Vss pins. This image is in the x-y plane.

Initial Failure Analysis Examination of the module shown in Figure 1 in the Failure Analysis Laboratory found no external evidence of the failure. Coordinate axes of the device were chosen as shown in Figure 1. Radiography was performed on the module in three orthogonal views: side, end, and top-down; as shown in Figure 2. For purposes of this paper the top-down x-ray view shows the x-y plane of the module. The side view shows the x-z plane, and the end view shows the y-z plane. No anomalies were noted in the radiographic images. Excellent alignment of components on the mini-boards permitted an uncluttered top-down view of the mini-circuit boards. The internal construction of the module was seen to consist of eight, stacked mini-boards, each with a single microcircuit and capacitor. The mini-boards connected with the external module pins using the gold-plated exterior of the package. External inspection showed that laser-cut trenches created an external circuit on the device, which is used to enable, read, or write to any of the eight EEPROM devices in the encapsulated vertical stack. Regarding nomenclature, the laser-trenched gold panels on the exterior walls of the package were labeled with the pin numbers. The eight miniboards were labeled TSOP01 through TSOP08, beginning at the bottom of the package near the device pins.

Pin-to-pin electrical testing confirmed that Vcc Pins 12, 13, 14, and 15 were electrically common, presumably through the common exterior gold panel on the package wall.

Likewise, Vss Pins 24, 25, 26, and 27 were common. Comparison to the xray images showed that these four pins funneled into a single wide trace on the mini-boards. All of the Vss pins were shorted to the Vcc pins with a resistance determined by the I-V slope at approximately 1.74 ohms, the low resistance indicating something other than an ESD defect. Similarly electrical overstress was considered an unlikely cause of failure as the part had not been under power since the time it was qualified at the factory. The three-dimensional geometry of the EEPROM module suggested the use of magnetic current imaging (MCI) on three, or more flat sides in order to construct the current path of the short within the module. As noted, the coordinate axes selected for this analysis are shown in Figure 1.

Magnetic Current Imaging SQUIDs are the most sensitive magnetic sensors known. This allows one to scan currents of 500 nA at a working distance of about 400 micrometres. As for all near field situations, the resolution is limited by the scanning distance or, ultimately, by the sensor size (typical SQUIDs are about 30 μm wide), although software and data acquisition improvements allow locating currents within 3 micrometres. To operate, the SQUID sensor must be kept cool (about 77 K) and in vacuum, while the sample, at room temperature, is raster-scanned under the sensor at some working distance z, separated from the SQUID enclosure by a thin, transparent diamond window. This allows one to reduce the scanning distance to tens of micrometres from the sensor itself, improving the resolution of the tool.

The typical MCI sensor configuration is sensitive to magnetic fields in the perpendicular z direction (i.e., sensitive to the in-plane xy current distribution in the DUT). This does not mean that we are missing vertical information; in the simplest situation, if a current path jumps from one plane to another, getting closer to the sensor in the process, this will be revealed as stronger magnetic field intensity for the section closer to the sensor and also as higher intensity in the current density map. This way, vertical information can be extracted from the current density images.

Chapter- 7

Chemical Force Microscopy & Near-Field Scanning Optical Microscope

Chemical force microscopy

Figure 1: Photograph of an AFM system which can be used for chemical force microscopy.

Chemical force microscopy (CFM) is a variation of atomic force microscopy (AFM) which has become a versatile tool for characterization of materials surfaces. With AFM, structural morphology is probed using simple tapping or contact modes that utilize van der Waals interactions between tip and sample to maintain a constant probe deflection amplitude (constant force mode) or maintain height while measuring tip deflection (constant height mode). CFM, on the other hand, uses chemical interactions between functionalized probe tip and sample. Choice chemistry is typically gold-coated tip and surface with R-SH thiols attached, R being the functional groups of interest. CFM enables the ability to determine the chemical nature of surfaces, irrespective of their specific morphology, and facilitates studies of basic chemical bonding enthalpy and surface energy. Typically, CFM is limited by thermal vibrations within the cantilever holding the probe. This limits force measurement resolution to ~1 pN which is still very suitable considering weak COOH/CH_3 interactions are ~20 pN per pair. Hydrophobicity is used as the primary example throughout this consideration of CFM, but certainly any type of bonding can be probed with this method.

Pioneering work

CFM has been primarily developed by Charles Lieber at Harvard University in 1994. The method was demonstrated using hydrophobicity where polar molecules (e.g. COOH) tend to have the strongest binding to each other, followed by nonpolar (e.g. CH_3-CH_3) bonding, and a combination being the weakest. Probe tips are functionalized and substrates patterned with these molecules. All combinations of functionalization were tested, both by tip contact and removal as well as spatial mapping of substrates patterned with both moieties and observing the complementarity in image contrast. Both of these methods are discussed below. The AFM instrument used is similar to the one in Figure 1.

Force of adhesion (tensile testing)

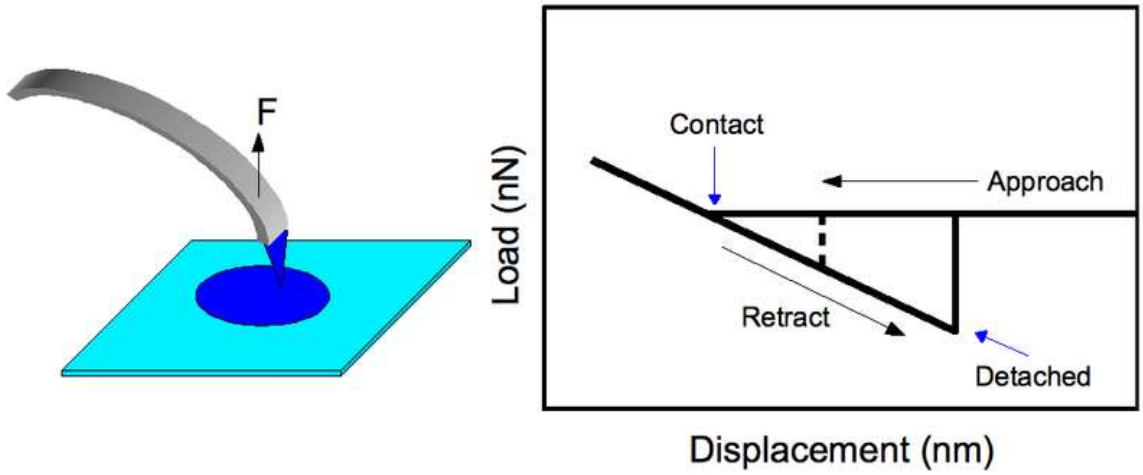

Figure 2: (Left) Probe tip being pulled from a similarly functionalized patterned area on the substrate to determine adhesion force. (Right) Typical force profile for adhesion force measurements. The dashed line is indicative of detachment for less probe-substrate interaction versus the solid line.

This is the simpler mode of CFM operation where a functionalized tip is brought in contact with the surface and is pulled to observe the force at which separation occurs, F_{ad} (see Figure 2). The Johnson-Kendall-Roberts (JKR) theory of adhesion mechanics predicts this value as

(1) $$F_{ad} = \frac{3}{2}\pi R W_{STM}$$

where $W_{SMT} = \gamma_{SM}+\gamma_{TM}-\gamma_{ST}$ with R being the radius of the tip, and γ being various surface energies between the tip, sample, and the medium each is in (liquids discussed below). R is usually obtained from SEM and γ_{SM} and γ_{TM} from contact angle measurements on substrates with the given moieties. When the same functional groups are used, $\gamma_{SM} = \gamma_{TM}$ and $\gamma_{ST} = 0$ which results in $F_{ad} = 3\pi R\gamma_{SM, TM}$. Doing this twice with two different moieties (e.g. COOH and CH_3) gives values of γ_{SM} and γ_{TM}, both of which can be used together in the same experiment to determine γ_{ST}. Therefore, F_{ad} can be calculated for any combination of functionalities for comparison to CFM determined values.

For similarly functionalized tip and surface, at tip detachment JKR theory also predicts a contact radius of

(2) $$r = \left(\frac{3\pi\gamma R^2}{K}\right)^{\frac{1}{3}}$$

with an "effective" Young's modulus of the tip $K=(2/3)(E/(1-\nu^2))$ derived from the actual value E and the Poisson ratio ν. If one knows the effective area of a single functional group, A_{FG} (e.g. from quantum chemistry simulations), the total number of ligands participating in tension can be estimated as $\pi r^2/A_{FG}$. As stated earlier, the force resolution of CFM does allow one to probe individual bonds of even the weakest variety, but tip curvature typically prevents this. Using Eq 2, a radius of curvature R<10 nm has been determined as the requirement to conduct tensile testing of individual linear moieties.

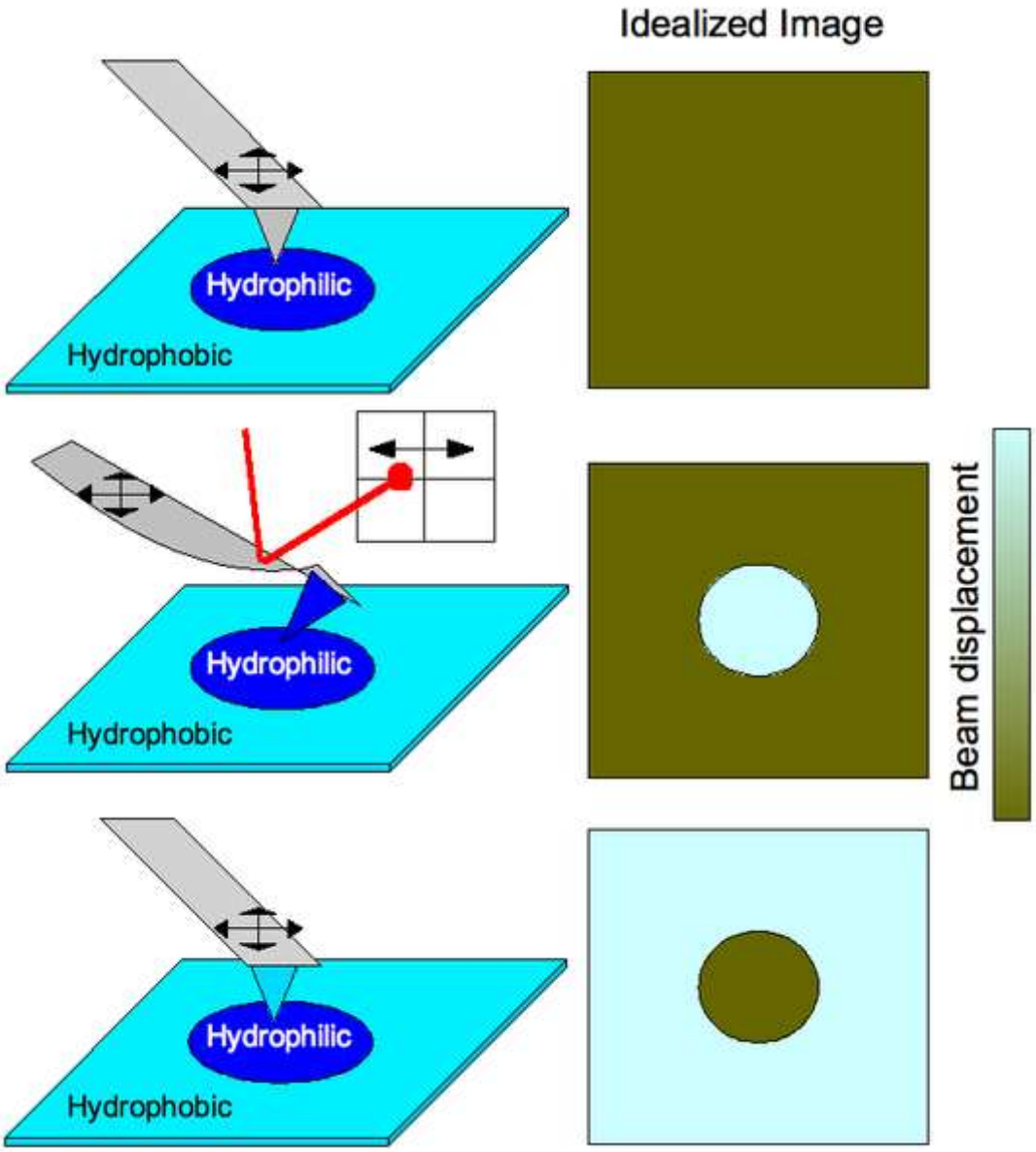

Figure 3: (Top) Scan of a patterned surface with regular tip (no functional groups) would produce an image with no contrast because the surface is morphologically uniform. (Middle) A hydrophilic tip on the hydrophilic functionalized portion of the surface causes the cantilever to bend due to strong interactions which is detected by laser deflection therefore producing a chemical profile image of the surface. (Bottom) Cantilever functionalization is switched such that the tip is bent when encountering hydrophobic areas of the substrate instead.

A quick note to mention is the work corresponding to the hysteresis in the force profile (Figure 2) does not correlate to the bond energy. The work done in retracting the tip is $W = \int F dx \approx \frac{1}{2} F_{max} \Delta x$, approximated due to the linear behavior of deformation

with F_{max} being the force and Δx being the displacement immediately before release. Using the results of Frisbie et al., normalized to the estimated 50 functional groups in contact, the work values are estimated as 39 eV, 0.25 eV, and 4.3 eV for COOH/COOH, $COOH/CH_3$, and CH_3/CH_3 interactions, respectively. Roughly, intermolecular bond energies can be calculated by: $E_{bond}=kT_B$, T_B being the boiling point. According to this, E_{bond} = 32.5 meV for formic acid, HCOOH, and 9.73 meV for methane, CH_4, each value being about 3 orders of magnitude smaller than the experiment might suggest. Even if surface passivation with EtOH were considered (discussed below), the large error seems irrecoverable. The strongest hydrogen bonds are at most ~1 eV in energy. This strongly implies that the cantilever has a force constant smaller than or on the order of that for bond interactions and, therefore, it cannot be treated as perfectly rigid. This does open an avenue for increasing the usefulness of CFM if stiffer cantilevers can be used while still maintaining force resolution.

Frictional force mapping

Chemical interactions can also be used to map prepatterned substrates with varying functionalities (see Figure 3). Scanning of a surface having varying hydrophobicity with a tip having no functional groups attached would produce an image with no contrast because the surface is morphologically featureless (simple AFM operation). Functionalizing a tip to be hydrophilic would cause the cantilever to bend when the tip scans across hydrophilic portions of the substrate due to strong tip-substrate interactions. This is detected by laser deflection in a position sensitive detector therefore producing a chemical profile image of the surface. Generally, a brighter area would correspond to a greater amplitude of deflection so stronger bonding corresponds to lighter areas of a CFM image map. When the cantilever functionalization is switched such that the tip is bent when encountering hydrophobic areas of the substrate instead, the complementary image is observed.

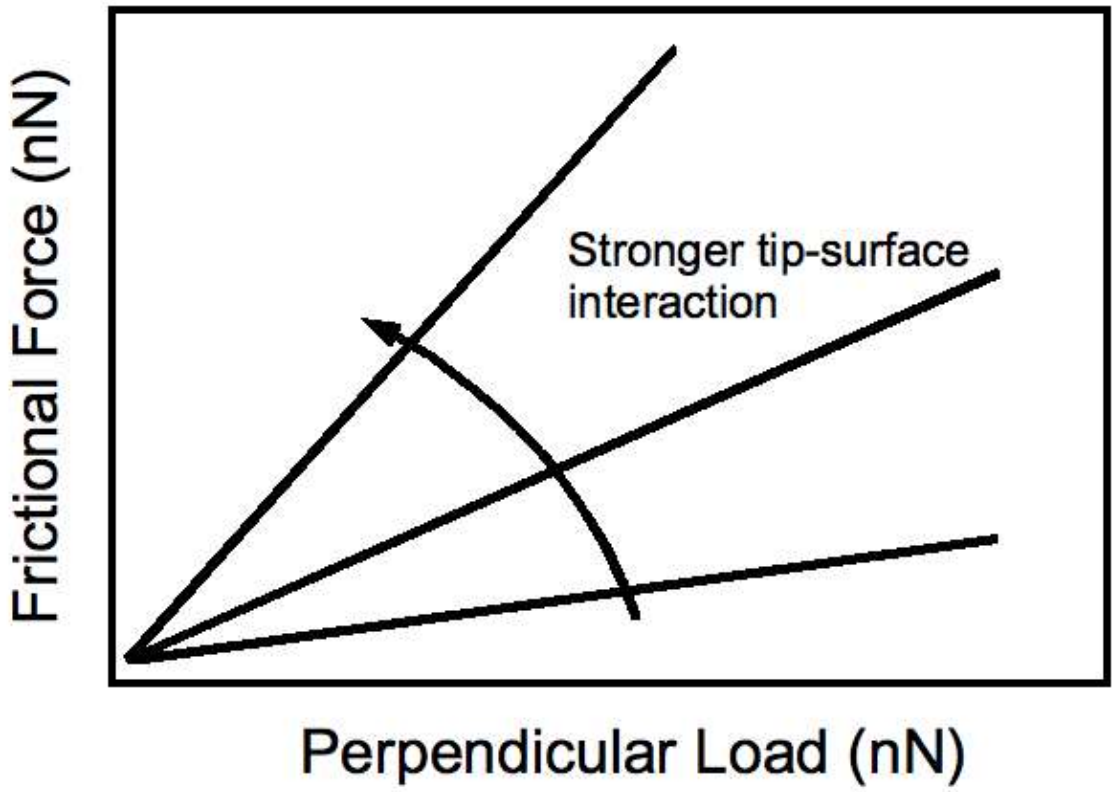

Figure 4: Typical response of frictional force to applied load by the tip. Stronger tip-substrate interactions result in steeper slopes.

Frictional force response to the amount of perpendicular load applied by the tip on to the substrate is shown in Figure 4. Increasing tip-substrate interactions produce a steeper slope, as one would expect. Of experimental importance is the fact that contrast between different functionalities on the surface may be enhanced with an application of greater perpendicular force. Of course, this comes at the cost of potential damage to the substrate.

Ambient: measurements in liquids

Capillary force is a major problem in tensile force measurements since it effectively strengthens the tip-surface interaction. It is usually caused by adsorbed moisture on substrates from ambient environment. To eliminate this additional force, measurements in liquids can be conducted. With X-terminated tip and substrate in liquid L, the addition to F_{ad} is calculated using Eq 1 with $W_{XLX} = 2\gamma_{LL}$; that is, the extra force comes from the attraction of liquid molecules to each other. This is ~10 pN for EtOH which still allows for the observation of even the weakest polar/nonpolar interactions (~20 pN). The choice of liquid is dependent on which interactions are of interest. When the solvent is immiscible with functional groups, larger than usual tip-surface bonding exists. Therefore, organic solvents are appropriate for studying van der Waals and hydrogen bonding while electrolytes are best for probing hydrophobic and electrostatic forces.

Applications in nanoscience

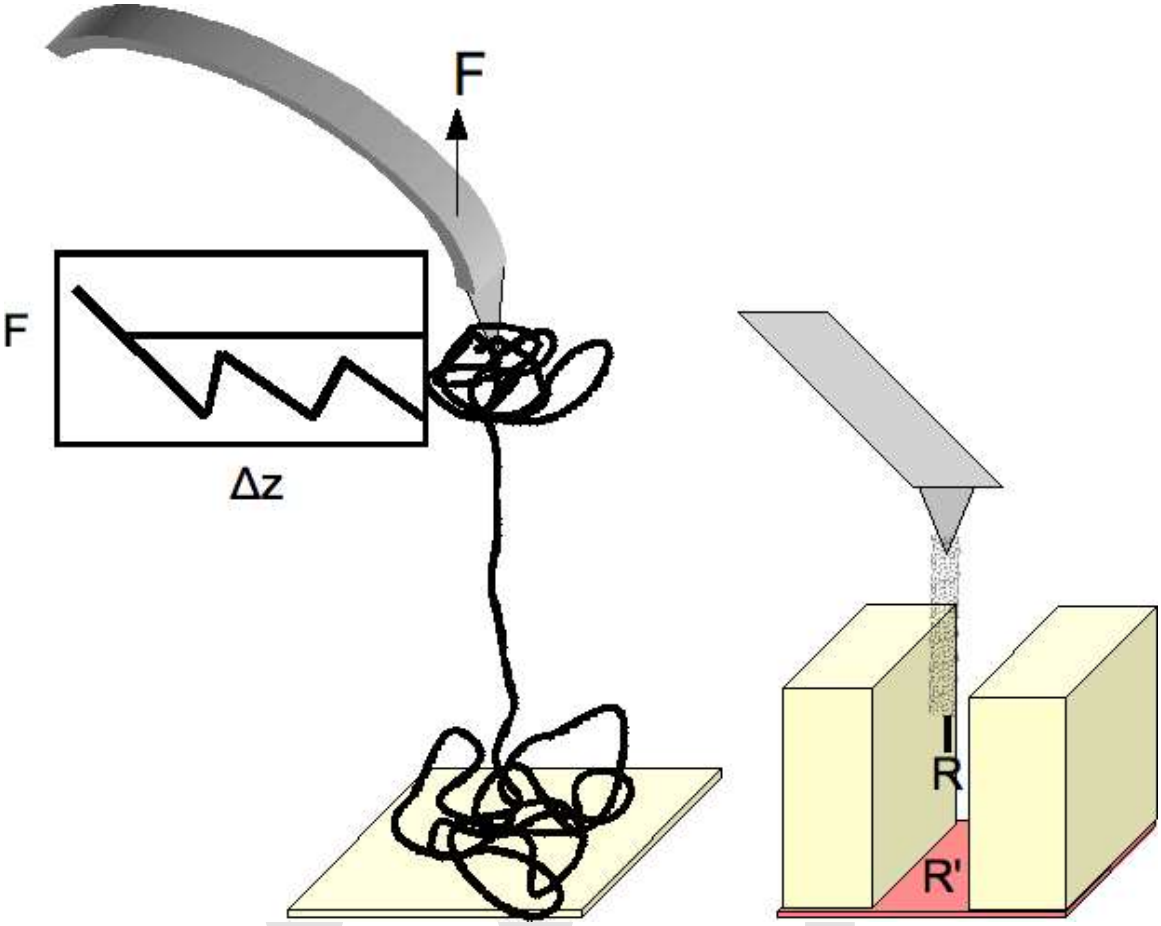

Figure 5: (Left) Utilizing CFM for the unfolding of complex proteins. The force response during strain is shown. (Right) Carbon nanotube terminated tip functionalized at the nanotube end.

A biological implementation of CFM at the nanoscale level is the unfolding of proteins with functionalized tip and surface (see Figure 5). Due to the increased contact area, the tip and the surface act as anchors holding protein bundles while they separate. As uncoiling ensues, the force required jumps indicating various stages of uncoiling: (1) separation into bundles, (2) bundle separation into domains of crystalline protein held together by van der Waals forces, and (3) linearization of the protein upon overcoming the secondary bonding. Information on the internal structure of these complex proteins, as well as a better understanding of constituent interactions are provided with this method.

A second consideration is one that takes advantage of unique nanoscale materials properties. The high aspect ratio of carbon nanotubes (easily >1000) is exploited to image surfaces with deep features.. The use of the carbon material broadens the functionalization chemistry since there are countless routes to chemical modification of nanotube sidewalls (e.g. with diazonium, simple alkyls, hydrogen, ozone/oxygen, and amines). Multiwall nanotubes are typically used for their rigidity. Because of their

approximately planar ends, one can estimate the number of functional groups that are in contact with the substrate knowing tube diameter and number of walls which helps in determining single moiety tensile properties. Certainly, this method has obvious implications in tribology as well.

Near-field scanning optical microscope

Near-field scanning optical microscopy (**NSOM**/**SNOM**) is a microscopic technique for nanostructure investigation that breaks the far field resolution limit by exploiting the properties of evanescent waves. This is done by placing the detector very close (distance much smaller than wavelength λ) to the specimen surface. This allows for the surface inspection with high spatial, spectral and temporal resolving power. With this technique, the resolution of the image is limited by the size of the detector aperture and not by the wavelength of the illuminating light. In particular, lateral resolution of 20 nm and vertical resolution of 2–5 nm have been demonstrated. As in optical microscopy, the contrast mechanism can be easily adapted to study different properties, such as refractive index, chemical structure and local stress. Dynamic properties can also be studied at a sub-wavelength scale using this technique.

NSOM/SNOM is a form of scanning probe microscopy.

History

E.H. Synge, a scientist, is given credit for conceiving and developing the idea for an imaging instrument that would image by exciting and collecting diffraction in the near field. His original idea, proposed in 1928, was based upon the usage of intense nearly planar light from an arc under pressure behind a thin, opaque metal film with a small orifice of about 100 nm. The orifice was to remain within 100 nm of the surface, and information was to be collected by point-by-point scanning. He foresaw the illumination and the detector movement being the biggest technical difficulties. John A. O'Keefe also developed similar theories in 1956. He thought the moving of the pinhole or the detector when it is so close to the sample would be the most likely issue that could prevent the realization of such an instrument. It was Ash and Nichols who, in 1972, first broke the Abbe's diffraction limit using radiation with wavelength of 3 cm. A line grating was resolved with a resolution of $\lambda_0/60$. It was twelve more years before the first papers that used visible radiation for near field scanning were published by Pohl et al., and Lewis et al. Both these works involved the use of a subwavelength metal coated optical aperture at the tip of a sharp pointed probe, and a feedback mechanism to maintain a constant distance of a few nanometers between the sample and the probe. Resolution as low as 25 nm (about $\lambda_0/20$) was achieved.

Theory

According to Abbe's Theory of Image Formation, developed in 1873, the resolving capability of an optical component is ultimately limited by the spreading out of each

image point due to diffraction. Unless the aperture of the optical component is large enough to collect all the diffracted light, the finer aspects of the image will not correspond exactly to the object. The minimum resolution (d) for the optical component are thus limited by its aperture size, and expressed by the Rayleigh criterion:

$$d = 0.61\frac{\lambda}{NA}$$

Here, λ_0 is the wavelength in vacuum; NA is the numerical aperture for the optical component (usually 1.3–1.4 for modern objectives). Thus, the resolution limit is usually around $\lambda_0/2$ for conventional optical microscopy.

This treatment only assumes the light diffracted into the far-field that propagates without any restrictions. NSOM makes use of evanescent or non propagating fields that exist only near the surface of the object. These fields carry the high frequency spatial information about the object and have intensities that drop off exponentially with distance from the object. Because of this, the detector must be placed very close to the sample in the near field zone, typically a few nanometers. As a result, near field microscopy remains primarily a surface inspection technique. The detector is then rastered across the sample using a piezoelectric stage. The scanning can either be done at a constant height or with regulated height by using a feedback mechanism.

Modes of operation

Aperture and apertureless operation

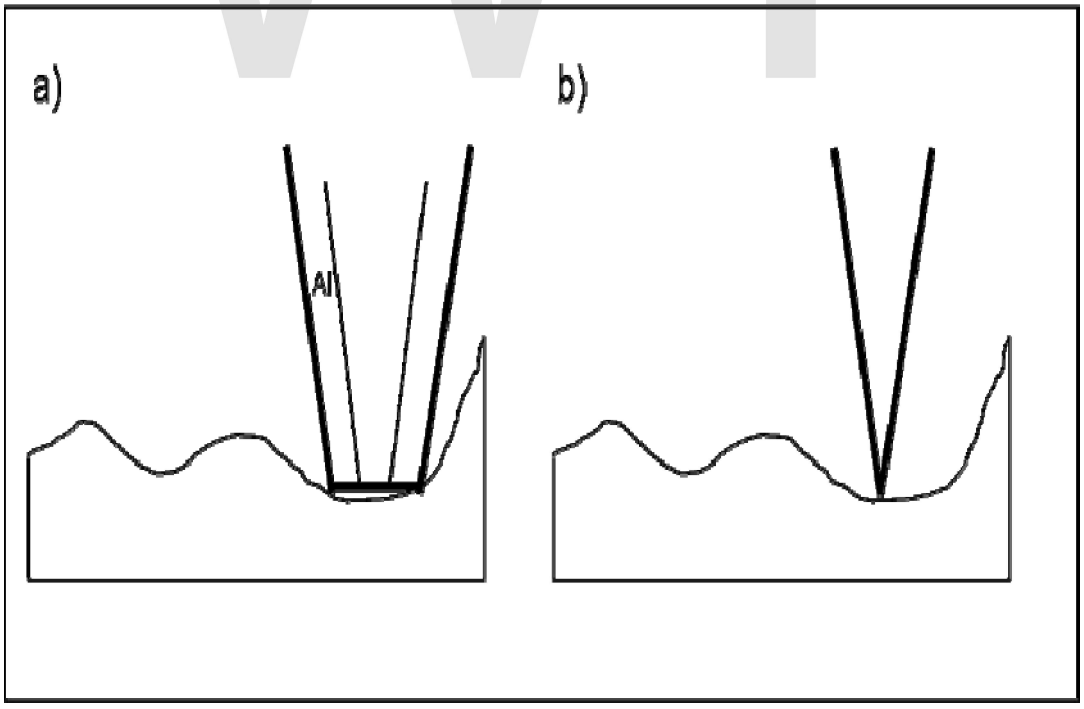

Sketch of a) typical metal-coated tip, and b) sharp uncoated tip.

NSOM can be operated in both an aperture and a non-aperture mode. As illustrated, the tips used in the apertureless mode are very sharp and do not have a metal coating.

Though there are many issues associated with the apertured tips (heating, artifacts, contrast, sensitivity, topology and interference amongst others), aperture mode remains more popular. This is primarily because apertureless mode is even more complex to set up and operate, and is not understood as well. There are five primary modes of apertured NSOM operation and four primary modes of apertureless NSOM operation. The major ones are illustrated in the next figure.

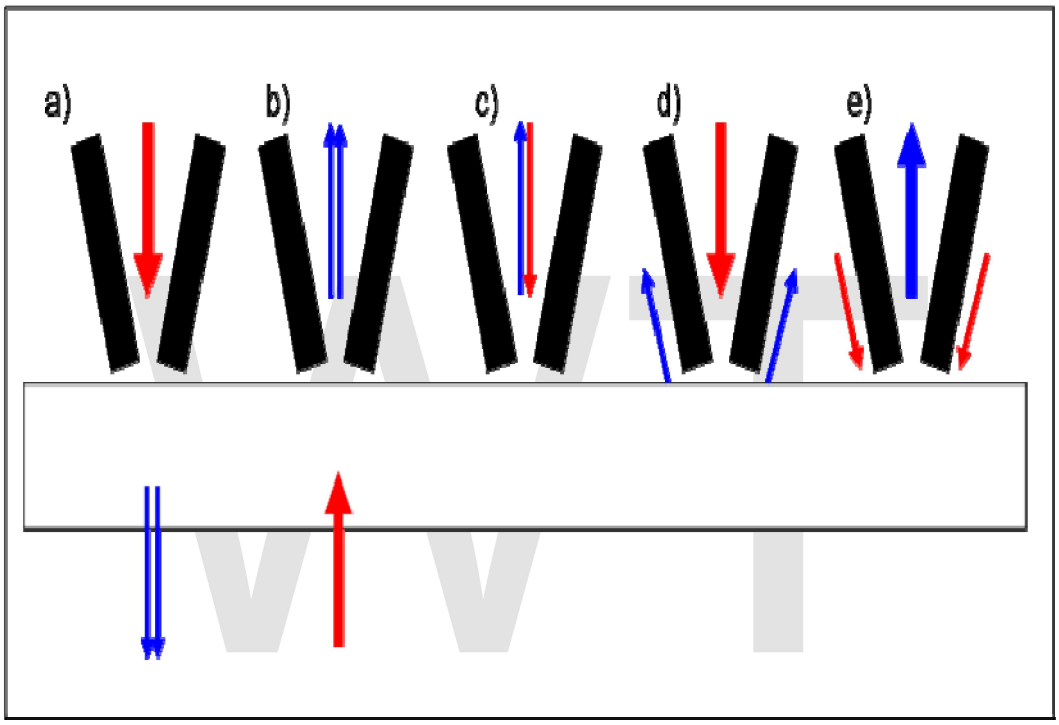

Apertured modes of operation: a) illumination, b) collection, c) illumination collection, d) reflection and e) reflection collection.

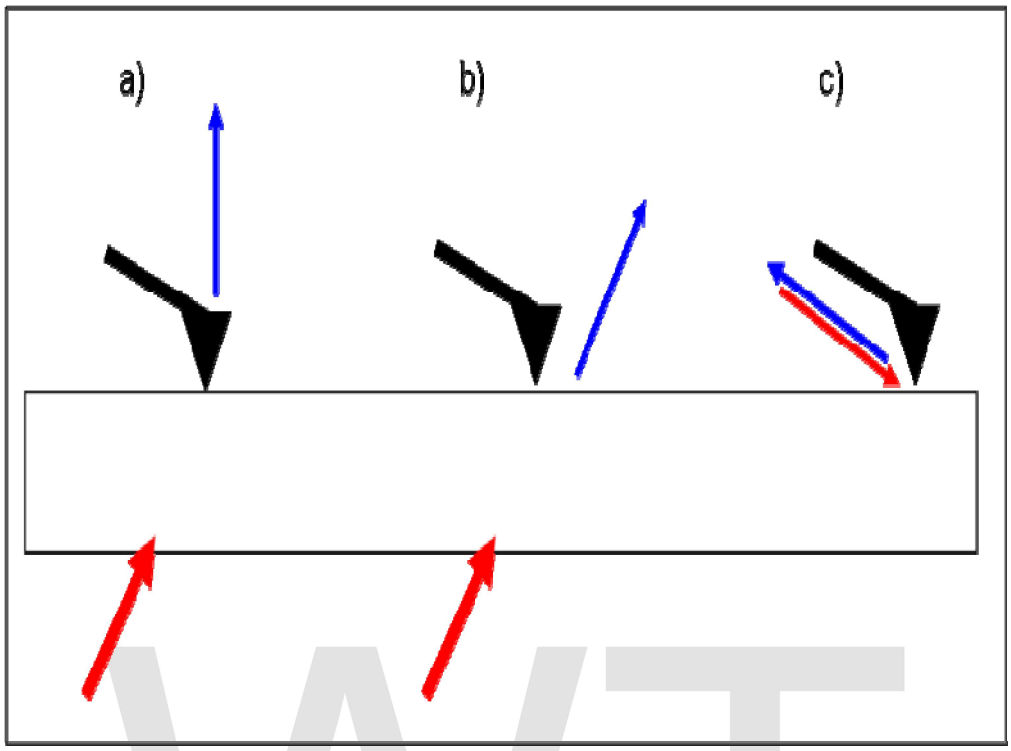

Apertureless modes of operation: a) photon tunneling (PSTM) by a sharp transparent tip, b) PSTM by sharp opaque tip on smooth surface, and c) scanning interferometric apertureless microscopy with double modulation.

Feedback mechanisms

Feedback mechanisms are usually used to achieve high resolution and artifact free images since the detector must be positioned within a few nanometers of the surfaces. Some of these mechanisms are:

- Constant force feedback: This mode is very similar to the feedback mechanism used in atomic force microscope (AFM). Experiments can be performed in contact, intermittent contact, and non-contact modes.
- Shear force feedback: In this mode, a tuning fork is mounted alongside the tip and made to oscillate at its resonance frequency. The amplitude is closely related to the tip-surface distance, and thus used as a feedback mechanism.

Contrast

It is possible to take advantage of the various contrast techniques available to optical microscopy though NSOM but with much higher resolution. By using the change in the polarization of light or the intensity of the light as a function of the incident wavelength, it is possible to make use of contrast enhancing techniques such as staining, fluorescence, phase contrast and differential interference contrast. It is also possible to provide contrast

using the change in refractive index, reflectivity, local stress and magnetic properties amongst others.

Instrumentation and standard setup

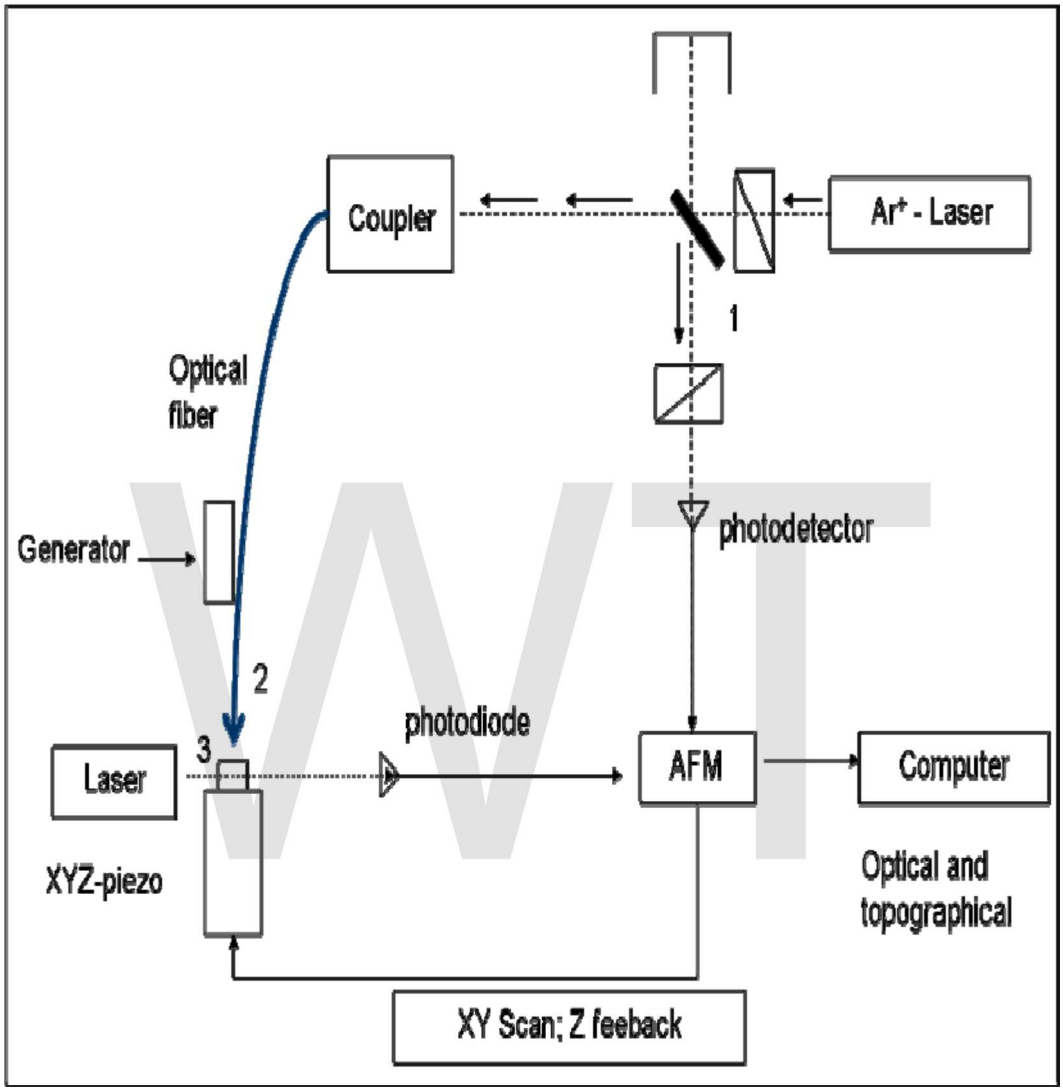

Block diagram of an apertureless reflection-back-to-the-fiber NSOM setup with shear-force distance control and cross-polarization; 1: beam splitter and crossed polarizers; 2: shear-force arrangement; 3: sample mount on a piezo stage.

The primary components of an NSOM setup are the light source, feedback mechanism, the scanning tip, the detector and the piezoelectric sample stage. The light source is usually a laser focused into an optical fiber through a polarizer, a beam splitter and a coupler. The polarizer and the beam splitter would serve to remove stray light from the returning reflected light. The scanning tip, depending upon the operation mode, is usually a pulled or stretched optical fiber coated with metal except at the tip or just a standard AFM cantilever with a hole in the center of the pyramidal tip. Standard optical detectors, such as avalanche photodiode, photomultiplier tube (PMT) or CCD, can be used. Highly

specialized NSOM techniques, Raman NSOM for example, have much more stringent detector requirements.

Near-field spectroscopy

As the name implies, information is collected by spectroscopic means instead of imaging in the near field regime. Through Near Field Spectroscopy (NFS), one can probe spectroscopically with subwavelength resolution. Raman SNOM and fluorescence SNOM are two of the most popular NFS techniques as they allow for the identification of nanosized features with chemical contrast. Some of the common near field spectroscopic techniques are:

- *Direct Local Raman NSOM:* Aperture Raman NSOM is limited by very hot and blunt tips, and by long collection times. However, apertureless NSOM can be used to achieve high Raman scattering efficiency factors (around 40). Topological artifacts make it hard to implement this technique for rough surfaces.
- *Surface Enhanced Raman Spectroscopy (SERS) NSOM:* This technique can be used in an apertureless shear-force NSOM setup, or by using an AFM tip coated with gold. The Raman signal is found to be significantly enhanced under the AFM tip. This technique has been used to give local variations in the Raman spectra under a single-walled nanotube. A highly sensitive optoacoustic spectrometer must be used for the detection of the Raman signal.
- *Fluorescence NSOM:* This highly popular and sensitive technique makes use of the fluorescence for near field imaging, and is especially suited for biological applications. The technique of choice here is the apertureless back to the fiber emission in constant shear force mode. This technique uses merocyanine based dyes embedded in an appropriate resin. Edge filters are used for removal of all primary laser light. Resolution as low as 10 nm can be achieved using this technique.
- *Near Field Infrared Spectrometry and Near Field Dielectric Microscopy*

Artifacts

NSOM is particularly vulnerable to artifacts that are not from the intended contrast mode. The most common root for artifacts in NSOM are:

- Tip Breakage During Scanning
- Striped Contrast
- Displaced Optical Contrast
- Local Far Field Light Concentration
- Topological Artifacts

Limitations

- Very low working distance and extremely shallow depth of field.
- Limited to study of surfaces.

- Not conducive for studying soft materials, especially under shear force mode.
- Long scan times for large sample areas or high resolution imaging.

Chapter- 8

Scanning Joule Expansion Microscopy

Scanning Joule Expansion Microscopy is a form of scanning probe microscopy heavily based on atomic force microscopy that maps the temperature distribution along a surface. Resolutions down to 10 nm have been achieved and 1nm resolution is theoretically possible. Thermal measurements at the nanometer scale are of both academic and industrial interest, particularly in regards to nanomaterials and modern integrated circuits.

Basic Principles

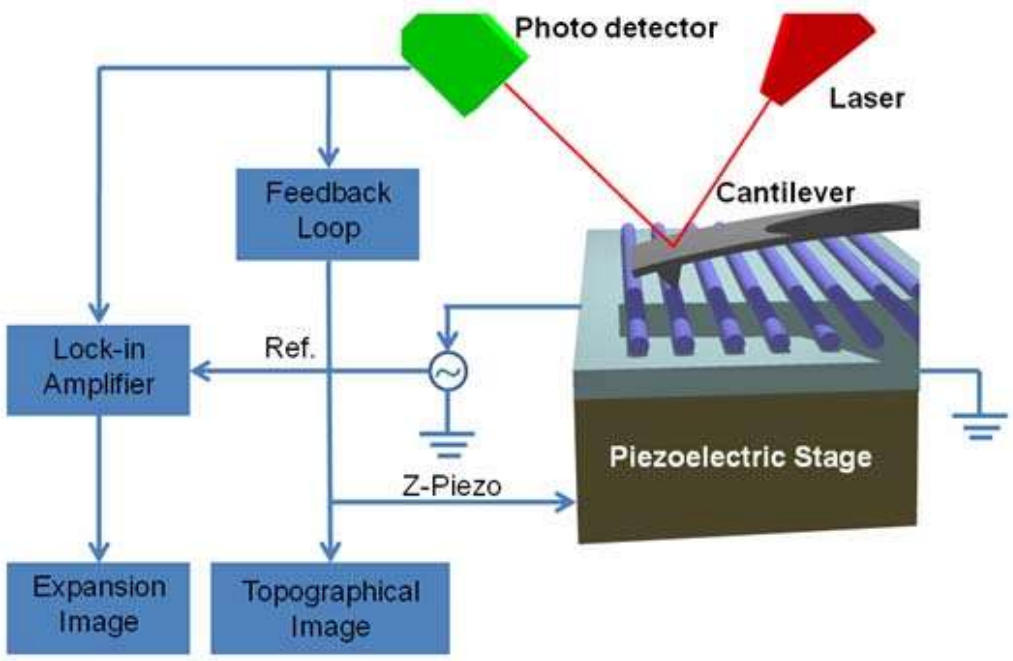

Simplified schematic of Scanning Joule expansion microscope.

Scanning Joule Expansion Microscopy (SJEM) is based on the contact operation model of Atomic Force Microscopy (AFM). During the operation, the tip on the cantilever is brought into contact with the surface of the sample. AC or pulsed electrical signal is applied to the sample creating Joule heating and resulting in periodic thermal expansion. At the same time, the laser, which is focused on the top surface of the cantilever and the photodiode of the equipment, detects the displacement of the cantilever. The detecting photodiode is composed of two segments, which normalizes the incoming signal deflected from the cantilever. This differential signal is proportional to the cantilever deflection.

The deflection signals are caused not only by sample topography, but also by the thermal expansion caused by Joule heating. Since AFM has feedback controller with a bandwidth, for example 20 kHz (different AFM may have different bandwidths), the signal below 20 kHz is captured and processed by the feedback controller which then adjusts the z-piezo to image surface topography. Joule heating frequency is kept well above 20 kHz to avoid feedback response and to separate topological and thermal effects. The upper limit of the frequency is limited by the decrease of thermoelastic expansion with the inverse power of the modulation frequency and the frequency characteristics of the cantilever arrangement. A lock-in amplifier is specially tuned to the Joule heating frequency for detecting only the expansion signal and provides the information to an auxiliary Atomic Force Microscopy channel to create the thermal expansion image. Usually expansion signals approximately 0.1 Angstroms start to be detected, although the resolution of SJEM highly depends on the whole system (cantilever, sample surface, etc).

By comparison, Scanning Thermal Microscopy (SThM) has coaxial thermocouple at the end of sharp metal tip. The spatial resolution of SThM critically depends on the thermocouple sensor size. Much effort has been dedicated to reducing sensor size to sub-micron scales. The quality and resolution of the images are very dependent on the nature of the thermal contact between tip and the sample; hence it is quite difficult to control in a reproducible way. The fabrication also becomes very challenging particularly for thermocouple sensor size below 500 nm. With optimization on the design and the fabrication, it was possible to achieve resolution around 25 nm. Scanning Joule Expansion Microscopy, however, has the potential of achieving similar to AFM resolution of 1~10 nm. In practice, however, the spatial resolution is limited to the size of the liquid film bridge between the tip and the sample, which is typically about 20 nm. The microfabricated thermocouples used for Scanning Thermal Microscopy are rather expensive and more importantly very fragile. Scanning Joule Expansion Microscopy has been used to measure the local heat dissipation of an in-plane gate (IPG) transistor to study hot spots in semiconductor devices, and thin-film alloy like cobalt-nickel silicide.

Signal acquisition and analysis

Signal obtained by the AFM (and captured by lock-in amplifier) are actually representations of the cantilever deflection at a specific frequency. However, besides thermal expansion, several other sources may also result in cantilever deflection.

Thermally induced cantilever bending

This is usually due to the mismatch in thermal expansion of two cantilever materials, for instance, silicon cantilever coated with a thin layer of metal (to increase the deflection). When heated, materials with higher expansion coefficient will expand more than the material with lower expansion coefficient. In this case, two materials, one in tensile strain, the other in compression strain, will induce substantial bending. However, this mechanism can be excluded for two reasons; first, cantilever coatings have been stripped experimentally and no change in signal was observed; second, the calculated thermal diffusion length in SiNx and Si cantilevers at the SJEM working frequency (typically 10KHZ~100KHZ) is small, much smaller than the length of the cantilever(typically 100 um).

Pressure waves

When the sample heats and contracts due to rapid Joule heating from an applied AC power source, pressure waves may be radiated from the sample. This wave may interact with the cantilever, causing additional deflection. However, this possibility is unlikely. For sinusoidal heating, the wavelength of the acoustic wave in air with speed of 340 m/s is about several millimeters, which is much larger than the length of cantilever. Furthermore, experiments have been carried out under vacuum, in which case there are no air pressure waves. In the experiment, it was observed that when the cantilever was out of contact with sample surface, no deflection signal was detected.

Piezoelectric effect

In piezoelectric materials, mechanical expansion occurs due to applied bias. Therefore, if the sample is such a material, an additional piezoelectric effect must be considered when analyzing the signal. Typically, piezoelectric expansion is linearly dependent on applied voltage and a simple subtraction can be used to correct for this effect.

Electrostatic force interaction

When a bias is applied to the sample for Joule heating, there is also an electrostatic force interaction between the tip and the sample. The tip-sample electrostatic force can be represented as $F=\frac{1}{2}\frac{dC}{dz}V^2$, in which C is the tip sample capacitance, and V is the voltage, Z is the tip and sample distance. Interestingly, this force also depends on V^2, the same as the expansion signal. Usually electrostatic force is small because the sample has been covered with a polymer layer. However, when applied voltage is large, this force needs to be considered. Electrostatic force does not depend on the frequency of the applied AC signal, therefore allowing for a simple method to differentiate and account for this contribution.

Thermal expansion

This is primary mode of signal and the main goal of SJEM. The substrate expands when Joule heated, resulting in change in the measured profile by the cantilever, resulting in a change in signal. However, thermal expansion coefficients can vary significantly. For example, the thermal expansion coefficients of metal are typically one order of magnitude higher than those of dielectric and amorphous materials; while the expansion coefficient of polymer is one order higher than those of metals. So by coating the sample surface with a layer of polymer, the expansion signal could be enhanced. More importantly, after coating, the signal only depends on the temperature, independent of the expansion coefficient of different materials, allowing for SJEM to be used for a wide array of samples. Expansion signal increases linearly with temperature and thus quadratically with voltage. In addition, expansion signal increases monotonically with the thickness of coating polymer, while the resolution will decrease due to greater thermal diffusion. Lastly, expansion signal decreases as the frequency increases.

Extraction of Temperature

By using the expansion signal, the temperature can be extracted as follows: the signal that captured by the lock-in amplifier is converted into the bending of cantilever. Using $\Delta L = \alpha_{CET} L \Delta T$,and applying the known expansion coefficient, $\alpha_{CET}$and polymer thickness, L(which could be measured by AFM or ellipsometer), the expansion signal is obtained. The smallest expansion that can be resolved is about 10pm. In order to extract accurate temperatures, additional modeling taking into account thermal expansion and cantilever bending is necessary. Moreover, calibration using a reference system, such as metallic films, is required.

Modeling

One dimensional transient finite element model

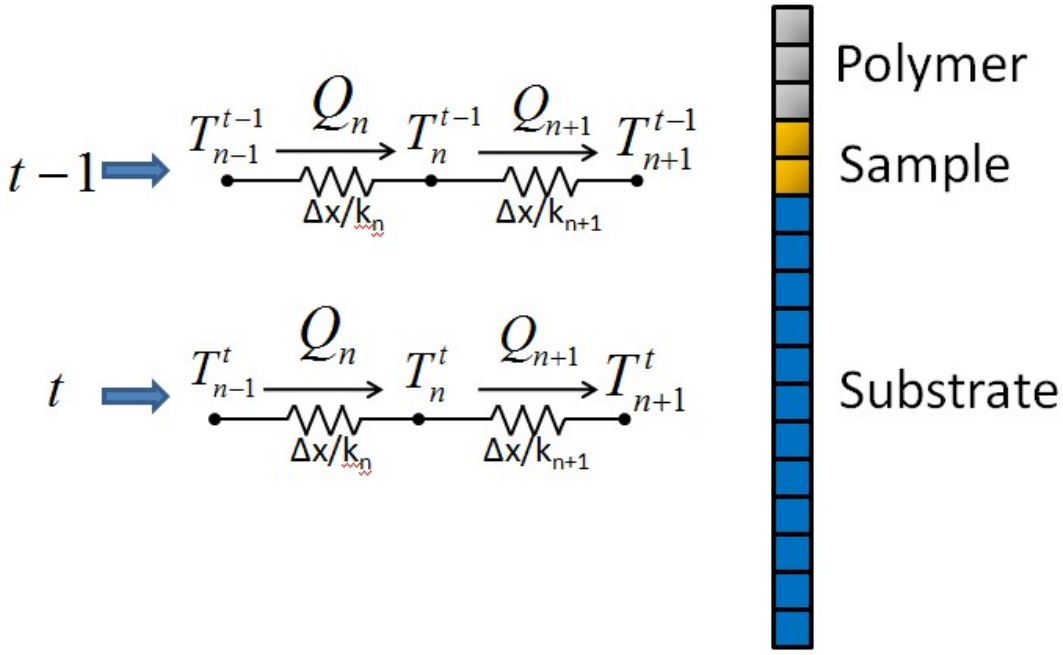

One dimensional finite element model for polymer-Sample(heater)-substrate sandwich structure

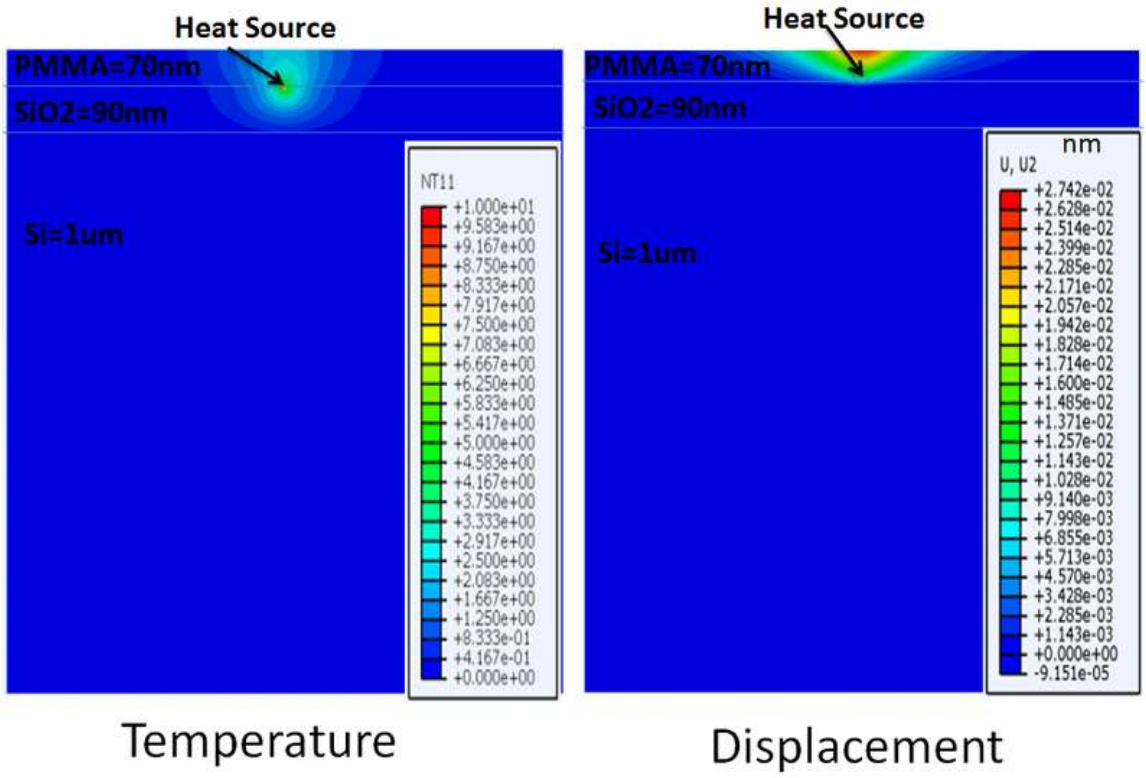

The temperature and expansion profile of a structure consisting of a single walled carbon nanotube sitting on SiO_2(90nm)/Si(1um) substrate, with a 70nm layer of PMMA on top(Simulated using Abacus).

When the sample is large enough, edge effects can be ignored. Therefore, a simple one dimensional finite element model can be a good approximation.

The basic thermal equation is:

$$\rho C_p \frac{dT}{dt} = \nabla (k \nabla T) + Q$$

Here, ρCp is the heat capacitance;K is the thermal conductivity and Q is the input power.

Rearrange the equation in a discrete form according to each element:

$$\rho C_p \frac{T_n^t - T_n^{t-1}}{\Delta t} = k_n \frac{T_{n-1}^t - T_n^t}{\Delta x^2} + k_{n+1} \frac{T_{n+1}^t - T_n^t}{\Delta x^2} + Q_n$$

Here, T_n^t represents the specific temperature of position element n at time element t. Using software could solve the equations and obtained the temperature T. The expansion magitude could be obtained by:

$$\Delta L = \alpha_{CET} L \Delta T$$

α_{CET} is the thermal expansion coefficient of the polymer and L is its thickness.

Two or three dimensional finite element model with electrical-thermal-mechanical coupling

Commercialized software can be used for 2D/3D finite element modeling. In such software, the appropriate differential equations for electrical, thermal and mechanical expansion are chosen and proper boundary conditions are set. In addition, electrical-thermal coupling exists in the sample because the resistance is a function of temperature. This is additionally accounted for by typical FEM software packages.

Applications

Integrated circuit interconnects

Miniaturization of modern integrated circuits has led to hugely increased current densities and therefore, self-heating. In particular, vias, or vertical interconnects, experience extreme local temperature fluctuations, which can strongly influence the electrical performance of multi-level interconnect structures. In addition, these large, highly-localized temperature fluctuations cause repeated stress gradients on the vias, ultimately leading to device failure. Traditional thermometry techniques use electrical characterization to determine resistivity and estimate the average temperature along an interconnect. However, this method is not able to characterize local temperature rises which may be significantly higher near vias due to their extremely high aspect ratios. Optical methods are diffraction limited to resolutions greater than 1um, far larger than most modern vias feature sizes. SJEM has been used to do in situ thermal mapping of these devices with lateral resolution in the sub-0.1 um range.

In addition, size effects also play an important role in modern interconnects. As dimensions of the metal decrease, thermal conductivity begins to decrease from that of the bulk material, further creating cause for concern. SJEM has been used to extract thermal conductivities of constrictions in different thicknesses of thin metallic films. The extracted values show agreement with those predicted by the Wiedemann-Franz law.

Integrated circuit transistors

Understanding thermal properties of transistors are vital for the semiconductor industry as well. Similar to interconnects, repeated thermal stresses can eventually lead to device failure. However, more importantly, electrical behavior, and therefore device parameters change significantly with temperature. SJEM has been used to map local hotspots in thin film transistors. By determining the location of these hotspots, they can be better understood and reduced or eliminated. One disadvantage to this method is that, like AFM, only the surface can be mapped. Consequently, additional processing steps would

be required in order to map buried features, such as most features in modern IC transistors.

Nanoscale materials

Nanoscale materials are becoming widely investigated for their many advantages in commercial electronics. In particular, these materials are known for excellent mobility as well as ability to carry high current densities. In addition, new applications have been realized for these materials including thermoelectrics, solar cells, fuel cells, etc. However, significant decrease in size scale in conjunction with increases in current density and device density leads to extreme temperature rises in these devices. These temperature fluctuations can influence electrical behavior and lead to device failure. Therefore, these thermal effects must be studied carefully, in situ, to realize nanoscale electronics. SJEM can be used for this purpose, allowing for in situ high-resolution thermal mapping.

Possible materials and devices for thermal mapping include high electron mobility transistors, nanotubes, nanowires, graphene sheets, nanomeshes, and nanoribbons, and other molecular electronic materials. In particular, SJEM can be directly used for characterization of band gap distributions in nanotube transistors, nanowires, and graphene nanomeshes and nanoribbons. It can also be used to locate hotspots and defects in these materials. Another example of a simple, direct application is thermal mapping of rough nanowires for thermolelectric applications.

Remaining Questions

Although SJEM is a very powerful technique for temperature detection, significant questions still remain regarding its performance.

This technique is far more complex than traditional AFM. Unlike AFM, SJEM needs to consider the type of polymer, the thickness of polymer used to coat the sample and the frequency to drive the device. This additional processing often can degrade or compromise the integrity of the sample. For micro/nano devices, wire-bonding is usually necessary to apply voltage, further increasing processing and decreasing throughput. During scanning, the magnitude of the voltage, frequency, and scanning speeds need to be considered. Calibration must also be done using a reference system in order to ensure accuracy. Finally, a complex model must be used to account for all these factors and parameters.

Second, there may be artifact effects near the edges (or steps). Near the edges where large height differences or material mismatches exist, artifact expansion signals are usually detected. The exact cause has not been found. It is widely believed that the tip sample interaction near the edges can account for these artifacts. At the edges, forces are present not only in the vertical direction but possibly also in the lateral direction, disrupting the cantilever motion. In addition, at a large step, loss of contact between the tip and the sample could result in an artifact in the image. Another concern is that the polymer

coating near the step may not be uniform, or possibly not continuous. Further investigations near edges and junctions need to be carried out.

Finally, interactions between the tip and electric field can occur when large gate biases are applied to the substrate. Fringing effects and other geometric concerns can lead to electric field concentrations, leading to large deviations from the normal baseline tip interaction which cannot be easily subtracted. This is especially problematic where the polymer expansion is small, leading to artifacts from this effect dominating. The contribution from these artifacts can be reduced by applying thicker polymer coatings or operating at a lower gate bias to decrease electric field. However, this occurs at the expense of resolution due to increased thermal diffusion in the thicker polymer layer as well as increased noise. In addition, devices may not be fully modulated at lower gate biases.

Chapter- 9

Other Types of Scanning Probe Microscopy

Scanning Hall probe microscope

Scanning Hall probe microscope (SHPM) is a variety of a scanning probe microscope which incorporates accurate sample approach and positioning of the scanning tunnelling microscope with a semiconductor Hall sensor. This combination allows to map the magnetic induction associated with a sample. Current state of the art SHPM systems utilize 2D electron gas materials (e.g. GaAs/AlGaAs) to provide high spatial resolution (~300 nm) imaging with high magnetic field sensitivity. Unlike the magnetic force microscope the SHPM provides direct quantitative information on the magnetic state of a material. The SHPM can also image magnetic induction under applied fields up to ~1 tesla and over a wide range of temperatures (millikelvins to 300 K).

Scanning voltage microscopy

Scanning voltage microscopy (SVM) -- sometimes also called *nanopotentiometry* -- is a scientific experimental technique based on atomic force microscopy. A conductive probe, usually only a few nanometers wide at the tip, is placed in full contact with an operational electronic or optoelectronic sample. By connecting the probe to a high-impedance voltmeter and rastering over the sample's surface, a map of the electric potential can be acquired. SVM is generally nondestructive to the sample although some damage may occur to the sample or the probe if the pressure required to maintain good electrical contact is too high. If the input impedance of the voltmeter is sufficiently large, the SVM probe should not perturb the operation of the operational sample.

SVM is particularly well suited to analyzing microelectronic devices (such as transistors or diodes) or quantum electronic devices (such as quantum well diode lasers) directly

because nanometer spatial resolution is possible. SVM can also be used to verify theoretical simulation of complex electronic devices.

For example, the potential profile across the quantum well structure of a diode laser can be mapped and analyzed; such a profile could indicate the electron and hole distributions where light is generated and could lead to improved laser designs.

In a similar technique, Scanning gate microscopy (SGM), the probe is oscillated at some natural frequency some fixed distance above the sample with an applied voltage relative to the sample. The image is constructed from the X,Y position of the probe and the conductance of the sample, with no significant current passing through the probe, which acts as a local gate. The image is interpreted as a map of the sample's sensitivity to gate voltage. A lock-in amplifier aids noise reduction by filtering through only the amplitude oscillations that match the probe's vibration frequency. Applications include imaging defect sites in carbon nanotubes and doping profiles in nanowires.

Spin polarized scanning tunneling microscopy

Spin polarized scanning tunneling microscopy (SP-STM) is a specialized application of scanning tunneling microscopy (STM) that can provide detailed information of magnetic phenomena on the single-atom scale additional to the atomic topology gained with STM. SP-STM opened a novel approach to static and dynamic magnetic processes as precise investigations of domain walls in ferromagnetic and antiferromagnetic systems, as well as thermal and current-induced switching of nanomagnetic particles.

How it works

An extremely sharp tip coated with a thin layer of magnetic material is moved systematically over a sample. A voltage is applied between the tip and the sample allowing electrons to tunnel between the two, resulting in a current. In the absence of magnetic phenomena, the strength of this current is indicative for local electronic properties.

If the tip is magnetized, however, electrons with spins matching the tip's magnetization will have a higher chance of tunneling. This is essentially the effect of tunnel magnetoresistance and the tip/surface essentially acts as a spin valve.

Since a scan using only a magnetized tip cannot distinguish between current changes due to magnetization or space separation, multi-domain structures and/or topological information from another source (frequently conventional STM) must be utilized. Then, magnetic imaging down to the atomic scale, i.e. for example in antiferromagnetic system, can be achieved.

Nowadays, antiferromagnetic tips are preferred since ferromagnetic tips induce magnetization reversal in the systems to be studied due to stray fields. In STM tunneling electrons come from the very same atom most close to the surface. Therefore, with the magnetization of this atom well defined, the tunneling current remains polarized for antiferromagnetic tips but without stray field.

Alternate method

Another way to obtain the magnetization distribution is to have the tip provide a strong stream of spin polarized electrons. One method to achieve this is to shine polarization laser light onto a GaAs tip, which produces spin polarized electrons due to spin-orbit coupling. The tip is then scanned along the sample much like conventional STM. One limitation of this method is that the most effective source of spin polarized electrons is obtained by having the incident laser light shine directly opposite of the tip, i.e. through the sample itself. This restricts the method to measuring thin samples.

Scanning ion-conductance microscopy

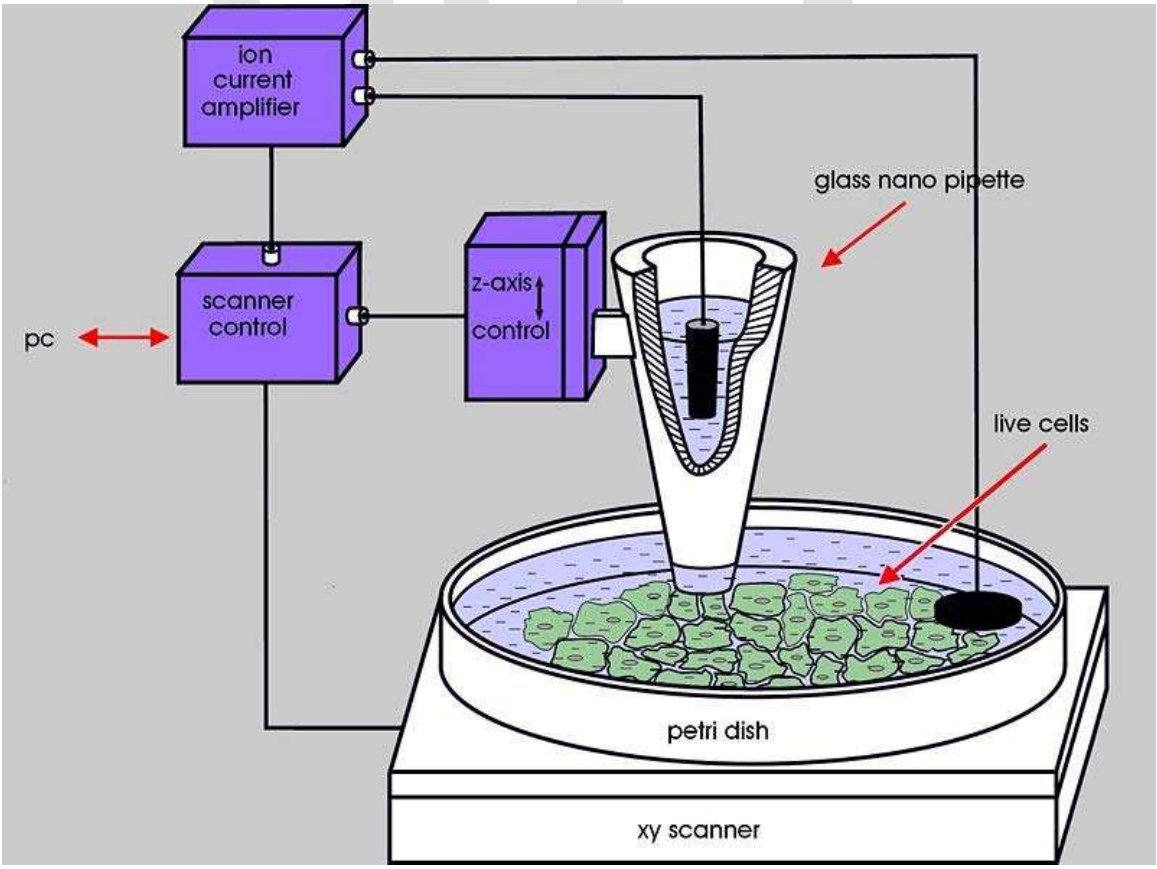

The **scanning ion-conductance microscope** (SICM) consists of an electrically charged glass micro- or nanopipette probe filled with electrolyte lowered toward the surface of the sample (which is non-conducting for ions) in an oppositely charged bath of electrolyte. As the tip of the micropipette approaches the sample, the ion conductance and therefore current decreases since the gap through which ions can flow, is reduced in size. Variations in the ion current are measured by an amplifier, and are used as a feedback signal by a scanner control unit to keep the distance between pipette tip and sample constant by applying corresponding voltages to the Z-piezo drive during the scanning procedure. Therefore, the path of the tip follows the contours of the surface.

The SICM can also sample and map the local ion currents above the surface. This is useful in imaging ion currents through membrane channels.

This scanning technique can be used on living tissues, whereas traditional SEM imaging necessitated killing the sample. Biological processes can now be observed whilst in action.

SICM is part of the larger family of scanning probe microscopy (SPM), and was specially designed for the sub-micrometer resolution scanning of soft non-conductive materials that are bathed in electrolyte solution.

Scanning gate microscopy

Scanning gate microscopy (SGM) is a scanning probe microscopy technique with an electrically conductive tip used as a movable gate that couples capacitively to the sample and probes electrical transport on the nanometer scale. Typical samples are mesoscopic devices, often based on semiconductor heterostructures, such as quantum point contacts or quantum dots. Carbon nanotubes too have been investigated.

In SGM one measures the sample's electrical conductance as a function of tip position and tip potential. This is in contrast to other microscopy techniques where the tip is used as a sensor, e.g., for forces.

SGMs were developed in the late 1990s from atomic force microscopes. Most importantly, these had to be adapted for use at low temperatures, often 4 kelvins or less, as the samples under study do not work at higher temperatures. Today an estimated number of ten research groups worldwide use the technique.

Scanning capacitance microscopy

Scanning capacitance microscopy (SCM) is a variety of scanning probe microscopy in which a narrow probe electrode is held just above the surface of a sample and scanned

across the sample. SCM characterizes the surface of the sample using information obtained from the change in electrostatic capacitance between the surface and the probe.

SCM uses an ultra-sharp conducting probe (often Pt/Ir or Co/Cr metal covering an etched silicon probe) to form a metal-insulator-semiconductor (MIS/MOS) capacitor with a semiconductor sample if a native oxide is present. When no oxide is present, a Schottky capacitor is formed. When the probe and surface are in contact, an AC bias is applied, generating capacitance variations in the sample which can be detected using a GHz resonant capacitance sensor. The tip is then scanned across the semiconductor's surface in 2D while the tip's height is controlled by conventional contact force feedback.

By applying an alternating bias to the metal-coated probe, carriers are alternately accumulated and depleted within the semiconductor’s surface layers, changing the tip-sample capacitance. The magnitude of this change in capacitance with the applied voltage gives information about the concentration of carriers (SCM amplitude data), whereas the difference in phase between the capacitance change and the applied, alternating bias carries information about the sign of the charge carriers (SCM phase data). Because SCM functions even through an insulating layer, a finite conductivity is not required to measure the electrical properties.

SCM resolution

On the conducting surfaces, the resolution limit is estimated as 2 nm. For the high resolution, the quick analysis of capacitance of a capacitor with rough electrode is required. This SCM resolution is an order of magnitude better than that estimated for the atomic nanoscope; however, as other kinds of the probe microscopy, SCM requires careful preparation of the analyzed surface, which is supposed to be almost flat.

Applications of SCM

Owing to the high spatial resolution of SCM, it is a useful nanospectroscopy characterization tool. Some applications of the SCM technique involve mapping the dopant profile in a semiconductor device on a 10 nm scale, quantification of the local dielectric properties in hafnium-based high-k dielectric films grown by an atomic layer deposition method and the study of the room temperature resonant electronic structure of individual germanium quantum dot with different shapes. The high sensitivity of dynamical scanning capacitance microscopy, in which the capacitance signal is modulated periodically by the tip motion of the atomic force microscope (AFM), was used to image compressible strips in a two-dimensional electron gas (2DEG) buried 50 nm below an insulating layer in a large magnetic field and at cryogenic temperatures.

Photothermal microspectroscopy

Photothermal microspectroscopy (PTMS), alternatively known as photothermal temperature fluctuation (PTTF), is derived from two parent instrumental techniques: infrared spectroscopy and atomic force microscopy (AFM). In one particular type of AFM, known as scanning thermal microscopy (SThM), the imaging probe is a sub-miniature temperature sensor, which may be a thermocouple or a resistance thermometer. This same type of detector is employed in a PTMS instrument, enabling it to provide AFM/SThM images: However, the chief additional use of PTMS is to yield infrared spectra from sample regions below a micrometer, as outlined below.

Technique

The AFM is interfaced with an infrared spectrometer. For work using Fourier transform infrared spectroscopy (FTIR), the spectrometer is equipped with a conventional black body infrared source. A particular region of the sample may first be chosen on the basis of the image obtained using the AFM imaging mode of operation. Then, when material at this location absorbs the electromagnetic radiation, heat is generated, which diffuses, giving rise to a decaying temperature profile. The thermal probe then detects the photothermal response of this region of the sample. The resultant measured temperature fluctuations provide an interferogram that replaces the interferogram obtained by a conventional FTIR setup, e.g., by direct detection of the radiation transmitted by a sample. The temperature profile can be made sharp by modulating the excitation beam. This results in the generation of thermal waves whose diffusion length is inversely proportional to the root of the modulation frequency. An important advantage of the thermal approach is that it permits to obtain depth-sensitive subsurface information from surface measurement, thanks to the dependence of thermal diffusion length on modulation frequency.

Applications

The two particular features of PTMS that have determined its applications so far are:

- spectroscopic mapping may be performed at a spatial resolution well below the diffraction limit of IR radiation, ultimately at a scale of 20-30 nm. In principle, this opens the way to sub-wavelength IR microscopy where the image contrast is to be determined by the thermal response of individual sample regions to particular spectral wavelengths.

- In general, no special preparation technique is required when solid samples are to be studied. For most standard FTIR methods, this is not the case.

Related technique

This spectroscopic technique complements another recently-developed method of chemical characterisation or fingerprinting, namely micro-thermal analysis (micro-TA). This also uses an “active” SThM probe, which acts as a heater as well as a thermometer, so as to inject evanescent temperature waves into a sample and to allow sub-surface

imaging of polymers and other materials. The sub-surface detail detected corresponds to variations in heat capacity or thermal conductivity. Ramping the temperature of the probe, and thus the temperature of the small sample region in contact with it, allows localized thermal analysis and/or thermomechanometry to be performed.

Magnetic resonance force microscopy

Magnetic resonance force microscopy (**MRFM**) is an imaging technique that acquires magnetic resonance images (MRI) at nanometer scales, and possibly at atomic scales in the future. MRFM is potentially able to observe protein structures which cannot be seen using X-ray crystallography and protein nuclear magnetic resonance spectroscopy. Detection of the magnetic spin of a single electron has been demonstrated using this technique. The sensitivity of a current MRFM microscope is 10 billion times better than a medical MRI used in hospitals.

Basic principle

The MRFM concept combines the ideas of magnetic resonance imaging (MRI) and atomic force microscopy (AFM). Conventional MRI employs an inductive coil as an antenna to sense resonant nuclear or electronic spins in a magnetic field gradient. MRFM uses a cantilever tipped with a ferromagnetic (iron cobalt) particle to directly detect a modulated spin gradient force between sample spins and the tip. As the ferromagnetic tip moves close to the sample, the atoms' nuclear spins become attracted to it and generate a small force on the cantilever. The spins are then repeatedly flipped, causing the cantilever to gently sway back and forth in a synchronous motion. That displacement is measured with an interferometer (laser beam) to create a series of 2-D images of the sample, which are combined to generate a 3-D image. The interferometer measures resonant frequency of the cantilever. Smaller ferromagnetic particles and softer cantilevers increase the signal to noise ratio. Unlike the inductive coil approach, MRFM sensitivity scales favorably as device and sample dimensions are reduced.

Because the signal to noise ratio is inversely proportional to the sample size, Brownian motion is the primary source of noise at the scale in which MRFM is useful. Accordingly, MRFM devices are cryogenically cooled. MRFM was specifically devised to determine the structure of proteins *in situ*.

Milestones

The basic principles of MRFM imaging and the theoretical possibility of this technology were first described in 1991. The first MRFM image was obtained in 1993 at the IBM Almaden Research Center with 1-μm vertical resolution and 5-μm lateral resolution using a bulk sample of the paramagnetic substance diphenyipicrylhydrazil. The spatial resolution reached nanometer-scale in 2003. Detection of the magnetic spin of a single

electron was achieved in 2004. In 2009 researchers at IBM and Stanford announced that they had achieved resolution of better than 10 nanometers, imaging tobacco mosaic virus particles on a nanometer-thick layer of adsorbed hydrocarbons.

Kelvin probe force microscope

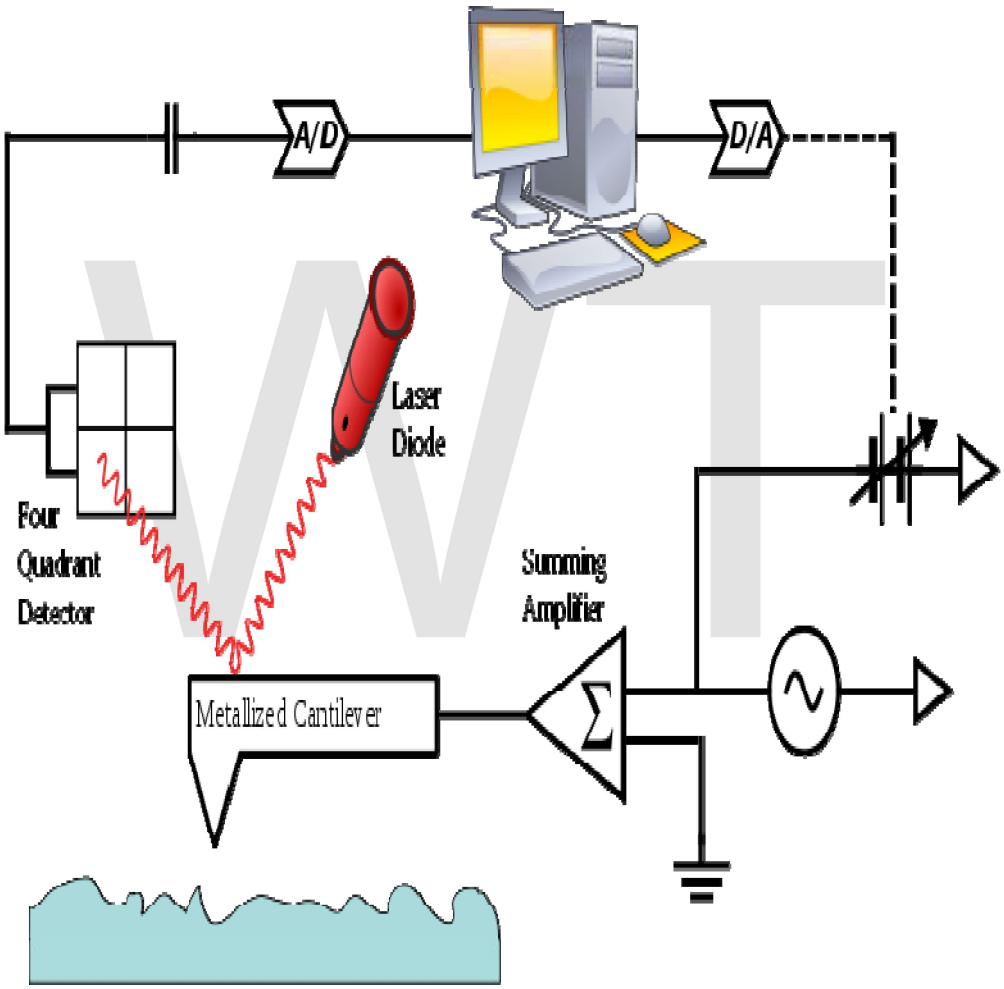

In Kelvin probe force microscopy, a conducting cantilever is scanned over a surface at a constant height in order to map the work function of the surface.

Kelvin probe force microscopy (*KPFM*), also known as **surface potential microscopy,** is a noncontact variant of atomic force microscopy (AFM) that was invented in 1991. With KPFM, the work function of surfaces can be observed at atomic or molecular scales. The work function relates to many surface phenomena, including catalytic activity, reconstruction of surfaces, doping and band-bending of semiconductors, charge

trapping in dielectrics and corrosion. The map of the work function produced by KPFM gives information about the composition and electronic state of the local structures on the surface of a solid.

KPFM is a scanning probe method where the potential offset between a probe tip and a surface can be measured using the same principle as a macroscopic Kelvin probe. The cantilever in the AFM is a reference electrode that forms a capacitor with the surface, over which it is scanned laterally at a constant separation. The cantilever is not piezoelectrically driven at its mechanical resonance frequency ω_0 as in normal AFM although an alternating current (AC) voltage is applied at this frequency.

When there is a direct-current (DC) potential difference between the tip and the surface, the AC+DC voltage offset will cause the cantilever to vibrate. The origin of the force can be understood by considering that the energy of the capacitor formed by the cantilever and the surface is

$$E = \frac{1}{2}C[V_{DC} + V_{AC}sin(\omega_0 t)]^2 = \frac{1}{2}C[2V_{DC}V_{AC}sin(\omega_0 t) - \frac{1}{2}V_{AC}^2 cos(2\omega_0 t)]$$

plus terms at DC. Only the cross-term proportional to the $V_{DC} \cdot V_{AC}$ product is at the resonance frequency ω_0. The resulting vibration of the cantilever is detected using usual scanned-probe microscopy methods (typically involving a diode laser and a four-quadrant detector). A null circuit is used to drive the DC potential of the tip to a value which minimizes the vibration. A map of this nulling DC potential versus the lateral position coordinate therefore produces an image of the work function of the surface.

A related technique, electrostatic force microscopy (EFM), directly measures the force produced on a charged tip by the electric field emanating from the surface. EFM operates much like magnetic force microscopy in that the frequency shift or amplitude change of the cantilever oscillation is used to detect the electric field. However, EFM is much more sensitive to topographic artifacts than KFPM. Both EFM and KPFM require the use of conductive cantilevers, typically metal-coated silicon or silicon nitride.

Working principle

The Kelvin probe force microscope or Kelvin force microscope (KFM) is based on an AFM set-up and the determination of the work function is based on the measurement of the electrostatic forces between the small AFM tip and the sample. The conducting tip and the sample are characterized by (in general) different work functions. When both elements are brought in contact, a net electric current will flow between them until the Fermi levels are aligned. The potential is called the contact potential (difference) denoted generally with V_{CPD}. An electrostatic force between tip and sample builds up, resulting from the net charge transfer. For the measurement a voltage is applied between tip and sample, consisting of a DC-bias V_{DC} and an AC-voltage $V_{AC} = sin(\omega_2 t)$ of frequency ω_0 at the second resonance frequency of the AFM cantilever

$$V = (V_{DC} - V_{CPD}) + V_{AC} \cdot \sin(\omega_2 t)$$

Tuning the AC-frequency to the second resonance frequency of the cantilever results in an improved sensitivity and allows the independent and simultaneous imaging of topography and the contact potential. As a result of these biasing conditions, an oscillating electrostatic force appears, inducing an additional oscillation of the cantilever with the characteristic frequency ω_2. The general expression of such electrostatic force not considering coulomb forces due to charges can be written as

$$F = -\frac{1}{2}\frac{dC}{dz}V^2$$

The electrostatic force can be split up into three contributions, as the total electrostatic force F acting on the tip has spectral components at the frequencies ω_2 and $2\omega_2$.

$$F = F_{DC} + F_{\omega_2} + F_{2\omega_2}$$

The DC component, F_{DC}, contributes to the topographical signal, the term $F_{\omega 2}$ at the characteristic frequency ω_2 is used to measure the contact potential and the contribution $F_{2\omega 2}$ can be used for capacitance microscopy.

$$F_{DC} = -\frac{dC}{dz}[\frac{1}{2}(V_{DC} - V_{CPD})^2 + \frac{1}{4}V_{AC}^2]$$
$$F_{\omega_2} = -\frac{dC}{dz}[V_{DC} - V_{CPD}]V_{AC}\sin(\omega_2 t)$$
$$F_{2\omega_2} = +\frac{1}{4}\frac{dC}{dz}V_{AC}^2\cos(2\omega_2 t)$$

For contact potential measurements a lock-in amplifier is used to detect the cantilever oscillation at ω_2. During the scan V_{DC} will be adjusted so that the electrostatic forces between the tip and the sample become zero and thus the response at the oscillation frequency ω becomes zero and at the same time response at frequency ω_2 become maximum. Since the electrostatic force at ω_2 depends on V_{DC} - V_{CPD}, V_{DC} corresponds to the contact potential. Absolute values of the sample work function can be obtained if the tip is first calibrated against a reference sample of known work function. Apart from this, one can use the normal topographic scan methods at the resonance frequency ω independently of the above. Thus, in one scan, the topography and the contact potential of the sample are determined simultaneously.

Electrochemical scanning tunneling microscope

The **electrochemical scanning tunneling microscope**, or **ESTM**, was invented in 1988 by Kingo Itaya in Japan. With ESTM, the structures of surfaces and electrochemical reactions in solid-liquid interfaces can be observed at atomic or molecular scales.

Electrochemical reactions occur in electrolytic solutions—for example electroplating, etching, batteries, and so on. On the electrode surface, many atoms, molecules, and ions adsorb and affect the reactions. In the past, in order to obtain information about the structure of electrode surfaces and reactions, the sample electrode was taken out of the electrolytic solution and measured under ultra high vacuum (UHV) conditions. In this case, the structure of the surface changed and could not be observed precisely. By using this microscope, however, these problems are resolved.

In electrolytic solutions, a very complicated electrical double layer of H_2O molecules and anions is formed. In this layer, as the distribution of anions changes with the potential of the electrode, it is necessary to control the reaction on the electrode. The potentials of the working electrodes (the sample and the tip) are controlled independently against a reference electrode. In this case, the tunneling bias voltage is the difference between the two potentials. A counter electrode is used to complete the current-carrying circuits with the working electrodes. By using these four electrodes, the electrochemical reaction is controlled precisely by the external voltage, and the surface in liquid can be observed.

Electrostatic force microscope

Electrostatic force microscopy (EFM) is a type of dynamic non-contact atomic force microscopy where the electrostatic force is probed. ("Dynamic" here means that the cantilever is oscillating and does not make contact with the sample). This force arises due to the attraction or repulsion of separated charges. It is a long-ranged force and can be detected 100 nm from the sample. For example, consider a conductive cantilever tip and sample which are separated a distance z usually by a vacuum. A bias voltage between tip and sample is applied by an external battery forming a capacitor, C, between the two. The capacitance of the system depends on the geometry of the tip and sample. The total energy stored in that capacitor is $U = -\frac{1}{2}C\Delta V^2$. The battery works to maintain a constant voltage, ΔV, between the capacitor plates (tip and sample). By definition, taking the negative gradient of the energy gives the force. The z component of the force (the force along the axis connecting the tip and sample) is thus:

$$F_{electrostatic} = \frac{1}{2}\frac{\partial C}{\partial z}\Delta V^2$$.

The electrostatic force can be probed by changing the voltage, and that force is parabolic with respect to the voltage. One note to make is that ΔV is not simply the voltage difference between the tip and sample. Since the tip and sample are often not the same material, and furthermore can be subject to trapped charges, debris, etc., there is a difference between the work functions of the two. This difference, when expressed in terms of a voltage, is called the contact potential difference, V_{CPD} This causes the apex of the parabola to rest at $\Delta V = V_{tip} - V_{sample} - V_{CPD} = 0$. Typically, the value of V_{CPD} is on the order of a few hundred millivolts. Forces as small as piconewtons can routinely be detected with this method.

With an electrostatic force microscope, like the atomic force microscope it is based on, the sample can be immersed in liquid.

Conductive atomic force microscopy

Conductive atomic force microscopy (C-AFM) is a variation of atomic force microscopy (AFM) and scanning tunneling microscopy (STM), which uses electrical current to construct the surface profile of the studied sample. The current is flowing through the metal-coated tip of the microscope and the conducting sample. Usual AFM topography, obtained by vibrating the tip, is acquired simultaneously with the current. This enables to correlate a spatial feature on the sample with its conductivity, and distinguishes C-AFM from STM where only current is recorded. A C-AFM microscope uses conventional silicon tips coated with a metal or metallic alloy, such as Pt-Ir alloy.

The C-AFM can be operated in the imaging mode and spectroscopic mode.

Imaging mode

In the conventional imaging mode, vibrating tip is scanned over a small sample area (typically square micrometres); a negative voltage bias is applied to the sample, and the electrons tunneling from the sample to the tip are being collected. This polarity is chosen for several reasons:

- The electron barrier in this case is the conduction band onset at the Si/oxide interface, which is better known than the tip/oxide interface.
- The emission area for substrate injection is homogeneous and depends mostly on the tip/sample contact area. On the contrary, the emission area in the case of tip injection depends on the shape of the tip.
- During the measurement, the tip is in contact with the sample, and many studies materials are hydrophilic. Therefore, the tip drags along water and other contaminants adsorbed at the sample surface. The applied voltage induces a high electrical field between the tip and the substrate. This field ionizes water, producing the OH^-. If a negative voltage is applied to the tip, the OH^- ions are

attracted to the surface of the sample; they oxidize it thereby permanently blocking the current flow. If a positive voltage is applied to the tip, the OH^- ions are dragged to the tip, oxidizing it and breaking the electrical circuit. However, whereas the studied sample may be unique, the tips are disposable and easy to replace, but after replacement, it is difficult to relocate exactly the same area. The tip degradation, as well as image quality, also depend on the scanning parameters.

Spectroscopic mode

In the spectroscopic mode, the tip is stationary, while the voltage is being swept. This allows recording conventional current–voltage characteristic from tiny areas of the sample, and thereby to extract information on the local electronic properties, such as local density of states.

Ballistic electron emission microscopy

Ballistic electron emission microscopy or BEEM is a technique for studying ballistic electron transport through variety of materials and material interfaces. BEEM is a three terminal scanning tunneling microscopy (STM) technique that was invented in 1988 at the Jet Propulsion Laboratory in Pasadena California by L. Douglas Bell and William Kaiser. The most popular interfaces to study are metal-semiconductor Schottky diodes, but metal-insulator-semiconductor systems can be studied as well.

When performing BEEM, electrons are injected from a STM tip into a grounded metal base of a Schottky diode. A small fraction of these electrons will travel ballistically through the metal to the metal-semiconductor interface where they will encounter a Schottky barrier. Those electrons with sufficient energy to surmount the Schottky barrier will be detected as the BEEM current. The atomic scale positioning capability of the STM tip gives BEEM nanometer spatial resolution. In addition, the narrow energy distribution of electrons tunneling from the STM tip gives BEEM a high energetic resolution (about 0.02 eV).